Molecular Investigation of Chemical-assisted Protein Rescue in Ocular Protein Folding Diseases

GONG, Bo

A Thesis Submitted in Partial Fulfilment

of the Requirements for the Degree of

Doctor of Philosophy

in

Ophthalmology and Visual Sciences

The Chinese University of Hong Kong

August 2010

ProQuest LLC
789 East Eisenhower Parkway
P.O. Box 1346
Ann Arbor, MI 48106-1346

Thesis/Assessment Committee

Professor Shu-Ping Fan (Chair)

Professor Chi-Pui Pang (Thesis supervisor)

Professor Hin-Fai Yam (Thesis supervisor)

Professor Prof Wing-Keung Liu (Committee Member)

Professor Yun-Chung Leung (External Examiner)

Abstract of thesis entitled:
Molecular investigation of chemical-assisted protein rescue in ocular protein folding diseases
Submitted by GONG Bo
For the degree of Doctor of Philosophy
At the Chinese University of Hong Kong in August 2010

Abstract

To date, many genes and mutations are identified to cause various ocular diseases. Some of them result in a disruption of protein folding, an important cause of disease pathogenesis and progression. In my laboratory, novel mutations of *crystallins* and *myocilin* have been identified to segregate with congenital cataract and primary open-angle glaucoma, respectively. In this thesis, I reported molecular investigations of the resultant protein variants and their altered cellular functions in relation to the clinical phenotypes that contributed to new understanding of the roles of these genes in ocular tissues. The experimental results also threw light on the underlying mechanisms involved in the onset and pathogenesis of the respective ocular diseases. Meanwhile, small chemicals were also tested to see if the altered protein features could be correctable.

In the study of *αA-crystallin (CRYAA)*, *G98R CRYAA* was cloned into a mammalian expression vector pcDNA6-His/myc version B and the sequence was confirmed by direct sequencing. Following lipophilic transfection to lens epithelial B3 cells, the recombinant mutated CRYAA protein was highly insoluble upon 0.5% Triton X-100 (Tx) extraction. It was retained and formed aggregation, and distributed in the endoplasmic reticulum (ER) along with the ER resident protein (protein disulfide isomerise). The wild-type (WT) CRYAA was found to be

soluble and diffusely distributed in the cytoplasm. The accumulation of G98R mutant induced ER stress, and the affected cells were prone to apoptosis. After treatment with a small chemical molecule, the natural osmolyte trimethylamine N oxide (TMAO), the Tx insolubility of mutant protein was reduced in dose- and time-dependent manners. It was also prone to be degraded via ubiquitin proteasome pathway (UPP). In mutant-expressing cells, the mutant protein aggregation was decreased after treatment. The ER stress and the rate of apoptosis were also alleviated, probably mediated by heat shock response, as demonstrated by the effect of TMAO on heat shock protein 70 expression.

The truncated *G165fsX8 γD-crystallin (CRYGD)* variant was studied to further examine the effects of small chemical-assisted protein rescue of a CRYGD mutant that causes congenital cataract. *G165fsX8 CRYGD* was identified in a Chinese family with nuclear type of congenital cataract. The mutation was cloned into a mammalian expression vector p3XFLAG-myc-CMV"-25 and sequence was confirmed by direct sequencing. Following lipophilic transfection to COS-7 cells, the G165fsX8 CRYGD mutant protein was significantly insoluble upon 0.5% Tx extraction and was mistrafficked to the nuclear envelope with co-localization with nuclear lamins, whereas WT protein was Tx soluble and nuclear located. Treatment with small chemical sodium 4-phenylbutyrate (4-PBA) substantially reduced the Tx insolubility and reversed the mutant protein to nuclear localization. This correction has resulted in better cell survival, probably via a heat-shock response, as demonstrated by heat-shock protein 70 up-regulation.

The third eye gene model was *myocilin (MYOC)*, the first identified gene responsible for primary open angle glaucoma. The aim of this study was to investigate if glaucoma-causing

MYOC variants, including D384N MYOC, could be correctable. *D384N MYOC* was identified in a Chinese family diagnosed with high tension juvenile-onset primary open-angle glaucoma. Disease causing mutations in *MYOC* (*R82C, C245Y, Q368X, P370L, T377M, D380A, D384N, R422C, R422H, C433R, Y437H, I477N, I477S and N480K*) were cloned into mammalian expression vector p3XFLAG-myc-CMV"-25 and the sequences confirmed by direct sequencing. Following lipophilic transfection to human trabecular meshwork (HTM) cells, the Tx solubility and secretion of MYOC and cell apoptosis were examined in the presence or not with small chemical treatments. 4-PBA, TMAO and deuterium oxide (D_2O), reduced the portion of insoluble fractions to various extents in the mutant proteins. The osmolytes TMAO and D_2O were more effective than 4-PBA in improving MYOC solubility. TMAO was further shown to improve the secretion and ER-Golgi trafficking of D384N MYOC, thereby reducing the ER stress and rescuing cells from apoptosis.

In summary, this thesis described my study on the biochemical properties of novel protein mutants of three different ocular disease genes (*CRYAA, CRYGD* and *MYOC*). The disrupted protein properties, such as protein solubility, mistrafficking and aggregation, could be resolved by treatment with small chemical molecules including TMAO and 4-PBA, by virtue of their chaperoning capabilities. Results of these studies showed how these chemicals correct the cellular defects associated with disrupted proteins. Given that these chemicals are cell-permeable and small in size, they should be tested in animal studies on their biological effects to lens opacity or elevated intraocular pressure.

摘 要

迄今為止，已有大量與眼科疾病相關的基因及突變被發現。這些基因可能導致病理生理改變和發展的蛋白折疊錯亂。我們實驗室已經發現了很多能引起先天性白內障和原發性開角型青光眼的相關基因及突變。本論文闡述了對這些突變基因以及它們導致的細胞功能和表型改變的分子水準的研究，以期揭示這些基因引起眼科疾病所起的作用，進而闡述眼科疾病發生和發展的分子機制。同時，在此課題中還對一些小分子化合物進行了檢測，研究它們是否可以修復這些突變基因引起的蛋白質錯亂征狀。

在對 αA-晶體蛋白的研究課題中，*CRYAA* 基因 *G98R* 突變克隆於真核表達載體 pcDNA6-His/myc version B 上並進行基因測序驗證其序列。其後，把構建好的質粒用脂質體轉染到人晶體上皮細胞 B3 細胞株中，發現 G98R 突變蛋白不溶於 Triton X-100x (Tx) 提取液中，以及在內質網中有聚集體形成。相反，野生型 αA 晶體蛋白可溶於 Tx 提取液中並且均勻分佈在細胞的胞質中。同時，這種聚集的突變蛋白可以引起內質網應激反應並容易導致細胞凋亡。當用小化學分子自然滲透物氧化三甲胺 (TMAO) 對 G98R 轉染的細胞進行處理時，可以按劑量和時間依賴性的方式使這些突變蛋白通過泛素-蛋白酶體途徑 (UPP) 降解。 同時，在這些被處理的轉染細胞中，聚集的突變蛋白，內質網應激反應以及凋亡率都有降低，這種現象可能是由於熱休克蛋白 70 (Hsp70) 表達量上升而引起的。

為了進一步檢測小化學分子對治療先天性白內障突變基因引起的蛋白質錯亂所起的作用，另外一個先天性白內障致病基因，*γD* 基因 *G165fsX8* 突變也被納入研究。同樣，這個突變基因被克隆到真核表達載體 p3XFLAG-myc-CMV"-25 並經過序列驗證以後，轉染

到 COS-7 細胞株中，發現 G165fsX8 突變蛋白不溶於 0.5%的 Tx 的提取液中，同時這種突變蛋白分佈在細胞核周圍的核質蛋白 lamin 中，相反，野生型γD 蛋白是可溶於 Tx 提取液中並分佈在細胞核內。在經過小分子化合物苯基丁酸鈉 (PBA) 處理以後，這些不溶性突變蛋白大大降低的同時，也發現它們在細胞核中重新表達。PBA 的這種修復作用同時也增加 Hsp70 的表達以及促進被轉染*γD* 基因 G165fsX8 突變的細胞生長速度。

第三個研究的基因是 *myocilin* (*MYOC*)，它是第一個被確認的原發性開角青光眼致病基因。在此課題中，主要目的是檢測小分子化合物是否對以下一些青光眼致病基因表達的蛋白有修復作用。它們包括在中國人群中發現的致高眼壓早期原發性開角青光眼的 *MYOC* 基因 *D384N* 突變，以及其它的突變基因 *R82C, C245Y, Q368X, P370L, T377M, D380A, D384N, R422C, R422H, C433R, Y437H, I477N, I477S* 和 *N480K MYOC*。這些基因先是克隆到真核表達載體 p3XFLAG-myc-CMV"-25 中，經過序列鑒定以後再轉染到小梁網細胞中，並對其 Tx 溶解性、MYOC 的分泌程度以及細胞凋亡率，在有或者無小分子化合物的處理條件下都進行進行了檢測。PBA，TMAO 和 D_2O 都可以不同程度地減少不溶性突變 MYOC 蛋白，並增強其分泌性。TMAO 和 D_2O 比 PBA 能更好地提高 MYOC 的可溶性和分泌性。TMAO 同時能促進 D384N 突變蛋白從內質網到高爾基體的轉運，而且降低內質網應激反應和減少細胞凋亡率。

綜上，此課題對 3 種不同致眼科疾病基因 (*CRYAA, CRYGD* 和 *MYOC*) 引起的蛋白性質改變進行了生物化學特徵方面的研究，揭示了一些具有分子伴侶特徵的小分子化合物，如 TMAO 和 PBA 可以幫助修復一些突變蛋白的特徵（可溶性、錯誤轉運以及聚集體

的形成）。此課題還分析了這些小分子化合物對突變基因導致的蛋白缺陷的修復機制。由於這些小分子化合物很小且具有膜滲透性的特徵，可以通過動物模型來進壹步研究和測試它們對動物晶體混濁以及眼壓升高的影響和生物效果。

Acknowledgements

First, I wish to express my greatest gratitude to my supervisor, Prof. Chi-Pui Pang, whose expertise, understanding, and patience, added considerably to my post-graduate experience. I appreciate his vast knowledge in many areas, and his assistance in writing reports (including papers, scholarship and fellowship applications, and this thesis). I also gave my whole-hearted appreciation to another supervisor Dr. Gary Hin-Fai Yam. During the three-year study, he provided lots of valuable guidance, insightful advice and continuous supports to my work. He helped me to step into a new and high level of cell biology in ophthalmology research. I am also indebted to Associate Prof. Christopher Kai-Shun Leung, Prof. Dorothy Shiu-Ping Fan, Ms. Pancy Oi-Sin Tam and Dr Wai-Ying Li for their useful discussion and technical assistance in my project.

I am also grateful to the other members of our laboratory. Many thanks were given to Miss Sylvia Chiang, Mr Kwok-Ping Chan and Dr Kai-On Chu for their nice technical support; to Dr Li-Yun Zhang, Dr Li-Yun Jia, Dr. Sharon Ka-Wai Lee, Dr Zhi-Wei Li, Mr Michael Tsz-Kin Ng, Dr Li-Jia Chen, Dr. Huan-Ming Liu, Dr Li Xu, Dr Xin Zhang, Dr Xiao-Ying Liang, Dr Shu Liu, Ms Nancy Lan Liu, Dr Ye Chong, Ms Yu-Qian Zheng and Dr Yu-Fei Teng for their helpfulness and friendship.

Finally, I would like to give my special thanks and love to my parents, elder brother and sister, and my girl friend Qin Xiao. They always stand beside me and offer their hands during my lengthy study period.

Table of Contents

List of Tables

List of Figures

Abbreviations

Nucleotides

A	Adenine
C	Cytosine
G	Guanine
T	Thymine

Amino acids

Ala A	Alanine
Arg R	Arginine
Asn N	Asparagine
Asp D	Aspartic acid
Cyc C	Cysteine
Gln Q	Glutamine
Glu E	Glutamic acid
Gly G	Glycine
His H	Histidine
Ile I	Isoleucine
Lys K	Lysine
Met M	Methionine
Phe F	Phenylalanine
Pro P	Proline
Ser S	Serine
Thr T	Threonine
Trp Q	Tryptophan
Tyr Y	Tryosine
Val V	Valine
Ter X	Stop codon

General

ATF6	Transcription factor 6
AD	Autosomal dominant
ADCC	Autosomal dominant congenital cataract
Bip	Binding immunoglobulin protein
Bp	Base pair
BSA	Bovine serum albumin
β-ME	β-mercaptoethanol
CC	Congenital cataract
CHOP	C/EBP-homologous protein
CRYAA	αA-crystallin
CRYAB	αB-crystallin
CRYBA1	βA1-crystallin
CRYBA2	βA2-crystallin
CRYBA3	βA3-crystallin
CRYBA4	βA4-crystallin
CRYBB1	βB1-crystallin
CRYBB2	βB2-crystallin
CRYBB3	βB3-crystallin
CRYGA	γA-crystallin
CRYGB	γB-crystallin
CRYGC	γC-crystallin
CRYGD	γD-crystallin
CRYGE	γE-crystallin
CRYGF	γF-crystallin
CRYGS	γS-crystallin
DAPI	4',6-diamidino-2-phenylindole
DMSO	Dimethylsulphoxide
DNA	Deoxyribonucleic acids
dNTPs	Deoxyribonucleotides

DTT	DL-dithiothreitol
ER	Endoplasmic reticulum
ERAD	ER-associated degradation
ECL	Enhanced chemiluminescence
EGTA	Ethylene Glycol Tetraacetic Acid
FBS	Fetal bovine serum
GAPDH	Glyceraldehyde phosphate dehydrogenase
GA	Golgi apparatus
Hsp70	Heat shock protein 70
IMP	Inner mitochondrial membrane potential
IRE1	Inositol requirement 1
JNK	c-Jun amino terminal kinase
Kb	Kilobase
MEM	Eagle's minimum essential medium
Ml	Milliliter (10^{-3}L)
mM	Milliliter (10^{-3}M)
mm	Millimeter
MYOC	myocilin
MW	Molecular weight
PACG	Primary angle closure glaucoma
PBA	Sodium 4-phenylbutyrate
PBS	Phosphate buffer solution
PCR	Polymerase chain reaction
PDI	Protein disulfide isomerase
PERK	Double-stranded RNA-activated protein kinase-like ER kinase
pI	Isoelectric point
POAG	Primary open-angle glaucoma
PMSF	Phenylmethyl sulfonylfluoride
QC	Quality control
RIPA	Radioimmunoprecipitation
RNA	Ribonucleic acid

SDS	Sodium dedecylsulfate
TMAO	Trimethylamine N-oxide
TUDCA	Tauroursodeoxycholic acid
Tx	Triton X-100
TEMED	N,N,N',N'-tetramethyl ethylenediamine
µl	Microliter (10^{-6} L)
µM	Microliter (10^{-6} M)
UPP	Ubiquitin-proteasome pathway
UPR	Unfolded protein responses
WT	Wild-type

Publications

1. Publications based on the work of this thesis

1.1 Research papers

1.1.1 **Gong B**, Zhang LY, Lam DS, Pang CP, Yam GH. Sodium 4-phenylbutyrate corrects the mutant phenotype of a structural protein: gammaD-crystallin. *Mol Vis.* 2010 Jun 4; 16: 997-1003.

1.1.2 Yam GH, **Gong B**, Jia LY, Fan L, Lam DS, Pang CP. Chemical chaperones correct mutant phenotype of myocilin-a potential treatment for glaucoma. Manuscript preparation.

1.1.3 **Gong B,** Zhang LY, Lam DS, Pang CP, Yam GH. Trimethyamine N-oxide alleviated the severe aggregation and ER stress caused by G98R A-crystallin. *Mol Vis.* 2009 Dec 19; 15: 2829-40.

1.1.4 Zhang LY, **Gong B,** Tong JP, Fan DS, Chiang SW, Lou D, Lam DS, Yam GH, Pang CP. A novel gammaD-crystallin mutation causes mild changes in protein properties but leads to congenital coralliform cataract. *Mol Vis.* 2009 Aug 6;15:1521-9.

1.1.5 Jia LY, **Gong B,** Pang CP, Huang Y, Lam DS, Wang N, Yam GH. Correction of the disease phenotype of myocilin-causing glaucoma by a natural osmolyte. *Invest Ophthalmol Vis Sci.* 2009 Aug;50(8):3743-9.

1.2 Conference papers

1.2.1 **Gong B,** Zhang LY, Lam DS, Pang CP, Yam GH. Chemical chaperones reduced aggregate formation of cataract-causing Gly98Arg alpha-crystallin. The Association for research in Vision and Ophthalmology, *Fort Lauderdale, Florida, USA*, May 3-7, 2009.

1.2.2 **Gong B,** Chu KY, Choy KW, Lam DS, Pang CP, Yam GH. Cataract-causing mutant alpha-crystallin altered the cellular response to oxidative stress. The XVIII International Congress of Eye Research, *Beijing, China*, Sep. 23-29, 2008.

2. Publications indirectly related or independent of the work of this thesis

2.1 Chan CK, Cheng AC, Leung CK, Cheung CY, Yung AY, **Gong B**, Lam DS. Quantitative assessment of optic nerve head morphology and retinal nerve fibre layer in non-arteritic anterior ischaemic optic neuropathy with optical coherence tomography and

confocal scanning laser ophthalmoloscopy. *Br J Ophthalmol.* 2009 Jun;93(6):731-5.

2.2 Liu M, **Gong B**, Qi Z. Comparison of the endogenous IK currents in rat hippocampal neurons and cloned Kv2.1 channels in CHO cells. *Cell Biol Int.* 2008 Dec;32(12):1514-20.

2.3 **Gong B**, Liu M, Qi Z. Membrane potential dependent duration of action potentials in cultured rat hippocampal neurons. *Cell Mol Neurobiol.* 2008 Jan;28(1):49-56.

1 General introduction

1.1 Protein biosynthesis

The protein building process in a cell is a multi-step process, beginning from amino acid synthesis/turnover to transcription of nuclear DNA to messenger RNA (mRNA), nucleocytoplasmic transport of mRNA, followed by translation (reading of mRNA and peptide synthesis) in the ribosomal complex. Once the pre-protein (usually with signal pepide in the N-terminus) is made, it is a target of post-translational modifications such that the mature protein is natively folded and functionally active.

1.1.1 Peptide synthesis

Peptide synthesis (translation) takes place in the ribosomal complex located on the cytosolic side of the endoplasmic reticulum (ER). The genetic information is carried by the nucleotide sequence of the mRNAs. They interact with the ribosomal complex, which contains one small and one large subunit, ribosomal RNA (rRNA) and proteins and ligases. In translation, mRNA is decoded according to the reading specified by the trinucleotide genetic code (codon) and serves as a template to guide the synthesis of amino acid chain. This is assisted by a succession of transfer RNA (tRNA) molecules charged with different amino acids through the base-pairing between codons (on mRNA) and anti-codons (on tRNAs). The amino acids are then linked together and extend to growing peptide chain. Altogher, translation proceeds in four phases: activation (charging of tRNA with appropriate amino acid), initiation (attachment of mRNA to ribosomal complex and reading of "START/FMet" codon, elongation (tRNA-amino acid by pairing

between codon and anticodon to growing peptide chain) and termination (reading of "STOP" codon to end the peptide synthesis).

Translation has an infidelity rate estimated at 1 amino acid out of 10^3-10^4 amino acids synthesize (Cochella and Green, 2005). Errors are caused by misacylation leading to tRNA loaded with inappropriate amino acid (Lee et al., 2006), selection of an incorrect tRNA during elongation process (Jakubowski and Goldman, 1992), incorrect selection of start codon, frame shifting, or incorrect termination.

In general, cells synthesize proteins that stay or function in the cytosolic region, nucleus mitochondria, lysosomes, peroxisomes, cell membrane and so on as well as being secretory to the extracellular space. Membrane-bound ribosomes synthesize polypeptides destined to the secretory and endocytic compartments (endoplasmic reticulum ER, Golgi apparatus, endosomes and lysosomes), to the plasma membrane.

1.1.2 Post-translational modifications

During peptide synthesis on the ribosomal complex, the growing peptide is co-translational translocated into the luminal region of the ER, through a signal peptide directed process. Once the peptide enters the ER, it is surrounded by various ER resident proteins, including molecular chaperones, foldases, and so on for the post-translational modifications, folding and protein assembly. Peptides are folded due to the inherent amino acid sequence and to assume a final native conformation, which we usually refer to the sequences of secondary, tertiary or higher structures. The folding processes

including formation of disulfide bond between cysteine molecules, or attachment of various side-chains, like during acetylation, phosphorylation, glycosylation and so on.

1.1.2.1 Phosphorylation

Reversible phosphorylation is one of the most important and well-studied post-translational modifications. Most commonly occurring on threonine, serine and tyrosine residues, phosphorylation plays critical roles in the regulation of many cellular processes, including cell cycle, growth, apoptosis and differentiation. Phosphorylation can have profound effects on regulating the function of the client protein (Johnson and Lewis, 2001). The phosphoryl group with a p*K*a of ~6.7 is likely to be predominantly dianionic at physiological pH. The property of a double negative charge (a property not carried by any of the naturally occurring amino acids) and the capacity for the phosphoryl oxygens to form hydrogen-bond networks confer special characteristics. Phosphorylation can activate enzyme activity through allosteric conformational changes, as observed for glycogen phosphorylase (Johnson and Barford, 1993) and many protein kinases that rely on phosphorylation by upstream kinases for activity (Russo et al., 1996). Phosphorylation can inhibit enzyme activity, as observed in isocitrate dehydrogenase, where the phosphate group acts as a steric blocking agent and does not promote any conformational change (Hurley et al., 1990), and in CDK2, where phosphorylation on Tyr15 impedes protein substrate recognition (Welburn et al., 2007). Phosphorylation can lead to recognition sites for other protein molecules, such as in the phosphotyrosine recognition SH2 domains important for regulation of kinases such as Src, ZAP70 (ζ -chain-associated protein kinase of 70 kDa), Fes and Abl protein. Recent results have shown how recognition of a

phosphotyrosine residue by the SH2 domain in Fes is coupled to substrate recognition through co-operative SH2-kinase-substrate interactions (Dube and Bertozzi, 2005).

1.1.2.2 N-linked glycosylaton

Another important and common post-translational modification of proteins is glycosylation, the covalent attachment of oligosaccharides. Carbohydrates in the form of asparagine-linked (N-linked) or serine/threonine-linked (O-linked) oligosaccharides are major structural components of many cell surface and secretory proteins. This addition and subsequent processing of carbohydrates (*glycosylation*) is the principal chemical modification to most proteins. Some glycosylation reactions occur in the lumen of the ER; others, in the lumina of the *cis-*, *medial-*, or *trans*-Golgi cisternae. Thus, the presence of certain carbohydrate residues on proteins provides useful markers to follow the protein movement along ER-Golgi route.

N-linked glycosylation is initiated by transfer of a core oligosaccharide from a membrane-bound dolichol phosphate anchor to consensus Asn-X-Ser/Thr residues in the polypeptide chain (Freeze, 2007), these protein start at the cytosolic face of the ER by the synthesis of a GlcNAc and mannose (Man) containing glycan chain onto the lipid dolichol phosphate. This chain is then flipped into the lumen of the ER, more Man and glucose (Glu) residues are added and oligosaccharyltransferase moves the finished GlcNAc2Man9Glu3 product onto the appropriate asparagine side chain of proteins. Before the protein is transported from the ER to the Golgi for further glycan processing, three Glu residues and one Man are removed in the complex quality control calnexin-

calreticulin cycle (Hossler et al., 2007). Glycosylation serves several purposes in protein folding. First, due to the hydrophilic nature of carbohydrates, glycosylation increases the solubility of glycoproteins and defines the attachment area for the surface of protein. Second, due to their large hydrated volume, oligosaccharides shield the attachment area from surrounding proteins. Third, oligosaccharides interact with the peptide backbone and stabilize its conformation (Wormald and Dwek, 1999). Lastly, sequential trimming of sugar residues is monitored by a lectin machinery to report on the folding status of the protein (Ellgaard et al., 1999).

1.1.2.3 O-linked glycosylaton

The exact mechanism of O-glycosylation is less established. The main forms of Golgi-derived O-glycans on higher eukaryotic secretory proteins are mucin type glycans and proteoglycans. Both mucins and proteoglycans can form very large sugar structures comprising up to 75% or more of the final molecular weight of the glycoprotein (Takahashi et al., 2001). Mucin synthesis starts in the Golgi apparatus with the addition of an N-acetylgalactosamine (GalNAc) residue to a Ser/Thr side chain. This is followed by formation of one of four distinct core structures by the addition of Gal and GlcNAc residues in various linkages (Freeze, 2007). These core structures serve as the foundation for the synthesis of a large variety of different glycans containing Gal, GlcNAc and NeuAc sugars (Fukuda, 1991). Therefore, these glycoproteins could stabilize the structure of proteins and promote their adequate sorting and quality control, and play crucial roles in cellular processes such as protein sorting, immune recognition, receptor binding, inflammation, and pathogenicity (Freeze, 2007).

In conclusion, there are enzymes removing some amino acids from the leading (N-terminal, amino) end of the peptide chain, giving two smaller peptides linked by disulfide bonding. All proteins before getting out of the ER-Golgi compartments and passing on to the subsequent sites, they must attain a correctly folded (or native) conformation to guarantee the correct folding and burial of every hydrophobic fragment / patch inside the peptide core (Hurtley and Helenius, 1989; Ibba and Soll, 1999; Wickner et al., 1999). As a result, the folding defects can be corrected and proteins are properly folded to a mature, functionally active state for the trafficking to the next intra- or extracellular location.

1.2 Protein quality control system

1.2.1 Protein quality control in the endoplasmic reticulum

In the biosynthesis of most peptides, protein quality control (QC) ensures that only correctly folded proteins exit the ER. Slowly folding or permanently unfolded proteins are retained in the ER and targeted for ER-associated degradation (ERAD) via the ubiquitin-proteasome pathway (Meusser et al., 2005).

The ER provides an optimized environment for protein folding and maturation. The presence of stringent QC system in the ER is essential for different reasons. By preventing the premature exit of folding intermediates and incompletely assembled protein from the ER, it extends the exposure of the substrates to the folding machinery in the ER and thereby improves the chance of correct maturation. This is because the downstream organelles in the secretory pathway do not generally support protein folding

(Mezzacasa and Helenius, 2002). Furthermore, ER QC ensures that proteins are not dispatched to terminal compartments when they are still incompletely folded and therefore potentially damaging the cell. This is well illustrated in the case of ion channels, transporters and receptors that the non-functional or partially function protein do not reach the plasma membrane, where their presence could be toxic to cells (Bichet et al., 2000). QC is also involved in processes such as gene regulation and nutrient storage, and may have extracellular carrier functions for ligands that have to be loaded in the ER before the proteins become secretion-competent (Brown et al., 2002).

1.2.2 ER stress

ER is an organelle that has essential roles in multiple cellular processes that are required for cell survival and normal cellular functions. These processes include intracellular calcium homeostasis, peptide synthesis and processing as well as steroid and lipid biosynthesis (Landry and Gies, 2008). All proteins entering the secretory pathway must pass through the ER. In the ER, proteins fold into their native conformation and undergo a multitude of post-translational modifications, including asparagine-linked glycosylation, and formation of intra and intermolecular disulfide bonds (Fewell et al., 2001). Due to the presence of ER QC, only correctly folded proteins leave the ER and are exported to the Golgi, while incompletely folded peptides are retained inside the ER for further folding opportunity or targeted for degradation, if the misfolding cannot be corrected (Ellgaard et al., 1999). Disruption of proper protein folding processes can be due to various means, such as mutations, altered post-translational modifications, presence of folding-incompetent proteins, hypoxia, or oxidation. These cause the

retention of proteins inside the ER or ER overloading. Hence it induces the ER stress and triggers the unfolded protein responses, following activation of downstream molecules (**Figure 1.1**). There are many metabolic diseases caused by protein accumulation in the ER and they are not prone to degradation. These metabolic disorders are termed as ER storage disease in the super-category of protein folding disorders (Kim and Arvan, 1998).

1.2.3 Unfolded protein responses

During the ER stress, accumulated misfolded or unfolded peptides activate an adaptive signaling cascade and trigger the unfolded protein responses (UPR) (Kozutsumi et al., 1988). Once activated, three ER-localized transmembrane signal transducers are recruited through the machinery involving BiP/GRP78 protein. In normal situation, the cellular BiP/GRP78 is preferentially associated with the signal transducer and silence their activities. However, with the presence of misfolded proteins, BiP/GRP78 is dissociated from its partners and binds preferentially to the exposed hydrophobic patches of the misfolded peptides. The dissociation leads to the activation of partner transducers. They are the protein kinase inositol requiring kinase-1 (IRE1) (Yoshida et al., 2001), double-stranded RNA-activated protein kinase-like ER kinase (PERK) (Harding et al., 2000b) and the transcription factor activating transcription factor 6 (ATF6) (Yoshida et al., 2001).

1.2.3.1 IRE1 activation

IRE1 is the first component of UPR that was identified initially in yeast (Shamu and Walter, 1996). IRE1 pathway regulates chaperone induction, ERAD, and expansion of

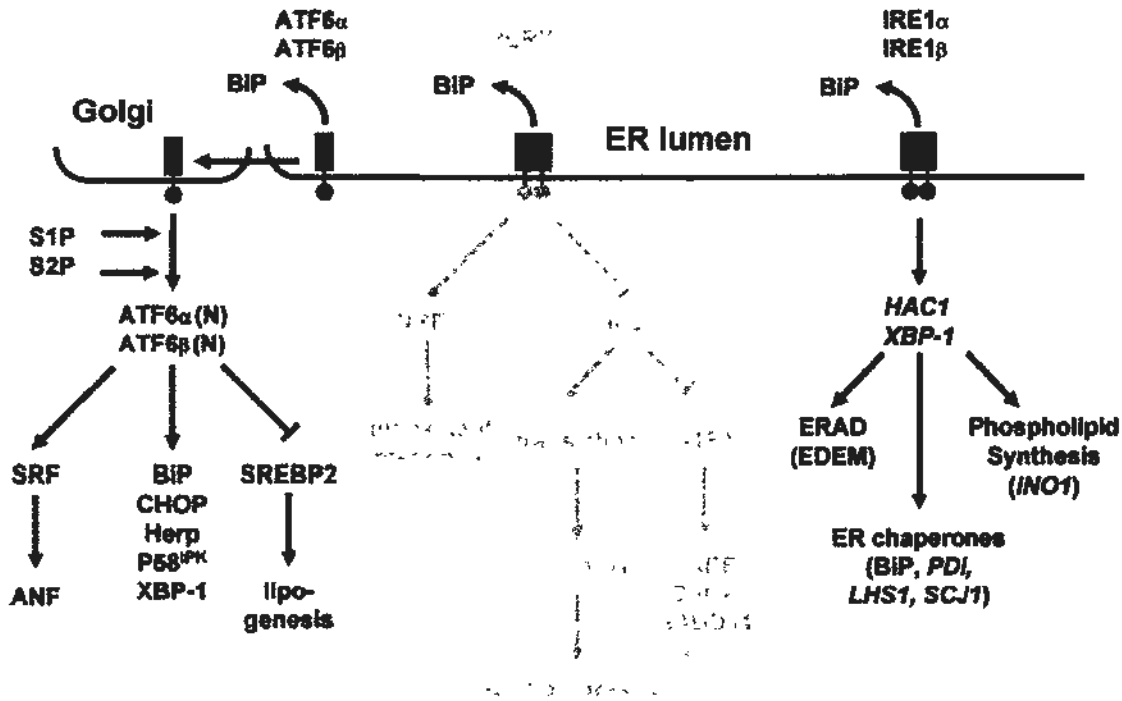

Figure 1.1 Overview of ER stress and unfolded protein response signalings. Normal eukaryotic cells have a stringent regulatory system of recognizing and processing of misfolded proteins. When there are misfolded proteins accumulated in the ER, the ER stress could be induced, which triggers specific responses termed as UPR. BiP, with its role as a central UPR molecule, binds preferentially to the hydrophobic peptide patches exposed on the misfolded protein surface. This causes a dissociation of the native complexes of BiP with PERK, ATF6 and IRE1, which subsequently lead to various signaling. Free PERK, via eIF2 inhibtion, blocks protein translation and causes G2/M cell cycle arrest and apoptosis. Free ATF6 activates CHOP for cell apoptosis. Free IRE1 activates XBP-1 for ERAD and expression of molecular chaperones to alleviate the ER burden (Martin et al., 2005, Review).

the ER lumen in response to the ER stress (**Figure. 1.1**). Further, this pathway is evolutionarily the oldest pathway, since it is present in all eukaryotes, and distinguished by unique features transducing the stress signal. IRE1 encodes an atypical type I transmembrane protein kinase endoribonuclease (Nikawa and Yamashita, 1992), consisting of an ER luminal dimerization domain, and cytosolic kinase and endoribonuclease domains. After dissociation of BiP from the ER luminal domain, IRE1 oligomerizes (Liu et al., 2002) and activates its RNase domain by autophosphorylation (Welihinda and Kaufman, 1996). However, occupancy of the ATP-binding pocket by ADP is sufficient for activation of the RNase domain after oligomerization (Papa et al., 2003). Mutations in the RNase domain of Ire1p abolished activation of an ERP72 CAT reporter construct (Tirasophon et al., 2000). Transient transfection experiments with kinase- and RNase-defective Ire1p indicated that two functional RNase domains were required for signaling by Ire1p (Tirasophon et al., 2000). The substrate for Ire1p endoribonuclease was first identified in yeast and is the mRNA for the bZIP transcription factor *HAC1* (Nikawa et al., 1996). Lastly, ER chaperone genes are activated, such as BiP, PDI, LHS1 and SCJ1.

1.2.3.2 ATF6 release

During the ER stress and dissociation from BiP binding, free ATF6 fragments migrate to the nucleus to activate transcription. ATF6 is an UPR transducer that bind ERSE motifs in the promoter regions of UPR responsive genes (Yoshida et al., 2001). There are two forms of ATF6, ATF6α (90 kDa) and ATF6β (110 kDa, also known as CREB-RP). Both of them require the presence of transcription factor NF-Y to bind to the ERSE (Li et

al., 2000). ATF6α interacts with the transactivation domain of serum response factor (SRF) and antisense ATF6α reduced serum induction of reporter constructs (Zhu et al., 1997). ATF6 forms a heterodimeric complex with the basic helix-loop-helix (bHLH) transcription factor sterol response element (SRE) binding protein 2 (SREBP2). This complex counters the lipogenic effects of SREBP2 by recruiting the histone deacetylase complex 1 (HDAC1) to the SRE to repress transcription (Zeng et al., 2004). In the nucleus, ATF6 interacts with the ER stress DNA element, thereby activating the transcription of different unfolded protein responsive genes, including Bip/GRP78, CHOP and other downstream genes (Li et al., 2000).

1.2.3.3 PERK activation

Similar as IRE1, PERK is a type I transmembrane kinase and is activated by the release of BiP from its ER luminal domain. PERK then oligomerizes and phosphorylates substrate proteins, translation initiation factor 2α (eIF2α) (Shi et al., 1999) and bZIP Cap'n'Collar transcription factor Nrf2 (Figure 1.1). Phosphorylation of eIF2α shuts-off the general protein translation (Harding et al., 1999). *Perk*$^{-/-}$ cells are sensitive to the ER stress and are partially rescued by translation inhibitors, e.g. cycloheximide (Harding et al., 2000a). Short-lived proteins are cleared from the cell during inhibition of translation. In the absence of PERK, eukaryotic cells, e.g. tunicamycin-treated yeast cells, are arrested in G2/M phase dependent on the function of the morphogenesis and pachytene checkpoint kinase Swe1p (Bonilla and Cunningham, 2003). Besides eIF2α, PERK also phosphorylates Nrf2, which contributes to the survival of cells from the ER stress. PERK

is a kinase that phosphorylates a subunit of eIF2α in response to ER stress (Liu et al., 2000). Phosphorylation of eIF2α activates transcription factor ATF4, which turns on the expression of BiP/GRP78 and CHOP, one of the pro-apoptotic factors. The elevation of CHOP results in down-regulation of Bcl-2, the activation of caspases, and finally initiate cell death events (McCullough et al., 2001).

Thus, BiP/GRP78, ATF4, CHOP, and caspase-12 are key proteins and enzymes that are activated by UPR. If this adaptive UPR is not capable to resolve the problem of ER stress, by removing improperly folded proteins, cell death pathways will be activated. Many caspases are recruited and ultimately results in apoptosis. Therefore, BiP and CHOP expression as well as caspase-12 activation in UPR are common cellular basis for many metabolic diseases involving the ER stress.

In human eyes, many ocular disorders are caused by the folding problems of candidate proteins, including cataract formation due to lens crystallin alterations and trabecular meshwork cell changes in myocilin-caused primary open-angle glaucoma. In my study, I employed the mutated G98R CRYAA and D384N MYOC as a model to study the UPR in human lens epithelial cells and human trabecular meshwork cells.

1.2.4 Protein degradation

Protein folding in the oxidizing environment of the ER is an energy requiring process. Under non-stressed conditions, newly synthesized proteins exist as unfolded intermediates along the protein-folding pathway. Once the ER stress is imposed, such as

by the depletion of energy, many folding intermediates become irreversibly trapped in low-energy states and accumulate. These unfolded proteins are retained in the ER through interaction with BiP, calnexin, and calreticulin. Eventually, unfolded or misfolded proteins in the ER lumen are retrotranslocated to the cytoplasm, where they are ubiquitinated and degraded by the proteasomes (Werner et al., 1996). This process is called the ER-associated degradation (ERAD), and is regulated by the UPR. Proteasomal degradation of misfolded proteins in the ER is required to protect from UPR activation. Proteasomal inhibition is sufficient to activate the UPR, which, in turn, induces the transcription of genes encoding components of ERAD (Travers et al., 2000). On the other hand, if the overload of unfolded or misfolded proteins in the ER is not resolved, prolonged UPR activation will lead to programmed cell death.

1.2.4.1 Ubiquitin-proteasome pathway (UPP)

The ubiquitin-proteasome pathway plays an important role in the selective degradation of many proteins, including damaged or non-native proteins. UPP is a major cytosolic proteolytic pathway in eukaryotic cells (Glickman and Ciechanover, 2002). Those substrates to be recognized for degradation are usually linked covalently to small-sized ubiquitin molecules. Attachment of poly-ubiquitin (ubiquitination) occurs through action of three classes of enzymes termed E1, E2, and E3. Normally, E1 exists as one dominant form in cells but E2 and E3 have multiple isoforms (Hegde, 2004). During ubiquitination, ubiquitin is first activated by E1, then passed on E2s and E3s (ubiquitin ligase) sequentially such that the activated polyubiquitin is linked to the substrate. The ubiquitin-associated ligation step is centrally important in determining the selectivity of protein

degradation. The selectivity is mostly determined by the substrate specificity of E3s. This is due to the E3 may select the substrate processed by a particular E2, which binds to specific non-catalytic amino or carboxyl terminal extension. Hence, E2 also contributes to the substrate selectivity for degradation. During ubiquitination, after the first ubiquitin molecule attached to the substrate, the next ubiquitin molecule is attached to an internal Lys residue in the first ubiquitin structure. In this process, a polyubiquitin chain grows on the substrate protein. The polyubiquitinated substrate is then recognized by the proteasome and is degraded to small peptides and amino acids (Hegde, 2004).

Degradation of proteins via UPP is a highly complex, temporally controlled and tightly regulated process that plays crucial roles in the maintenance and regulation of many cellular pathways and processes, including differentiation, proliferation, cell cycling, apoptosis, transcription, signal transduction, antigen processing and presentation, and protein homeostasis and recycling (Naujokat and Hoffmann, 2002). Thus, it is not surprising that aberration and deregulation of UPP could contribute to the pathogenesis of many human diseases, such as cancer, neurodegenerative, autoimmune, genetic and metabolic disorders (Herrmann et al., 2008; Naujokat and Hoffmann, 2002). Consequently, an improved understanding of the mechanisms that underlie the regulation of UPP will lead to the development of diagnostic, therapeutic and preventive strategies in the future. We also draw attention to the recent links between another proteolytic process in the cell called autophagy and the UPP in contributing to ocular diseases. In my project, mutant G98R CRYAA was degraded by UPP after treatment with a natural osmolyte, and the degradation was inhibited by MG132 (a reversible inhibitor to UPP).

1.2.4.2 Autophagy

Autophagy means auto phagos or self eating. During autophagy, portions of cell content are delivered to the lysosomes (in mammals) or vacuole (in plant, fungi) for degradation. Autophagy is, among other degradative pathways, strongly induced at nutrient starvation conditions and leads to bulk degradation of cytoplasmic components (proteins and organelles). This results in a retrieval and recycling of building blocks for further metabolism or energy production and the synthesis of components essential for survival at nutrient starvation conditions (Klionsky, 2005). In cells defective in autophagy, the total intracellular pool of amino acids is strongly reduced, leading to the inability of cells to synthesize proteins that are essential for survival (Onodera and Ohsumi, 2005). Similar results have been observed in Atg22 mutant cells in which autophagy is normally functioning, but amino acid efflux to the cytosol is compromised due to the absence of putative vacuolar amino acid transporter Atg22 (Yang et al., 2006). Autophagy also serves in the functions of cellular housekeeping as it may remove exhausted, redundant or unwanted components. In this way, autophagy acts as an anti-aging mechanism (Bergamini, 2006), supports cell remodeling during development (Levine and Klionsky, 2004) or contributes to the cellular defense against pathogens (Mizushima et al., 2008).

Reflecting the importance of autophagy in maintaining cell vitality, various quality control machineries exist together with mechanisms removing misfolded, exhausted or redundant proteins/organelles, even at the sub-organelle level. The currently known autophagy processes are sub-divided in three pathways: chaperone mediated autophagy

(CMA), macro- and microautophagy. Of these, CMA is as yet only described in mammals and involved in the degradation of single, soluble proteins (Dice, 2007). In contrast, macro- and microautophagy occur in a wide range of eukaryotes including mammals, plants and fungi and lead to the degradation of portions of the cytoplasm, which may include cell organelles (Kundu and Thompson, 2008; Uttenweiler and Mayer, 2008). In my project, I also looked into the autophagy of G98R CRYAA using its specific inhibitor 3-methyladenine, but it was not degraded through this pathway.

1.2.4.3 Lysosome-associated protein degradation

Lysosomes are the major organelles responsible for proteolytic degradation and recycling. They are single or double membrane-bound organelles containing various proteolytic enzymes capable of digesting an array of biological polymers, including proteins, nucleic acids, carbohydrates and lipids (Dice and Terlecky, 1990). They degrade both functional and damaged proteins and organelles. This ensures a continuous renewal and recycling of cellular constituents and avoids the accumulation of warn out components.

1.2.5 ER stress-induced apoptosis

If UPR fails to resolve the celllular defects associated with protein misfolding, the cells will go for apoptosis as a self-suicidal event. In response to the ER stress, apoptosis is signaled through both mitochondria-dependent and/or -independent pathways. The ER serves as a site where apoptosis signals are first generated and integrated to elicit the

death response. Topologically, the ER lumen is equivalent to the extracellular space. Thus, it is not surprising that ER stress activates a combination of intrinsic and extrinsic apoptotic pathways. Thea intrinsic pathway responds to intracellular insults, e.g. DNA damage, and an extrinsic pathway responds to extracellular stimuli (**Figure 1.2**), which is triggered by self-association of cell surface receptors, recruitment of caspases, mainly caspase-8, and initiation of a caspase cascade. Here several mechanisms include PERK/eIF2-dependent transcriptional induction of the pro-apoptotic transcription factor CHOP, Bak/Bax-regulated Ca^{2+} release from the ER, IRE1-mediated activation of ASK1 (apoptosis signal-regulating kinase-1)/JNK (c-Jun amino terminal kinase) and activation of pro-caspase 12 (ER stress-induced caspase-dependent apoptosis) (Malhotra and Kaufman, 2007). Activated IRE-1 recruits Jun N-terminal inhibitory kinase (JIK) to activate apoptosis-signaling kinase 1, which in turn activates the c-jun N-terminal kinase (JNK) pathway (Lee et al., 2002). This activates mitochondria/Apaf1-dependent caspases. Procaspase-12 is an ER-associated proximal effector of apoptosis. Activated caspase-12 cleaves the pro-caspase-9 to become active, which further turns on caspase-3, leading to apoptosis (Mandic et al., 2003).

It is known that oxidative stress is a significant contributing factor to ER stress-induced apoptosis (Jiang et al., 2009). Many pathologies, including eye diseases, are found associated with ER stress-induced apoptosis (Carbone et al., 2009; Mulhern et al., 2007; Raguenez et al., 2009). In my study, a glaucoma-causing mutation (D384N) of myocilin caused trabecular meshwork cell apoptosis through the induction of ER stress (Jia et al., 2009a). Also, the cataract-causing G98R CRYAA expression activated ER stress and the lens epithelial B3 cells were prone to apoptosis (Gong et al., 2009).

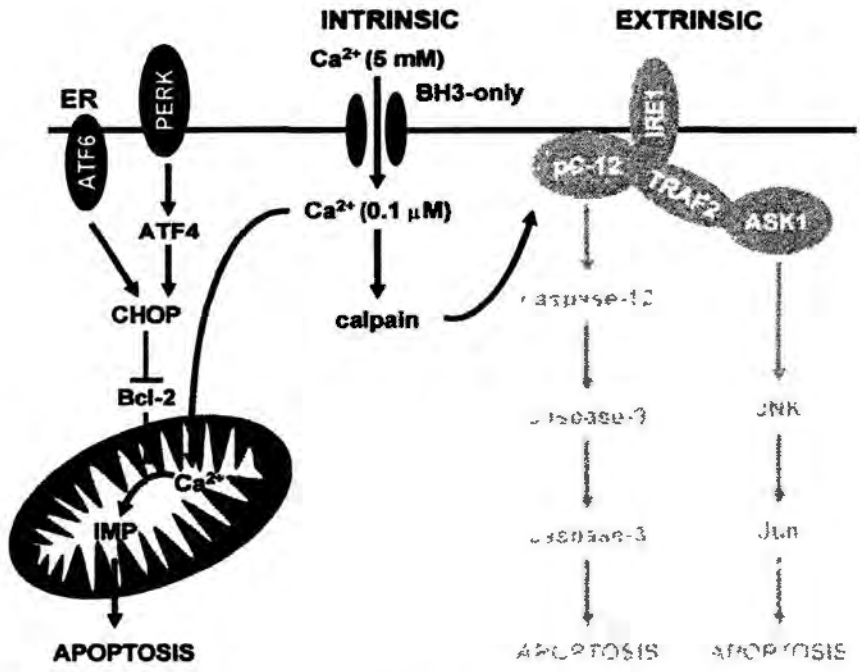

Figure 1.2 Apoptosis pathways regulated by ER stress and unfoled protein response. Two major pathways control apoptosis- an intrinsic pathway resonding to intracellular insults, and an extrinsic pathway responding to extracellular stimuli (Martin, 2005).

1.3 Protein folding disease

1.3.1 Protein folding and misfolding

Protein folding is a process by which a polypeptide folds into its characteristic and functional three-dimensional structure from random coil. The folding of the translated linear strand of amino acids into a fully functional three-dimensional protein is one of the most complex challenges facing the cellular protein factory (Dobson, 2003). The ER could provide an optimized environment for protein folding. Folding occurs very rapidly, probably within milliseconds of production of the string of amino acids, and results in 3-D conformations which usually are quite stable, with specific biological functions (Yang and Gruebele, 2003).

Each linear chain of amino acids translated from mRNA exists as an unfolded polypeptide or random coil. It lacks any developed three-dimensional structure, which is determined by the inherent amino acid sequence. During folding, amino acids interact with each other to produce a characteristic three dimensional structure, known as the native state (Stevens and Argon, 1999).

The folding of proteins thus facilitates the production of discrete functional entities, including enzymes and structural proteins, which allow the various processes associated with life to occur. Importantly, folding not only allows the production of structures which can perform particular functions in the cellular milieu, but also it prevents inappropriate interactions between proteins, in that folding hides elements of the amino acid sequence which if exposed would react non-specifically with other proteins (Leandro and Gomes,

2008). Restriction of interactions to those which are necessary and desirable for life is crucial in the intracellular environment where many thousands of proteins are present and required to perform precisely specified functions. Evolutionary pressure thus has favored those proteins which fold in such a way that appropriate reactive elements are exposed and unwanted reactivities are hidden.

1.3.1.1 Principles of protein folding

For any given protein, the number of possible conformations, as defined by the number of native and total interactions of its residues, is determined by its amino acid sequence. Each conformation has a certain free energy. Plotting of all free energies versus their corresponding conformations yields a distinctive energy surface or landscape for the protein. On this energy landscape, the protein folds along several competing pathways leading to conformations with ever decreasing free energies until a transition state is crossed (Dobson and Ellis, 1998). Folding stops when the conformation with the lowest free energy is reached. In many cases, this conformation is identical to the native conformation of the protein (Chan and Dill, 1998). Thus, the primary amino acid sequence of a protein is the major determinant for the folding of protein, a phenomenon first summarized in Anfinsen's dogma (Leandro and Gomes, 2008). Kinetically, protein folding is initiated by a hydrophobic collapse, in which several hydrophobic side chains shield each other from surrounding water (Stevens and Argon, 1999). Burial of electrostatic interactions, such as salt bridges or hydrogen bonds, in the hydrophobic core limits the number of possible conformations for the folding protein, and is a major determinant in the folding pathway (Stevens and Argon, 1999). Individual structures, e.g.

α-helices or β-turns fold within 0.1-1 μsec (Snow et al., 2002). Small proteins fold in less than 50 μsec (Yang and Gruebele, 2003) without significantly populating intermediate states (Dobson, 2003). Compared to the rate of protein folding, translation of mRNAs is slow and proceeds at ≈4-6 amino acid residues/sec (Mayor et al., 2003). To form secondary and tertiary structural elements in which residues far apart in the amino acid sequence, e.g. β-sheets or disulfide bonds, the preceding residues must be maintained in a folding competent state until the interacting partners are added to the polypeptide chain. This problem is exacerbated by the high protein concentration *in vivo*. For example, the protein concentration in the ER is ≈100 g/L (≈2 mM), and even the assembly of IgG heavy and light chains, whose concentration in the ER of an antibody secreting plasma cell is ≈4-6 μM, can in principle be a diffusion controlled process (Stevens and Argon, 1999). Thus, it is necessary to shield folding proteins displaying hydrophobic patches on their surface from inadvertently colliding and interacting with other maturing and mature proteins.

1.3.1.2 Protein folding in the ER

The ER differs significantly from the cytosol topologically, in its chemical composition, and in its protein folding machinery. All these differences can significantly affect protein folding in the ER. The ER is a membrane bound compartment, and its luminal space is topologically equivalent to the extracellular space. Proteins destined for the ER are directed to the ER through a predominantly hydrophobic signal sequence and have to, either co- or post-translationally, traverse the ER membrane through the Sec61p complex (Walter and Johnson, 1994). The presence and timing of cotranslocational signal

sequence cleavage with folding of the polypeptide chain affects the folding pathway. As in the cytosol, the pH in the ER is near neutral. In mammalian cells, the ER is the major site for Ca^{2+} storage. ER luminal Ca^{2+} concentrations reach ~5 mM, compared to 0.1 μM in the cytosol (Orrenius et al., 2003). ER luminal Ca^{2+} concentrations rapidly and frequently fluctuate as the ER's Ca^{2+} pool is mobilized during intracellular signaling (Webb and Miller, 2003). Ca^{2+} can participate in electrostatic interactions in proteins and through these alters the hydrophobic interactions. Thus, the effect of fluctuations in the ER's Ca^{2+} pool on protein folding depends on the protein. More importantly, the majority of the ER-resident molecular chaperones and foldases are vigorous Ca^{2+} binding proteins. Perturbation of the ER's Ca^{2+} pool affects their folding, activity, and interactions with other chaperones.

1.3.1.3 Protein folding machinery

The protein folding machinery of the ER consists of three classes of proteins: foldases, molecular chaperones, and the lectins calnexin, calreticulin, and EDEM. Foldases are enzymes that catalyze steps in protein folding to increase their rate. Prominent examples are *cis-trans* peptidyl-prolyl isomerases (PPI/immunophilins), which catalyze the *cis-trans* isomerization of peptidyl-prolyl bonds and PDIs. Molecular chaperones facilitate protein folding by shielding the unfolded regions from surrounding proteins. They do not enhance the rate of protein folding. According to their cytosolic counterparts, they are classified into several groups: class HSP70 chaperones in the ER are BiP/GRP78/Kar2p, Lhs1p (Cer1p/Ssi1p) (Oda et al., 2003), and GRP170 (Lin et al., 1993). BiP also participates in the translocation of nascent polypeptide chains into the ER. HSP90 class

chaperone GRP94/endoplasmin recognizes a subset of peptide substrates, in a manner coordinated with other chaperones, e.g. BiP (Melnick et al., 1994), and facilitates the display of immunogenic peptides on MHC class I complexes (Argon and Simen, 1999). In addition, PDI has disulfide-dependent and -independent chaperone activity (Tsai et al., 2001). Preferential interaction of unfolded proteins with the ER-resident molecular chaperones constitutes the second arm of the quality-control machinery in the ER.

1.3.1.4 Protein misfolding

However, some unmodified proteins could not fold properly and function normally, leading to misfolded protein problem. These incompletely folded proteins have exposed hydrophobic residues and are prone to self-aggregation and inappropriate interaction with other molecules within the crowded cellular environment. Ultimately, this leads to malfunctioning of living systems and protein imbalance.

The disorder in proteins is the precise manner in which natively soluble proteins of distinct primary structure undergo partial unfolding and aberrant refolding to produce highly stable oligomers and polymers with novel properties. It is clear that supraphysiological concentrations, coupled with prolonged time and certain biochemical conditions, underlie the initiation of oligomerizaton process. One instructive example that has been studied in some detail is lysozyme, a protein that causes a fatal systemic amyloidosis only when it bears one of two inherited missense mutations, I56Q or D67H. Crystallography of the wild-type and mutant variants revealed subtle but structurally significant changes at the interface between the α- and β-domains and this suggests that

this region is less constrained in both mutants (Booth et al., 1997). In agreement, circular-dichroism studies during conditions of heat denaturation that lead to fibril formation showed that both mutants were less thermostable. Moreover, near the midpoint of the heat-driven unfolding process, the mutants formed partly folded intermediates with considerable helical structure but no persistent tertiary interactions (Booth et al., 1997). Wild-type lysozyme unfolds into a partly structured intermediate only when thermal denaturation is performed at very low pH (Haezebrouck et al., 1995).

Nowadays, there are a number of diseases sharing a common aspect in that they all appear to involve inappropriate folding of a particular protein. These diseases are sometimes lumped together under the heading of the protein folding diseases resulted from misfolded proteins.

1.3.2 Protein folding diseases

It has become increasingly apparent that there are a number of diseases, sharing a common cause of perturbation of protein folding, but they have different symptoms and aetiologies. In many cases, misfolded proteins are recognized to be undesirable and consequently directed to protein degradation machinery in the cell. Hence many protein misfolding diseases are characterized by absence of a key protein, as it has been recognized as dysfunctional and eliminated by the cell's own machinery. Diseases caused by lack of a functioning protein, due to its degradation as a consequence of misfolding, include cystic fibrosis (misfolded CFTR protein) (Thomas et al., 1995) and Marfan syndrome (misfolded fibrillin) (Whiteman et al., 2006). Other than that, many protein

folding diseases are characterized by it's the protein deposition in insoluble aggregates. Diseases caused by protein aggregation include Alzheimer's disease (deposits of amyloid beta and tau), type II diabetes (deposits of amylase), Parkinson's disease (deposits of alpha synuclein) and so on (Dobson, 2001; Horwich, 2002; Kelly, 1998).

Protein misfolding appears at least in some cases to be due to mutations (missing or incorrect amino acids) which destabilize the encoded protein products and they are more likely to fold incorrectly.

In conclusion, the manner in which a newly synthesized chain of amino acids transforms itself into a perfectly folded protein depends both on the intrinsic properties of the amino acid sequence and on the multiple contributing influences from the crowded cellular milieu. Folding and unfolding are crucial ways of regulating biological activity and targeting proteins to different cellular locations. In addition, processes as apparently diverse as translocation across membranes, trafficking, secretion, immune response and regulation of cell cycle are directly dependent on folding and unfolding events (Radford and Dobson, 1999). Failure to fold correctly, or to remain correctly folded, will therefore give rise to deleterious living systems and hence to diseases (Dobson, 2001; Horwich, 2002; Thomas et al., 1995). Therefore, accumulation of misfolded proteins that escape the cellular quality-control mechanisms is a common feature of a wide range of highly debilitating and increasingly prevalent diseases.

1.3.3 Protein folding diseases in the eye

The accumulation of unfolded or misfolded proteins leading to pathology takes place in a wide variety of organs and tissues, also including different parts of the eye. So far, the best studied ocular protein folding diseases are cataract in the lens and retinitis pigmentosa in the retina, but accumulation of misfolded proteins also occurs in other parts of the eye causing various disorders, i.e. in the lens, cornea, retina, vitreous, conjunctiva, optic nerve, and so on. As the complicated structure of eye, any disturbance could cause eye diseases and lead to blindness. Furthermore, protein deposition in eye tissues may take place as a result of (a) systemic amyloidosis, (b) presence of naturally unfolded proteins and (c) mutations or post-translational modifications of proteins that become prone to aggregation as a result of such modifications.

1.3.3.1 Lens

The lens is a transparent, biconvex structure that, along with the cornea, helps to refract light to be focused on the retina (**Figure 3.1**). Cataract is the opacity of lens due to the accumulation of protein aggregate formation that obstructs the passage of light through the lens, thereby blocking light from reaching the photoreceptors (**Figure 3.1**). Protein folding diseases in the lens became known earlier than that in other eye tissues (Harding, 1972), because cataract formation can be monitored in real time by non-invasive, highly sensitive optical techniques. The major protein component of lens aggregation is α-crystallin and βγ-crystallins (Chen et al., 1997). Their post-translational modifications play a major role in cataractogenesis (Ecroyd and Carver, 2009; Meehan et al., 2004; Zhang et al., 2008). Mutations in crystallin genes are also associated with

cataract development (Graw, 1999; Graw, 2004; Graw, 2009; Jung et al., 2009). For example, some mutations in γ-crystallin gene cause the formation of large amyloid-like intranuclear inclusions containing the altered γ-crystallins leading to cataract (Graw, 2009). Aggregation and deposition of other misfolded proteins (both wild type and mutant) in the lens also cause cataract. For example, the transgenic mice expressing mutant intermediate filament protein vimentin had aggregate and accumulation of vimentin inclusions in the lens, and cataract development (Bornheim et al., 2008). In a knock-in mouse model, alphaA-crystallin R49C mutation influenced the architecture of lens fiber cell membranes and enhanced protein insolubility, resulting in posterior and nuclear cataract formation (Andley, 2009; Xi et al., 2008). In our work on G98R CRYAA, which is identified to cause presenile nuclear cataract, we observed aggregate formation in the transfected lens epithelial B3 cells.

1.3.3.2 Trabecular meshwork and optic nerve

In trabecular meshwork (TM) cells, myocilin (MYOC) protein is expressed but with unidentified function in the eye. Mutations of myocilin gene account for up to 35% of juvenile-onset and approximately 4% of adult-onset primary open-angle glaucoma (POAG) (Fingert et al., 2002; Yam et al., 2007b). Currently, more than 90 myocilin mutations have been identified among patients with POAG (Human Gene Mutation Database http://www.hgmd.cf.ac.uk/ac/gene.php?gene=MYOC). Various glaucoma-associated myocilin mutants are misfolded and are retained inside cells by the protein quality control recognizing non-native conformers. They are converted into detergent insoluble intracellular aggregates blocking the secretion (Gould et al., 2006; Jacobson et

al., 2001; Yam et al., 2007b). Hence, myocilin-associated glaucoma may be considered as a protein folding disease (Aroca-Aguilar et al., 2008; Carbone et al., 2009; Jia et al., 2009a; Liu and Vollrath, 2004).

1.3.3.3 Retina

Protein aggregation and deposition in the retina leading to retinal dystrophies often occur due to mutations in the retinal genes, post-translational modifications of retinal proteins or due to the presence of aggregation prone naturally unfolded proteins. Several retinal dystrophy genes have mutations that make the proteins misfold and become aggregation prone with subsequent loss of normal protein function. One of the mechanisms of retinitis pigmentosa (RP) is caused by the accumulation of mutated rhodopsin protein. More than 140 mutations in rhodopsin causative for RP have been described (http://www.sph.uth.tmc.edu/RetNet). Misfolding of rhodopsin in the transmembrane, intradiscal and cytoplasmic domains has been known to cause RP (Kaushal and Khorana, 1994; Roof et al., 1994; Sung et al., 1993). And also, age-related macular degeneration (AMD) is a late-onset, neurodegenerative retinal disease that shares several clinical and pathological features with Alzheimer's disease, including extracellular deposits containing amyloid-beta (Aβ) peptides, apoE protein, complement and other components. A pathogenic role for amyloid in AMD has been demonstrated (Yoshida et al., 2005) and further proven by detecting of non-fibrillar oligomeric Aβ in the drusen of AMD eyes (Ding et al., 2008; Luibl et al., 2006; Yoshida et al., 2005).

1.3.3.4 Cornea, vitreous and ciliary body

Similar to the lens, cornea is transparent for light transmission. Accumulation of damaged or denatured proteins is detrimental for corneal function because such species can lead to corneal cloudiness and increased light scattering. Such proteins are amyloid-P component, gelsolin (Kivela et al., 1994), lactoferrin (Araki-Sasaki et al., 2005), keratoepithelin (βig-h3 or TGFBIp) (Tai et al., 2009)in cornea-specific deposition diseases.

Vitreoretinal amyloidosis is usually associated with mutations in genes encoding amyloid precursor protein transthyretin (TTR) and found as part of the familial amyloidotic polyneuropathy (FAP) syndrome. FAP comprises of a genetically heterogeneous group of disorders characterized by amyloid deposition in different organs, including in eye tissues. Currently, more than 80 TTR mutations have been described (R.B. Bhisitkul and 1037 (Eds.)). As an example, vitreous opacities requiring vitrectomy were revealed in patients with FAP due to Ile84Ser substitution in the TTR protein (Zolyomi et al., 1998).

Deposition of amyloid and its precursors in the perineurium of ciliary nerves and the walls of ciliary vessels has been described in patients with familial amyloidosis, Finnish (FAF; Meretoja' s syndrome). The deposits can be revealed by Congo red staining, use of antisera to amyloid-P component and gelsolin Asn-187 fragment (Kivela et al., 1994).

1.4 Prospectives of corrections against misfolded proteins

Protein misfolding and aggregation is implicated in an increasing number of human conformational diseases including eye disorders. Since protein misfolding is the structural rearrangement within a protein that transform it into a pathological species, the corrections of such disorders may be based on the approaches that prevent the formation of the pathological conformation or destroy it.

1.4.1 Principles for correcting protein folding

Native state of protein always corresponds to the structure that is the most thermodynamically stable under physiological conditions. *In vitro*, many unfolded proteins are able to fold to their native conformations spontaneously. Most proteins in the cell adopt a compact, globular fold that determines their stability and function. Partial protein unfolding under conditions of cellular stress results in the exposure of hydrophobic regions normally buried in the interior of the native structure. Interactions involving the exposed hydrophobic surfaces of misfolded protein conformers lead to the formation of toxic aggregates, including oligomers, protofibrils and amyloid fibrils.

For the native protein, each conformation has a certain free energy. Plotting of all free energies versus their corresponding conformations yields a distinctive energy surface or landscape for the protein. On this energy landscape, the protein folds along several competing pathways leading to conformations with ever decreasing free energies until a transition state is crossed (Dobson and Ellis, 1998). Folding stops when the conformation with the lowest free energy is reached. In many cases this structure is identical to the

native conformation of the protein (Chan and Dill, 1998). Thus, the primary amino acid sequence of a protein is the major determinant for the folding of a protein. Kinetically, protein folding is initiated by a hydrophobic collapse, in which several hydrophobic side chains shield each other from surrounding water (Stevens and Argon, 1999). Thus, it is necessary to shield folding proteins displaying hydrophobic patches on their surface from inadvertently colliding and interacting with other maturing and mature proteins. For example, most small molecules are thought to have a general role in the folding of newly synthesized polypeptides *in vivo*, they could bind transiently to small hydrophobic regions exposed on unstructured nascent chains and thus decrease the free energy between polypeptides, change the charges on protein surface and stablize the misfolded proteins, to prevent aggregation and premature folding as elongation proceeds. Aggregation in the newly synthesized proteins is a high-order process that is greatly favoured by increases in protein concentration and temperature, because it is driven by the interaction of hydrophobic regions that are transiently exposed on the surface of partially folded intermediate states, causing identical chains close together to form aggregation. Application of these small molecules to reduce hydrophobic regions on the misfolded protein thus could rescue the protein misfolding and reduce protein aggregation.

1.4.2 Potential corrections against protein folding diseases

A significant number of human disorders (e.g. Alzheimer's disease, Parkinson's disease, Huntington's disease, amyotrophic lateral sclerosis and type II diabetes) are characterized by protein misfolding and aggregation. Generally, there are several novel

and promising therapeutic strategies targeting these protein folding diseases: firstly, inhibiting protein aggregation with peptides or small molecules identified via structure-based drug design or high-throughput screening; second, interfering with post-translational modifications that stimulate protein misfolding and aggregation; and lastly, upregulating molecular chaperones or aggregate clearance mechanisms.

So, in summary, although the concept of protein misfolding as a factor in the causation of many diseases may one day lead to a new class of therapeutics, the chaperones, nevertheless the search for cures for highly complex diseases such as Alzheimer's will not be easy, therefore, we can look forward to a no folds barred struggle between medical research and misfolded proteins, and also, we would expect to see some significant pharmaceutical activity for cures in this field.

1.4.3 Potential corrections against protein folding diseases in the eye

The advantage of the eye for the development of such treatment is that several ocular tissues are readily accessible for topical delivery of therapeutics such as lens or cornea. To achieve these goals several therapeutic strategies can be used. There are several potential approaches in the corrections of protein folding diseases in the eye.

1.4.3.1 Small chemicals with chaperone activities

Many endogenous molecules are now known to participate in different cellular functions. They assist protein folding, stabilize proteins under stress conditions and

maintain polypeptide chain components in a loosely folded state for translocation across membranes (Hartl, 1996). Regulated expression of these endogenous molecules is a cellular defense against misfolded proteins and this machinery monitoring and regulating protein folding and quality control are parts of a more general proteostasis network (Balch et al., 2008; Powers et al., 2009). Thus, the cellular defense could be regulated through the expression of molecular chaperones in cells by expressing transgenic chaperones (or their peptide fragments) in order to suppress the misfolding of pathogenic proteins. This can also induce special endogenous chaperones (such as up-regulation of small Hsp70) by administration of low molecular weight substances and using inhibitors of pathological chaperones. Many paper have reported that cellular defense could be fulfilled by molecular chaperones dedicated to facilitate the efficient folding and reverse the unfolding (Bukau et al., 2006; Chapple and Cheetham, 2003; Chapple et al., 2001; Ellis, 2001a; Ellis, 2001b; Kosmaoglou et al., 2008). These chaperones bind to aggregation-prone regions of proteins, for example the hydrophobic stretches or cystein residues, and change the local conformation of the polypeptide in a way that corrects the unfolding. They also undergo non-covalent interactions with exposed hydrophobic surfaces of non-native proteins and stabilize them against irreversible aggregation. For example, the study of chaperone αA-crystallin revealed its functional unit -19 amino acid hydrophobic peptide fragment (amino acid position70 to -88) was responsible for the chaperone function of the protein. This peptide can be used as a universal chaperone for controlling protein aggregation (Santhoshkumar and Sharma, 2004).

In recent years, a group of exogenous small molecules that are freely diffusible in cells

and with chaperoning activity (collectively termed as chemical chaperones) has successfully corrected a variety of misfolded proteins and the associated cellular defects or protein folding abnormalities (Bian et al., 2008; Burrows et al., 2000; Caciotti et al., 2009; Janovick et al., 2009; Jiang et al., 2009; Tveten et al., 2007; Yam et al., 2007b). These small chemicals have been shown to reverse the misfolding or mislocalization of several mutant plasma membrane, lysosomal, and secretory proteins. They are a diverse group of substances including glycerol, polyols, dimethylsulfoxide (DMSO), deuterated water, tauroursodeoxycholic acid (TUDCA), trimethylamine N-oxide (TMAO) and sodium 4-phenylbutyrate (PBA). The mechanism of action, though not fully understood, may involve an improvement and stabilization of protein folding environment, prevention of non-productive protein interactions, reduction of aggregate formation and alteration of endogenous chaperone activity. This facilitates the protein trafficking and reduces the aberrant intracellular accumulation of misfolded proteins and subsequently cytotoxicity (Jiang et al., 2009; Kanki et al., 2009; Kolter and Wendeler, 2003; Papp and Csermely, 2006; Ulloa-Aguirre et al., 2004). Chaperone-assisted therapy may be applicable to a variety of proteins associated with pathological conditions. Inherited protein folding diseases, including cystic fibrosis, Alzheimer's disease, prion-related diseases, familial Parkinsonism, spinocerebellar diseases and lysosomal storage diseases, are caused by abnormal localization and/or aggregation of proteins that lead to cell dysfunction and tissue damage (Gregersen, 2006).

In this project, we sought to investigate if the altered protein features (such as aggregates and mistrafficking) of mutant proteins (mutant CRYAA, CRYGD and MYOC)

could be correctable by small chemcials (TMAO, PBA and so on).

1.4.3.2 Other approaches

A number of different approaches under development include drugs which affect the processing of the precursor proteins, clearance of the misfolded protein, and which inhibit or prevent the conformation changes.

Pharmacological chemical is a relatively new concept in the treatment of human genetic diseases resulting from misfolded proteins. They present an attractive alternative to transplantation due to its low risk and an alternative to enzyme replacement therapy due to lowered expense and oral availability, and they selectively bind to a target protein and increase its stability. The binding of the pharmacological molecules helps the protein fold into its correct three-dimensional shape. So far, more and more attentions focus on this field. For example, pharmacological molecules could mediate the folding and stabilization of the P23H-opsin mutant associated with autosomal dominant retinitis pigmentosa (Noorwez et al., 2003).

In addition, immune system activation can increase the clearance of the disease-associated proteins. These conformation-based approaches appear to hold the best promise for therapies for this devastating group of disorders. Development of monoclonal antibodies with chaperone-like activities that would be able to neutralize the toxic gain of function of misfolded proteins represent another novel promising immunological concept in the treatment of conformational diseases (Kontsekova et al., 2009). Gene therapy can

be used to alleviate the burden of accumulation of misfolded proteins, e.g. insertion of normal genes to replace the function of mutant proteins, expression of recombinant chaperones, elimination of mutant unfolded proteins using small interfering RNA (siRNA) or self-looped short hairpin RNAs (shRNAs).

Finally, therapeutic strategies based on combination therapies improving different steps in the proteostasis network capacity (proteostasis regulators) and stabilizing specific proteins (small chemicals) are currently under development (Balch et al., 2008; Powers et al., 2009). There is hope that they will delay onset or decrease impact of protein folding diseases.

2 Objectives and study design

Many worldwide blindness are caused by different kinds of genetic eye diseases, such as cataract, glaucoma, age-related macular degeneration (AMD), and retinitis pigmentosa (RP). These major eye diseases which are potentially blinding, including cataract and glaucoma, may be affected by disruptions in protein structures. The lens opacity in cataract may attribute to misfolding in the secondary structure of crystallins. In glaucoma, disrupted structural behaviors of myocillin affect the geometry of the extracellular matrix at the trabecular meshwork which in turn obstruct aqueous outflow and lead to elevation of intraocular pressure. The latter is causing progressive optic nerve damages, which is the pathologic basis of glaucoma. In this study, I conduct *in vitro* investigations on variants of *CRYAA (αA-crystallin)* and *CRYGD (γD-crystallin)* in congenital cataract and *MYOC (myocilin)* in primary open-angle glaucoma. These genes are of interest to me and my laboratory because of their causative effects to blinding diseases.

My work mainly examine if the altered protein features caused by disease-causing mutations could be correctable by agents stabilizing the proteins towards a more native conformation. The correction might alleviate cell damages from the ER stress due to the retention of misfolded mutant protein by the ER quality control system, ultimately resulting in better cell survival. Possible biological mechanism of chaperone action will also be elucidated.

Presenile cataract-causing *G98R CRYAA* was expressed in lens epithelial B3 cells by lipophilic transfection. The *G98R mutation* of *CRYAA* gene was identified in an Indian family diagnosed with presenile nuclear type of cataract. When expressed in lens epithelial cells, the mutant protein was reported to have reduced solubility and was suggested to be misfolded (Singh et al., 2006). Hence, I attempted to investigate if the misfolding features and cellular responses could be corrected by chemical chaperone. Various parameters concerning G98A CRYAA protein expression in transfected B3 cells will be examined, including detergent solubility, subcellular localization, protein aggregation and degradation, ER stress, unfolded protein responses, heat-shock and cell stress signaling and cell apoptosis.

A premature *truncated G165fsX8 (c.494delG) CRYGD mutant* identified in a Chinese family with congenital nuclear type of cataract, had much reduced detergent solubility and mistrafficking to the nuclear envelope (Zhang et al., 2007b). This was hypothesized to influence nuclear translocation and lens fibre cell differentiation in normal lens development. My study was aimed to examine these altered protein features could be reduced by treatment with chemical chaperones.

The theory of small chemical-assisted protein rescue was also testified in myocilin, which is reported to cause 2-5% of primary open-angle glaucoma (POAG) with elevated intraocular pressure (IOP). Wildtype or disease-causing mutants (aggressive type causing high IOP-associated juvenile-onset POAG: *C245Y, Q368X, P370L, D384N, R422H, C433R, Y437H, I477N, I477S and N480K*; and mild variants without a rise of IOP: *R82C,*

T377M, D380A and R422C) were expressed in human trabecular meshwork cell line. After treatment or not with small chemicals, the cells were collected for examination of MYOC features, including MYOC secretion and detergent solubility, cellular localization, aggregation, ER stress and cell apoptosis.

3 Effects of small chemicals on the misfolding of cataract-causing mutant αA-crystallin

3.1 Introduction

3.1.1 Cataract

Cataract is defined as lens opacification causing light scattering. The lens is normally transparent and is responsible for direct and focus light rays on the retina for image perception. In cataract lens, the light transmission is deterred or blocked by the cloudy opacities, resulting in blurred vision (**Figure 3.1**). Cataract is a leading cause of visual impairment worldwide. Estimated by The World Health Organization in 2004, cataract is accounted for about 50% of the visual impairment or disability (Resnikoff et al., 2004). Hence, it becomes a global burden due to the high medical cost and the poor life quality.

Cataract is categorised into two major groups: age-related cataract and congenital cataract (CC) (Haargaard et al., 2004). Majority of cataract is age-related or senile cataract, which occurs in older age people and tends to be multi-factorial lens disorder. Genetic variations and environmental factors are the risk factors for the development of lens opacity. Congenital cataracts appear in early age and it is less common than senile cataract, however it is responsible for about one-tenth of childhood blindness worldwide. CC is inherited in a Mendelian fashion, and a number of disease-causing genetic loci and genes have been identified (Gilbert and Foster, 2001).

For senile cataract, lens opacification is caused by risk factors that could potentially

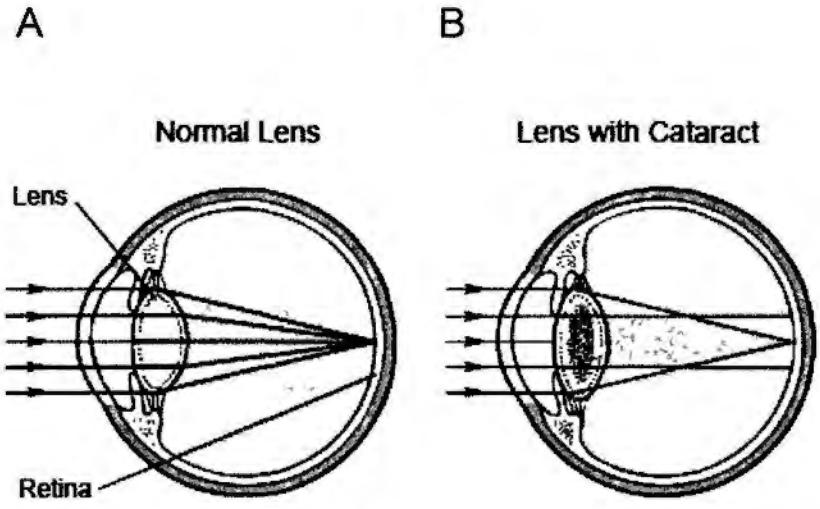

Figure 3.1 Light pathway in eyes. (A) Light rays pass through the normal lens and focus on the retina. **(B)** Some light rays are blocked by the lens opacities leading to a defocusing (modified from Augusteyn, 2007).

damage the lens structure and properties on both molecular and cellular levels. Risk factors include the UV exposure and radiation, trauma, surgical injury, use of systemic and ocular drugs, cigarette smoking, alcohol consumption, malnutrition, as well as chronic diarrhea (Brian and Taylor, 2001; Delcourt et al., 2005; Ferrufino-Ponce and Henderson, 2006). In mature lens, crystallin proteins practically have no major turnover and their expression remain stable in the lens body throughout one's lifetime. Hence, constant insults from products formed by photochemical reactions that bombard the lens proteins would introduce instability to lens structure and composition. For example, when the expression of α-crystallins with chaperone capability is altered due to environmental changes, those lens proteins that maintain in good shape by α-crystallins would precipitate and prone to aggregate either reversibly or irreversibly, resulting in a disruption of the structural uniformity of lens and, ultimately causing opacity formation (Andley, 2007; Truscott, 2005). Studies have shown that aggregation of crystallins could be attributed to the post-translational modifications of proteins through different processes, including mixed disulfide formation, glycation cross-linking by UV, transglutaminase or disulfides as well as phosphorylation, deamidation, and proteolysis (Lampi et al., 2002). Cellular changes involving membrane interaction (Fan et al., 2005), deregulated proteolytic denaturation of crystallins (Nixon, 2003), and disruption of osmotic balance (Miyazawa et al., 2007) are also possible causes of cataractogenesis.

3.1.1.1 Congenital cataract

Congenital cataract (CC) refers to the opacification of human lens presented or becoming manifested in early childhood. It causes the visual impairment of children and

even blindness if inappropriately treated. The lens opacification is unilateral or bilateral. In a Danish nation-wide study, 36% of CC was unilateral and 64% bilateral (Haargaard et al., 2004). This data is consistent with the result of a United Kingdom study (34% unilateral and 66% bilateral).

Cataracts can be isolated or occurs in association with different metabolic diseases and genetic syndromes (Hejtmancik JF et al., 2001), such as aniridia, microphthalmia, anterior segment mesenchymal dystrophy (ASMD), persistent hyperplastic primary vitreous (PHPV), and so on, or associated with systemic disorders, like hereditary hyperferritinaemia-cataract syndrome, desmin-related myopathies, Down's syndrome, juvenile chronic arthritis, diabetes, galactosaemia, and so on. Among them, isolated CC is a predominant clinical presentation. It was reported to account for 71% of CC in Danish and 56% in UK (Haargaard et al., 2004; Rahi and Dezateux, 2000). Isolated congenital cataracts tend to be highly penetrative Mendelian traits, with autosomal dominant mode of transmission more common than autosomal recessive. Among isolated inherited cataracts, 89% are autosomal dominant congenital cataract (ADCC), 7% autosomal recessive congenital cataract (ARCC), 2% X-linked, whereas the remaining are nonclassified (Haargaard et al., 2004). Currently, there are 39 genetic loci being mapped for isolated or primary cataracts. Of these, several are associated with additional abnormalities, mostly as part of developmental syndromes. These tend to result from mutations in genes encoding transcriptional activators, and some have been identified through sequencing of candidate genes in patients with developmental anomalies.

3.1.1.2 Genes and mutations causing congenital cataracts

Twenty-six of the 39 mapped loci for isolated congenital or infantile cataracts have been identified with candidate genes carrying specific mutations. Of the cataract families that carry specific gene changes, about half of them show disease-causing mutations in the family of crystallins, about 15% have mutations in the connexin family, and the remaining is due to gene changes for heat shock transcription factor-4 (HSF4), aquaporin-0 (AQP0, MIP), and beaded filament structural protein-2 (BFSP2) and so on. Correlation between the pattern of mutant protein expression and the morphology of resulting cataract is commonly observed. On the other hand, inheritance of the same mutation in different families or even the same mutation within the family can result in radically different cataract morphologies and severities. This suggests that additional genes or environmental factors might modify the expression of the primary mutation associated with cataracts. Conversely, cataracts with similar or identical clinical presentations can result from mutations in completely different genes.

3.1.2 Crystallins

Crystallins is accounted for 95% of water-soluble lens proteins and about 35% of the wet weight of lens fibre cells. They are cytoplasmic proteins. In human lens, the major crystallins are alpha (α), beta (β) and gamma (γ) types. α-crystallin exists as a heteropolymeric complex with copolymer of αA- and αB-crystallins present in an approximate 3:1 stoichiometric ratio. β-crystallins are a large family of closely related polypeptides that exist as oligomers, and γ-crystallins are monomeric proteins. So far, 14 types of crystallin have been found in young human lens, including 12 primary gene

products of CRYAA, CRYAB, CRYBA1, CRYBA2, CRYBA3, CRYBA4, CRYBB1, CRYBB2, CRYBB3, CRYGC, CRYGD, CRYGS and two NH_2-terminally truncated products of CRYBA3, BRYBB1 (Lapko et al., 2003). Analysis of micromolar concentrations in lens showed that α-, β- and γ-crystallins had ratios of 12, 13.5 and 9, respectively. These integral ratios suggest that crystallin molecules are probably packed in highly ordered arrays in the lens.

Crystallins are responsible for maintaining the structure, refractive index and optical properties of lens fibre cells. They contribute to the transparency and refractive power of lens by short-range interactions among themselves in a highly concentrated protein matrix. In general, the biosynthesis of crystallins after birth is continuous only within the first year of life (Augusteyn, 2007) and the crystallin pool remains constant throughout one's lifespan until the aging process starts. Given the importance of crystallin expression in lens fibre cells, crystallin genes and their mutation are highly attended in the study of cataract formation

The native α-crystallin protein complexes are the largest in molecular size (> 1,000 kDa) among different crystallins. They are mainly composed of two related proteins, αA- and αB-crystallins in a molar ratio of roughly 3:1, which are encoded by two different genes, *CRYAA* and *CRYAB*, located on different chromosomes. Both αA- and αB-crystallin have a conserved heat shock domain composed of 80 amino acid residues, which is engaged in the contact of subunits and is the core functional domain (Derham and Harding, 1999; Narberhaus, 2002). Both genes contain three exons of similar size. In

rodents (mouse, rat, hamster and rabbit), an alternative spliced product is observed in 10-20% of αA-crystallin encoding gene (*CRYAA*): additional 69 base-pairs from the intron 1 are included in the mature mRNA, leading to 23 amino acids longer than the usual αA-crystallin. At the protein level, the insertion is present between the amino acid residues 63 and 64 and it is named as αA^{ins}-crystallin. Native α-crytallin isolated from the lens is a hetero-oligomeric complex (about 800 kDa in molecular size) with CRYAA (about 20 kDa) and CRYAB (about 20 kDa) subunit (Sun and Liang, 1998). The α-crystallins belong to the family of small heat-shock proteins, of which they share a common central domain of about 90 amino acid residues. It is folded into a β-sandwich conformation and has variable N- and C-terminal extensions. Since this domain was firstly recognized in the α-crystallin, it is named as the "α-crystallin domain" (Augusteyn, 2004; de Jong et al., 1998). Conformational study with recombinant CRYAA and CRYAB displayed these two subunits having different secondary and tertiary structure (Sun et al., 1997), though they share about 60% sequence homology (Bloemendal and de Jong, 1991).

Expression of *CRYAA* and *CRYAB* genes has been characterized in a variety of species (including human mouse, hamster, rat, chicken and rabbit). In human lens, both subunits of α-crystallin are expressed predominantly in differentiated lens fiber cells and at low levels in epithelia (Andley et al., 2000). CRYAA is mainly expressed in lens and less common in other tissues, whereas CRYAB is expressed at a relatively high level in numerous tissues outside lens (**Table 3.1**). Additionally, CRYAB but not CRYAA can be induced by stresses, and is highly expressed in degenerative diseases and tumors

Table 3.1 The α-crystallins.

(Graw, 2009)

Gene	Chromosome[a]		Mouse cDNA source[b]	Protein	Function
	Mouse	Human			
CRYAA	17 (31.8)	21q22 (43.5) OMIM: 123580	Lens, extraembryonic tissue; pituitary gland; placenta; spleen	αA-crystallin; 173 aa; 20 kDa αA^{ins}-crystallin; 196aa; 25 kDa	Structural protein Chaperone Autokinase Gene activator
CRYAB	9 (50.6)	11q22 (111.3) OMIM: 123590	Lens, brain; kidney; heart; extraembryonic tissue; mammary gland; liver; muscle; testis;vthymus; lung; pancreas; thyroid; skin; uterus; ovary; colon; diaphragma; limb; placenta	αB-crystallin; 175aa; 22 kDa	Structural protein Heat-shock protein

[a] MB according to ENSEMBL databases (http://www.ensembl.org; 2008) in brackets.

[b] According to the Jackson Lab database (http://www.informatics.jax.org).

(Kantorow and Piatigorsky, 1998). This differential distribution indicates that these subunits may have diverse roles in human tissues.

The main feature of native α-crystallin complex in the lens is its protein chaperoning activity (Sun and MacRae, 2005). The basic characteristics of α-crystallins are summarized in Table 3.1. Moreover, experimental evidence have suggested that α-crystallin is involved in the remodelling and protection of cytoskeleton (actin, tubulin or intermediate filaments), inhibition of apoptosis and resistance to stress (Andley, 2007). Generally, α-crystallins represent a major class of water-soluble proteins in lens. Their functions are mainly in the context of protecting the lens against stress, in particular against oxidative stress, acting as small heat-shock proteins and molecular chaperone to stabilize the native conformation and normal activity of client proteins, and to maintain the cellular cytoskeleton.

The β- and γ-crystallins belong a super-family of crystallin and they share a common feature of anti-parallel β sheets, which are referred as the ''Greek key motif'' because of its similarity (in schematic drawings) to paintings on ancient Greek pottery. β-crystallins are highly heterogeneous and are divided into acidic and basic groups, characterized by the C-terminal extension (present in the basic group but not in the acidic group). Both β- and γ-crystallins are composed of two conservative domains. In all members of β- and γ-crystallin super-family, this motif occurs four times (Jaenicke and Slingsby, 2001).

3.1.3 Mutant crystallins

Mutant *crystallin* genes are strong candidates of cataract formation. Mutations in *α-*, *β-* and *γ-crystallin* have been linked to hereditary cataracts. So far, a number of mutations of crystallin genes have been identified.

More than twelve cataract-causing mutations have been identified in *α-crystallin*: *CRYAA* (including *W9X, R12C, R21L, R21W, R49C, R54W, G98R,* and *R116C*) and *CRYAB* (including *P20S, R120G, D140N* and *R157H*). *R116C* in human *CRYAA* was the first dominant cataract mutation being characterized (Litt et al., 1998). This mutation was reported independently in several other unrelated families **(Table 3.2)** suggesting it as a hotspot mutation in *CRYAA* gene. In a French family having *R116C* mutation, a non-lens phenotype of an iris coloboma was diagnosed in addition to the nuclear cataract (Beby et al., 2007). Moreover, missense *R116C* and nonsense *W9X* mutations in *CRYAA* have been linked to autosomal dominant (Litt et al., 1998) and recessive (Mackay et al., 2003) forms of non-syndromic cataracts, respectively. Dominant mutations of R116C in human CRYAA and V124E in mouse CRYAA were found to lie within the phylogenetically conserved core 'α-crystallin domain', whereas another dominant R49C mutation in human CRYAA is outside the core domain (Mackay et al., 2003). Recessive mutations of W9X and R54H in mammalian CRYAA were close to the N-terminal region. The same mutation can give rise to heterogeneous phenotypes in different families: *R116C CRYAA* was identified in families with zonular nuclear cataract (Litt et al., 1998) and also in families with fan-shaped cataract (Vanita et al., 2006). *R49C CRYAA* was found in families having lens opacities of nuclear type. No clinical description of the autosomal

Table 3.2 Mutations in mouse and human CRYAA genes

(Graw, 2009)

nt Position[a]	bp Exchagne	Aa Position[a]	aa Exchange	Biological consequence
Mouse mutations				
160	C→T	54	Arg→Cys	Dominant cataract, small lens, microphthalmia
161	G→A	54	Arg→His	Recessive cataract
352	T→G	118	Tyr→Asp	Dominant cataracts, small lens
371	T→A	124	Val →Gln	Dominant cataracts,microphthalmia
Human mutations				
27	G→A	9	Trp→stop	Recessive cataract
34	C→T	12	Arg→Cys	Two cases in distinct families; dominant cataract& microcornea
61	C→T	21	Arg→Trp	Dominant cataract, microcornea and microphthalmia
62	G→T	21	Ary→Lys	Dominant dense central cataract
149	C→T	49	Arg→Cys	Dominant nuclear cataract
160	C→T	54	Arg→Cys	Recessive total cataract, microcornea; dominant cataract
292	G→A	98	Gly→Arg	Dominant progressive total cataract
347	C→T	116	Arg→Cys	Six independent cases of dominant cataract with variable phenotype

[a] Beginning at coding sequence (start codon ATG)

recessive cataract morphology associated with the W9X mutation in CRYAA has been described (Pras et al., 2000). However, the premature termination resulting from *W9X* mutation may mimic the changes observed in the CRYAA knock-out mouse in a homozygous state. In case of G98R mutation, the mutant protein exists as larger oligomers and exhibited reduced protein chaperoning activity (Murugesan et al., 2007). In addition to the nine *CRYAA* mutations in human, four mouse *CRYAA* mutants were also characterized (Table 2). One mutation, c.160C>T (leads to Arg54Cys change), found in both mouse and human, showed different inheritance traits (recessive in human but dominant in mouse). In contrast, another mutation in the same codon (c.161G>A, leads to R54H change) identified in mouse had the transmission of a recessive mode of inheritance.

In contrast to *CRYAA* with a definite relationship of gene mutations with the formation of cataracts, the role of αB-crystallin is more heterogeneous. Homozygous *CRYAB* knock-out mice did not display any disease phenotype (Brady et al., 1997). In human, nine *CRYAB* mutations have been reported. Only several of them are associated with dominant cataracts, and others are suggested to be causative for desmin-related myopathy or dilated cardiomyopathy.

Meanwhile, genetic studies have identified mutations of *β-* and *γ-crystallin* genes leading to various forms of cataract. he first mutation of *β-crystallin* gene was described in 1991 by Chambers and Russell for the Philly-cataract in mouse (Chambers and Russell, 1991). After that, a mutation in human *CRYBA1* gene was identified to be causative for

the congenital zonular cataract (Graw, 2009). Similar to other crystallins, the cataract phenotypes caused by *γ-crystallin* mutations are quite varied and there is no specific genotype-phenotype correlation.

3.1.4 Mutant crystallins causing protein folding diseases

Many cataract-causing mutations of crystallin genes result in a disruption of protein structure and conformation when expressed in the lens fibre cells. It has been reported that α-crystallin functions as a molecular chaperone to bind to partially unfolded polypeptides and maintain them in a refolding-competent state, preventing lens protein aggregation and reducing the risk of cells undergoing apoptosis (Peschek et al., 2009). Also, mutant α-crystallin could be insoluble and prone to aggregate, causing cell death (Xi et al., 2008). Misfolded mutant protein has a loss of chaperone activity and altered protein-protein interactions (Fu and Liang, 2003) (Singh et al., 2006). This is evidenced by the R116C mutant CRYAA with diminished protective ability against stress-induced lens epithelial cell apoptosis (Andley et al., 2002). Moreover, mutations in γ-crystallin are associated with protein aggregation and lens fiber cell denucleation, as well as self-aggregation of lens protein leading to lens opacification (Talla et al., 2006; Wang et al., 2007).

3.1.5 Effects of small chemicals on mutant crystallins

There have been many reports showing the use of chemical compounds of low molecular mass and with chaperoning activity to correct the defective trafficking or

reduce protein aggregation that associated with diseases (Mu et al., 2008). These molecules are cell permeable and can freely diffusible in tissues and cells. The mechanism of action is not fully understood, though may involve the stabilization of improperly folded proteins, prevention of non-productive interactions with other proteins, reduction of aggregate formation and alteration of folding environment or endogenous chaperone activity. This facilitates an efficient transport of affected proteins to the intracellular or extracellular destinations (Papp and Csermely, 2006). It has been shown that small chemicals, like PBA, TMAO, and TUDCA, suppressed the ER stress and reduced cell apoptosis in cultured lens epithelial cells and prevented cataract formation in galactose-fed rat (Mulhern et al., 2007).

Hence, correction of protein folding and trafficking problems could rescue the damaged cells and reverse the disease course. In my study, I tested if the altered protein properties of G98R mutant CRYAA could be reversed by treatment with small chemicals. As for G98R CRYAA, it has a substitution of glycine to arginine resulting in an increase of negative charge and hydrophobicity on the protein surface, possibly a cause of protein misfolding.

3.1.6 Selected *mutant* αA-crystallins

From a repertoire of congenital cataract-causing *CRYAA* mutants (such as *R12C, R21L, R49C, G98R and R116C*), *G98R CRYAA* was mainly studied in transfected Human lens epithelial B3 cells. In 2006, Santhiya and co-workers (Santhiya et al., 2006) reported a new mutation (c.292G>A) of *αA-crystallin* , which was a change of glycine to arginine at

the 98th amino acid position. This mutation was observed in three members of an Indian family with the earliest onset of the nuclear type of cataract at the age of 16 and vision loss by the age of 24. The mutation leads to a gain of positive charge. This was supported by studies that mutations at arginine residues were associated with a loss of positive charge in α-crystallin, causing an altered structure and possible the protein functions (Murugesan et al., 2007). To investigate the effect of this mutation on the structure and chaperone function of αA-crystallin, purified G98R CRYAA protein was expressed in lens cells (Vanita et al., 2006). A loss of chaperone activity was shown by an increase of DTT-induced aggregation of insulin, suggesting that it might lead to a folding defect of the whole protein. The mutant forms were partially folded, aggregation-prone and existed as heterogeneous populations of very large oligomers, which lacked the chaperone activity. Also it was reported that G98R mutant CRYAA showed significantly more bis-ANS binding than the wild-type (WT) protein, which indicates that the mutant protein might have more exposed hydrophobic sites (Murugesan et al., 2007). The role of G98R mutation in CRYAA structural stability and subunit exchange was also revealed by its unfolding at lower concentrations of urea compared to WT CRYAA (Singh et al., 2007). The mutant protein was more susceptible to proteolysis than the WT protein and transiently populated fragments that were prone to aggregation. Subunit exchange studies using fluorescence resonance energy transfer showed that the mutant protein formed mixed oligomers with WT protein (Singh et al., 2007). The mutant protein was more susceptible to thermal aggregation, whereas mixed oligomer formation led to a decreased propensity to aggregate. Co-expression of WT CRYAA with G98R mutant in *E. coli* cells rescued the mutant protein from the formation of inclusion bodies (Singh et al., 2007).

These observations might underlie the molecular basis for the presenile type of cataract, in spite of severe folding defect and aggregation of the mutant G98R CRYAA. In my study, this G98R mutant CRYAA was expressed in cultured human lens epithelial B3 cells to study the protein solubility in detergent extraction, subcellular localization and aggregation, and cell stress and apoptosis.

3.2 Materials and methods

3.2.1 WT CRYAA expression construct

Total ocular mRNA was extracted from human aborted fetus at week 14 with RNeasy mini kit (Qiagen, Valencia, CA, USA) following the protocol provided by the manufacturer. Reverse transcription was performed with oligo (dT) primer (Roche, Bael, Switzerland) and SuperScript^{TM} III reverse transcriptase (Invitrogen, Carlsbad, CA, USA). Primers with two restriction enzyme cutting sites were designed to amplify the full-length WT cDNA of *CRYAA*. A 548 base-pair *EcoRI/XhoI* fragment encompassing the full-length 519 base-pair open reading frame of *CRYAA* was ligated into the *EcoRI/XhoI* sites of a mammalian expression plasmid pcDNA6-His/myc version B (Invitrogen) (**Figure 3.2**) to obtain the construct pHis/myc-CRYAA^{WT}.

3.2.2 Site-directed mutagenesis and mutant constructs

pHis/myc-CRYAA^{WT} was used as a template to generate specific mutations of *CRYAA* (*R21L, R49C, G98R, R116C*) using QuikChange II Site-Directed Mutagenesis kit (Stratagene, La Jolla, CA) and oligonucleotides (**Table 3.3**). The mutant constructs were

pcDNA™6/*myc*-His Vector

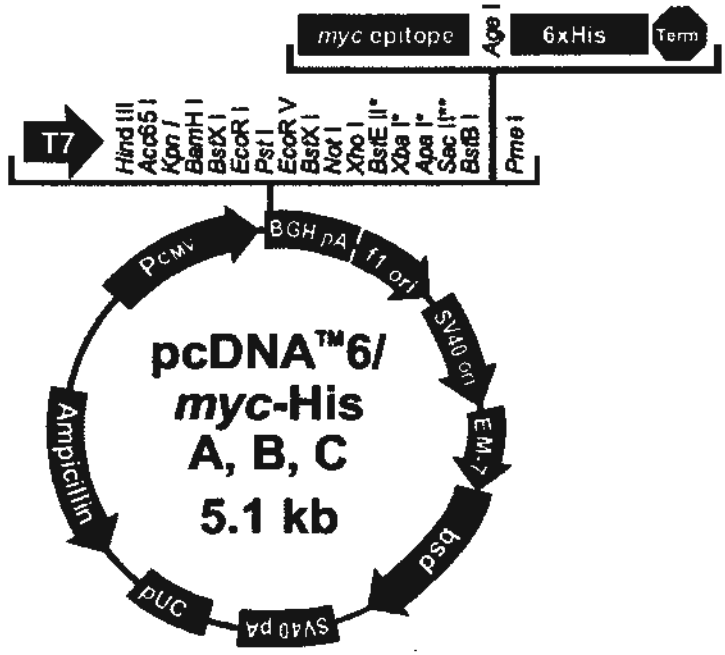

Multiple Cloning Site of Version B

Below is the multiple cloning site for pcDNA™6/*myc*-His B. Restriction sites are labeled to indicate the cleavage site. The boxed nucleotides indicate the variable region. The multiple cloning site has been confirmed by sequencing and functional testing. The sequence of pcDNA™6/*myc*-His B is available for downloading from our website at www.invitrogen.com or from Technical Support (page 17).

T7 promoter/priming site — Hind III — Acc65 I — Kpn I — BamH I

```
861  ATTAATACGA CTCACTATAG GGAGACCCAA GCTGGCTAGT TAAG CTT GGT ACC GAG CTC GGA
                                                   Leu Gly Thr Glu Leu Gly
```

BstX I* — EcoR I — Pst I — EcoR V — BstX I* — Not I

```
923  TCC ACT AGT CCA GTG TGG TGG AAT TCT GCA GAT ATC CAG CAC AGT GGC GGC CGC
     Ser Thr Ser Pro Val Trp Trp Asn Ser Ala Asp Ile Gln His Ser Gly Gly Arg
```

Xho I — Xba I — Apa I — Sac II — BstB I — myc epitope

```
977  TCG AGT CTA GAG GGC CCG CGG TTC GAA CAA AAA CTC ATC TCA GAA GAG GAT
     Ser Ser Leu Glu Gly Pro Arg Phe Glu Gln Lys Leu Ile Ser Glu Glu Asp
```

Age I — Polyhistidine tag — Pme I

```
1028 CTG AAT ATG CAT ACC GGT CAT CAT CAC CAT CAC CAT TGA GTTT AAACCCGCTG
     Leu Asn Met His Thr Gly His His His His His His ***
```

BGH Reverse priming site

```
1081 ATCAGCCTCG ACTGTGCCTT CTAGTTGCCA
```

*Note that there are two *BstXI* sites in the polylinker.

Figure 3.2 Map of eukaryotic expression vector pcDNA6/myc-His used for *CRYAA* cloning (Invitrogen websites).

Table 3.3 Sense oligonucleotides for site-directed mutagenesis in *CRYAA*

Mutation	Oligonucleotides (sense, 5' to 3') (bold underlined alphabet indicated specific base change)	Expression constructs
R21L (c.62G>T)	TGGGGCCCTTCTACCCCAGCC**T**GCTGTTCGACCAG TTTTTCG	pHis/myc-CRYAA^{R21L}
R49C (c.145C>T)	TCCACCATCAGCCCCTACTAC**T**GCCAGTCCCTCTT CCGCACCG	pHis/myc-CRYAA^{R49C}
G98R (c.292G>A)	GTGGAGATCCAC**A**GAAAGCACAACGAG	pHis/myc-CRYAA^{G98R}
R116C (c.346C>T)	ACATTTCCCGTGAGTTCCAC**T**GCCGCTACCGCCTG CCGTCC	pHis/myc-CRYAA^{R116C}

named as pHis/myc-CRYAA^{R21L}, pHis/myc-CRYAA^{R49C}, pHis/myc-CRYAA^{G98R}, pHis/myc-CRYAAR^{116C}. pHis/myc-CRYAA^{R12C} was introduced by Zhang LY (Zhang et al., 2009b) in our lab.

3.2.3 Amplification of WT and mutant constructs

3.2.3.1 Transformation

The recombinant constructs of *WT* and mutant *CRYAA* were transformed into *E. coli* DH5α competent cells (Invitrogen) to expand constructs. First, less than 10 ng construct DNA was transferred to 25 μl of competent cells, mixed well and incubated on ice for 30 minutes. The mixture was heat-shocked at 42°C for 45 seconds, followed by incubation on ice for 2 minutes. Then added 300 μl SOC medium (Invitrogen) was added to the bacterial mixture and was incubated at 37°C for 1 hour with shaking at 255 rpm. The transformation mixture was plated on agar plates containing 1 μg/ml ampicillin and incubated at 37°C for 16 hours. The colonies were picked and incubated in a starter culture (2 ml LB medium with ampicillin in a round-bottom tube) for 8 hours at 37°C with shaking at 255 rpm, followed by DNA extraction.

3.2.3.2 MiniPrep and MidiPrep to extract DNA

The vector DNA was extracted using QIAGEN Plasmid Extraction Kit. MiniPrep protocol was used to prepare up to 20 μg of plasmid DNA and MidiPrep was to prepare up to 100 μg of plasmid DNA. (1) Bacterial cell pellet was first harvested by spinning at

6000 g for 10 minutes at 4°C. The pellet was resuspended in Buffer P1 (added with RNase A, ice-cold) and mixed well, Then Buffer P2 was mixed at room temperature for 5 minutes, and ice-code P3 was added and mixed well and kept on ice for 10 minutes, and centrifuged at 6000 g for 20 minutes at 4°C; (2) QIAGEN-tip was equilibrated with buffer QBT followed by loading of clear supernatant from lysate spinning and let flow-through by gravitation. The QIAGEN-tip was washed 3 times with wash buffer QC. (3) QIAGEN-tip was placed in clean tubes for DNA elution with elution buffer QF by gravitation and DNA was precipitated with $1/5^{th}$ volume of isopropanol. DNA pellet was obtained by centrifugation at full speed at 4°C for 30 minutes. The pellet was washed with 70% ethanol and re-pellet by spinning. The pellet was briefly dried and resuspended in nuclease-free distilled water.

3.2.3.3 DNA direct sequencing

To confirm the correct sequence and mutation introduced in the construct, direct sequencing was performed with specific primers for *CRYAA*, including 1F: 5'- CGG GAC AAG TTC GTC ATC TT and 1R: 5'- GCA GAC AGG GAG CAA GAG AG; 2F: 5'- CTC CAG GTC CCC GTG GTA and 2R: 5'- AGG AGA GGC CAG CAC CAC; 3F: 5'- CTG TCT CTG CCA ACC CCA and 3R: 5'- CTG TCC CAC CTC TCA GTG. Sequencing reactions using BigDye terminator v3.1 cycle sequencing kit (Applied Biosystems, Foster, CA, USA) were done under the condition provided by the manufacturer. After reactions, samples were precipitated by ammonium acetate mixed with absolute ethanol at -80°C for 15 minutes, then pellet was washed by 70% ethanol. The precipitated DNA samples were resuspended in Hi-Di™ formamide and denatured at

95°C for 2 minutes. Then, the fluorescence was read and reported by ABI PRISM™ 3130xl DNA genetic analyzer. For sequence changes of introduced mutations, both forward and reverse sequencing were performed to confirm the alterations.

3.2.4 Cell culture and transfection

Human lens epithelial B3 cells (American Tissue Culture Collection, Manassas, VA) were cultured in Eagle's Minimal Essential medium (MEM, Invitrogen) supplemented with 10% fetal bovine serum (FBS, Invitrogen) and antibiotics (100 units/ml penicillin G and 100 μg/ml streptomycin sulfate, Invitrogen) and incubate at 37°C in a humidified chamber with 5% CO_2 balanced with air. Before transfection, negligible expression of endogenous *CRYAA* in B3 cells was verified by quantitative PCR with primers for *CRYAA*: forward, 5'- CGG GAC AAG TTC GTC ATC TT; reverse, 5'- GCA GAC AGG GAG CAA GAG AG. To prepare cells for DNA transfection, B3 cells were plated at a density of 10^5 cells/cm^2 in 60-mm (in diameter) tissue culture dish (Nalgen Nunc, Rochester, NY, USA). Transient transfection was done with WT and mutant constructs by using FuGene HD transfection reagent (Roche, Basel, Switzerland). A ratio of 1 μg DNA mixed with 3 μl FuGene HD reagent was taken, and the mixture was incubated in Opti-MEM® I supplemented with GlutaMAX™-I (Invitrogen) for 30 minutes. The FuGene-DNA complex was added to cells in 0.5 ml volume of Opti-MEM® I for 6-8 hours. Then, 5 ml of serum-added MEM was added to cells for further culture and fresh medium was replenished every 2 days. Except for those specified, all reagents were purchased from Invitrogen Company.

3.2.5 Treatment by small chemical molecules

Small chemical treatment was started at 24 hours after transfection. Trimethylamine N-oxide (TMAO, 25 to 300 mM, Sigma) (dissolved in water), 4-phenylbutyric acid (4-PBA, 0.2 to 2 mM, triButyrate, Triple Crown America Inc, Perkasie, PA), glycerol (1 to 5%, Sigma) or dimethylsulfoxide (DMSO, 0.5 to 1%, Sigma) was added to the medium for transfected cell culture. Fresh culture medium containing specified drug was replenished every 2 days.

3.2.6 Protein analysis by western blotting

3.2.6.1 Monitoring expression level of total protein

Cells were lysed at a concentration of 2.5 $x10^6$ cells/ml radioimmunoprecipitation (RIPA) buffer containing 50 mM Tris-HCl (Sigma), 150 mM sodium chloride, 1% Nonidet P-40 (Sigma), 0.25% sodium deoxycholate (Sigma), protease inhibitor cocktail (Roche) and 1 mM phenylmethyl sulfonylfluoride (PMSF; Sigma) for 30 minutes on ice. After centrifugation, the supernatant was collected and denatured in sample buffer with a final concentration of 50 mM Tris HCl (pH 6.8), 2% sodium dodecylsulfate (SDS, BioRad, Hercules, CA), 10% glycerol, 0.002% bromophenol blue, 1% 2-mecaptoethanol, and 50 mM DL-dithiothreitol (DTT; Sigma). The cell pellet was washed with ice-cold PBS and denatured in SDS sample buffer (including 50 mM Tris HCl (pH6.8), 10% glycerol, 2% SDS, 0.002% bromophenol blue, 50 mM DTT, 1% 2-mecaptoethanol,) containing 9 M urea (BioRad) at 95 °C for 5 minutes. All protein samples were stored at -20 °C for further usage.

The protein samples equivalent to $7.5x10^4$ cells were analyzed by 15% SDS-polyarcylamide gel electrophoresis (PAGE). Gel and buffer were prepared according to different concentrations of gel. Briefly, for 10% resolving gel, reagents including 6.7 ml 30% acrylamide/Bis solution (29:1, BioRad), 5 ml 4x Tris.HCl/SDS (pH 8.8), 100 µl 10% ammonium persulphate, 20 µl TEMED (AMRESCO) and 8.2 ml distilled water, were mixed in a 15 ml tube and poured to the glass plate sandwitch, with distilled water added on top of the gel to prevent evaporation during gel polymerization. Stacking gel solution with 4% acrylamide was prepared by mixing 1.33 ml 30% acrylamide/Bis solution (29:1, BioRad), 2.5 ml 4x Tris.HCl/SDS (pH 6.8), 50 µl 10% ammonium persulphate, 10 µl TEMED and 6.1 ml distilled water, and was added on the top of the resolving gel and a comb with 10 or 15-well was inserted and gel was left to polymerize. After gel polymerization, the wells were rinsed with distilled water and connected to the proper gel setup as indicated by the product manual. Sample loading was conducted by applying 20-50 µg protein to each well. Five µl of size standard marker (Precision plus protein™ dual color standards, BioRad) was applied to indicate protein sizes after separation. The electrophoresis was started with a constant 70 voltage (V) for 30 minutes for sample concentration followed by a constant 150 V for 1 hour for protein separation. After gel running, the resolved proteins were immobilized onto the nitrocellulose membrane (BioRad) by blotting at a constant 100 V for 60 to 90 minutes in ice cold transfer buffer (1.92 M glycine, 0.25 M Tris.base, pH 8.3). After blotting, the membrane was washed in distilled water, then TBST (20 mM Tris-HCl pH 7.4, 150 mM NaCl, and

0.05% Tween 20) for 5 minutes, followed by blocking in 5% skimmed milk in TBST for 1 hour at room temperature.

After blocking, the membrane was incubated with different antibodies including horseradish peroxidase (HRP)-conjugated antibody against myc (BD Biosciences, San Jose, CA) recognizing CRYAA, glyceraldehyde phosphate dehydrogenase (GAPDH; Sigma), β-actin (Sigma) or monoclonal antibodies against BiP (BD BioSciences), GADD153/CHOP (Santa Cruz Biotech, Santa Cruz, CA), caspase-3 (Santa Cruz), phosphorylated ER kinase (PERK, Santa Cruz) respectively, and appropriate HRP-conjugated Ig secondary antibodies. All antibodies are listed in **Table 3.4**. The staining signal was revealed by enhanced chemiluminescence (ECL, Amersham, Bucks, UK) using a ChemiDoc^{TM} System (BioRad). Gel imaging and band densitometry was obtained and measured by Quantity One 4.6.2 (BioRad). Except for those specified, all reagents were purchased from Sigma.

3.2.6.2 Monitoring Triton X-100 solubility of target protein

For Triton X-100 (Tx) solubility analysis, cells were washed twice with ice-cold PBS and added with lysis buffer, which contained 100 mM Tris-HCl (pH 7.4), 3 mM ethylene glycol tetraacetic acid (EGTA, Sigma), 5 mM $MgCl_2$, 0.5% Tx (Sigma), protease inhibitor cocktail (Complete, Roche), and 1 mM PMSF, for 2 minutes on ice. After centrifugation, the supernatant containing Tx-soluble protein was denatured in SDS sample buffer. The pellet containing Tx-insoluble protein was washed twice with ice-cold PBS, sonicated, and denatured in urea-SDS buffer (Zhang et al., 2007b). Tx-soluble and

Table 3.4 Concentrations of antibodies used in Western Blot.

Antibodies	Company	Origin	Concentration
Anti-MYC	Santa Cruz, CA, USA	Mouse	1:1000
Anti-GAPDH	Sigma	Mouse	1:2000
Anti-β-actin	Chemicon	Mouse	1:2000
Anti-Bip	BD BioSciences	Rabbit	1:1000
Anti-GADD153/CHOP	Santa Cruz CA, USA	Rabbit	1:1000
Anti-caspase3	Santa Cruz CA, USA	Mouse	1:1000
Anti-PERK	Santa Cruz CA, USA	Mouse	1:1000
Horseradish peroxidase-conjugated IgG	Amersham, Piscataway, NJ	Goat anti mouse	1:5000
Horseradish peroxidase-conjugated IgG	Amersham, Piscataway, NJ	Goat anti rabbit	1:5000

Tx-insoluble proteins from samples equivalent to $7.5x10^4$ cells were analyzed by 15% SDS-PAGE and immunoblotted using different antibodies against myc, GAPDH, β-actin (refer to Section 3.2.6.1).

3.2.6.3 Statistical analysis on protein expression level

After ECL imaging, relative signal densities representing the amounts of target proteins were measured by calculating the band densities with Quantity One 4.6.2, followed by normalization over the house-keeping protein GAPDH (for soluble protein) and β-actin (for insoluble protein). Data from the different groups were statistically analyzed using independent Student *t* test.

3.2.7 Immunofluorescence

Transfected cell grown on glass coverslips were fixed with freshly-prepared 2% neutral buffered paraformaldehyde (Sigma) in 0.1 M PBS, permeabilized with 0.05% Tx and 0.15% saponin (Yam et al., 2007a) and detected with a mouse monoclonal anti-myc antibody (recognizing CRYAA, Sigma, 200 ng/ml) followed by appropriate fluorescence conjugated IgG secondary antibody (Alexa Fluor® 488 IgG or RedX IgG goat anti-mouse conjugate, Invitrogen, 300 ng/ml) and nuclei counterstained with 4'-6-diamidino-2-phenylindole (DAPI; Sigma, 100 ng/ml). The staining was observed using a Leica DMRB fluorescence microscope (Leica, Wetzlar, Germany) equipped with SPOT RT color system (Diagnostic Instruments, Serling Heights, MI, USA).

For a semi-quantitative evaluation of cytoplasmic CRYAA aggregates, more than 200 cells per sample were analyzed. We graded CRYAA aggregation from 0 to 3+: 0, no aggregate; 1+, few dot-like aggregates; 2+, more dot-like aggregates and 3+, extensive large aggregates. The staining index, indicative of phenotype severity, was calculated using the formula: 4(3+)%+2(2+)%+1(1+)% (Yam et al., 2005).

3.2.8 Confocal double immunofluorescence

CRYAA tranfected cells grown on glass coverslips were fixed as described in Section 3.2.7. After blocking, myc immunoreactivity was detected by mouse monoclonal anti-myc antibody followed by Alexa Fluor® 488 IgG or RedX IgG goat anti-mouse conjugate. The open antigen binding sites on the secondary antibodies were saturated by normal goat serum. Then, endoplasmic reticulum (ER) was labeled using another mouse monoclonal antibody against protein disulfide isomerase (PDI, BD BioSciences, 200 ng/ml) followed by Rhodamine Red-X goat anti-mouse IgG (Invitrogen, 300 ng/ml). After nuclear staining by DAPI, samples were examined with confocal scanning microscopy (LSM 510 META, Carl Zeiss, Gottingen, Germany).

3.2.9 Terminal apoptosis assay

Fixed cells were stained for myc and red X-conjugated secondary antibody and nuclei counterstained with DAPI. Samples were examined by fluorescence microscopy (DMRB) equipped with a color imaging system (Spot RT). Terminal apoptosis rate was

represented as percentage of cells with fragmented nuclei. For each experiment (n=3), 10 random images (x40 objective) were analyzed.

3.2.10 Transcription analysis

3.2.10.1 RNA extraction and purification

Total RNA was obtained by a RNA purification kit (RNeasy kit, Qiagen, Valencia, CA) and an on-column DNase digestion kit (RNase-free DNase kit, Qiagen). Cells cultured in 60-mm dish were directly lysed in 350 μl RLT buffer added with 1% β-ME. The lysate was spun through a QIAshredder spin column at 6000 g for 3 minutes for complete lysis and release of RNA and DNA. The sample was then transferred to a new microcentrifuge tube and added with 350 μl 70% ethanol, and mixed well by vortex. The sample, up to 700 μl including precipitates that might have formed, was transferred to an RNeasy spin column placed in a 2 ml collection tube (supplied), and centrifuged for 60 sec at 6000 g. The flow-through was discarded. Buffer RW1 (700 μl) was added to the RNeasy spin column, and centrifuged for 60 seconds at 6000 g to wash the spin column membrane. After discarding the flow-through, 500 μl Buffer RPE was added to the RNeasy spin column, and centrifuged for 60 seconds at 6000 g to wash the spin column membrane. The flow-though was discarded and 500 μl Buffer RPE was added to the RNeasy spin column and centrifuged for 2 minutes at 6000 g to wash the spin column membrane. The RNeasy spin column was placed in a new 1.5 ml collection tube, with 25 μl RNase-free water directly added to the spin column membrane, and centrifuge for 1 minute at 6000 g to elute the RNA. The collected RNA was quantified using NanoDrop ND-1000 UV-Vis

spectrophotometer (NanoDrop technologies, Wilmington, DE, USA) and NanoDrop 3.1.0 sofware. The absorbencies at wavelengths of 260 nm and 280 nm were measured. The reading at 260 nm was the concentration of RNA and the ratio of reading 260 nm over 280 nm represented the RNA purity. In this study, the ratios were between 1.8 and 2.0.

3.2.10.2 RNA reverse transcription

Reverse transcription, taken to transcribe RNA to the first strand complementary DNA (cDNA), was performed with random hexanucleotide primer (Roche, Basel, Switzerland) and reverse transcriptase (SuperScript™ III; Invitrogen). Reagents were mixed according to the manufacturer's protocol. Firstly, the mixture (0.5 mM random primer, 0.5 mM dNTP mixture, 1000 ng total RNA, and water to 13 µl volume) was incubated at 65 °C for 5 minutes, then added First Strand Buffer, 0.05 M DTT, RNaseOUT Recombinant RNase inhibitor, SuperScript III RT enzyme, and continued incubation at 25°C for 5 minutes, and 50°C for 60 minutes, followed by 70°C for 15 minutes to stop reaction by enzyme inactivation. The cDNA was stored at -20 °C until further use.

3.2.10.3 Semi-quantitative reverse transcription-polymerase chain reaction (RT-PCR)

Semi-quantitative RT-PCR was applied to amplify and detect target genes. Primers used to amplify for CRYAA, heat-shock protein 70 and 90 as well as other stress markers, were listed in **Table 3.5**. The reaction components for PCR were prepared according to the manufacture's protocols (Invitrogen). The reaction mixture included 50 mM $MgCl_2$ (1.5 µl), 10x PCR buffer (2.5 µl), 10 mM dNTP (0.5 µl), primers (0.3 µl), Taq DNA

Table 3.5 Expression primer sequences.

Gene	GeneBank Accession No.	Specific primer sequences (5' to 3')	Product size (bp)
αA-crystallin (*CRYAA*)	U05569	F: CGGGACAAGTTCGTCATCTT R: GCAGACAGGGAGCAAGAGAG	203
Heat-shock protein 70 (*Hsp70*)	NM05345	1F: AAGTACAAAGCGGAGGACG 1R: GATGGGGTTACACACCTGC 2F: TGCTGATCCAGGTGTACGAG 2R: CGTTGGTGATGGTGATCTTG	249 185
Heat-shock protein 90α (*Hsp90α*)	NM005348.3	F: ACCCAGACCCAAGACCAACCG R: ATTTGAAATGAGCTCTCTCAG	141
Superoxide dismutase (*SOD*)	NM000454.4	F: AGGGCATCATCAATTTCGAGC R: CAAGGGAATGTTTATTGGGCG	430
αB-crystallin (*CRYAB*)	NM001885.1	F: TCACCTAGCCACCATGGACATCGCCA R: CAAAAGCTTATTACTATTTCTTGGGGG	541
Metallothionein 1M (*MT*)	NM176870.2	F: GCAAAGAGTGCAAATGCACCTC R: TCAGGCACAGCAGCTGCACT	125
Interleukin-6 (*IL-6*)	NM000600.2	F: CTGGTCTTTTGGAGTTTGAGGTATACC R: CCATGCTACATTTGCCGAAGA	295
Glyceraldehyde 3-phosphate dehydrogenase (*GAPDH*)	BC014085	F: GAAGGTGAAGGTCGGAGT R: GAAGATGGTGATGGGATTTC	225

polymerase (0.2 µl) and distilled water to a final volume of 25 µl. The mix was denatured to 94 °C followed by 30 cycles of 94 °C (denaturation) for 30 seconds, 55 to 60 °C (annealing) for 30 seconds and 72 °C (extension) for 30 seconds, then a final extension at 72 °C for 7 min. PCR products were then analyzed by agarose gel electrophoresis.

3.2.10.4 Agarose gel electrophoresis for DNA visualization

Agarose gel electrophoresis was applied to resolve and quantify the PCR product of target genes. Agarose gel (2%) was made by dissolving 1 g agarose (Sigma) in 50 ml 1x TAE (Tris-acetic acid-EDTA) buffer (BioRad) with microwave heating. The gel solution was added with ethidium bromide (0.01%) and poured to the agarose gel holder (BioRad). After insertion of comb (8 to 15 wells), the gel solution was allowed to solidify for 30 minutes at room temperature.

The gel was then placed in the appropriate gel tank 0.5x TAE running buffer and the wells were rinsed by the buffer. DNA samples were first mixed with DNA loading dye (Invitrogen) in a ratio of DNA: dye = 5:2 vol/vol. The mixtures were loaded to the wells, as well as DNA size standard (50 base-pair) markers (BioRad). The gel was run at a constant 100 V for 25 minutes under the blue frontier reached the lower one-third of the gel. DNA bands were visualized under UV transillumination using Gel Doc (BioRad). Images were captured and band densitometry was analyzed by Quantity One 4.0.3 (BioRad).

3.3 Results

3.3.1 Expression of WT and cataract-causing CRYAA mutants in B3 cells

Human lens epithelial B3 cell line was used in this study. Before transfection, negligible expression of endogenous *CRYAA* in B3 cells was verified by RT-PCR (**Figure 3.3**). This result was consistent with the earlier description that B3 cells ceased to produce αA-crystallin after passage 11 (Fleming et al., 1998). A repertoire of congenital cataract-causing *CRYAA* mutants (*R12C, R21L, R49C, G98R and R116C*) and *WT CRYAA* were cloned into the pcDNA6-His/myc expression vector and verified by direct sequencing (**Figure 3.4**), *R12C CRYAA* was introduced by Zhang (Zhang et al., 2009b) in our lab. They were transfected to human lens epithelial B3 cells (at seeding density of $2x10^4$ cells/cm^2), respectively. They were characterized for protein solubility and cellular localization.

At 48-hour post-transfection, protein samples using RIPA lysis method was collected and analyzed by western blotting for myc, representing CRYAA. The expression of pHis/myc-CRYAA^{G98R} was different from WT and other CRYAA mutants (**Figure 3.4A**). The expression of G98R CRYAA was almost 10-fold less than that of WT and other CRYAA mutants even upon transfection with different ratios of pHis/myc-CRYAA^{G98R} DNA to Fugene HD reagent. Normally, the optimized ratio of DNA to Fugene HD reagent is 1:3 when transfection. As for G98R CRYAA, different ratios of them (1:2, 1:3, 1:4, 1:5) could not come about high transfection efficacy, suggested that there were changes of microstructure for G98R CRYAA. When we tested the molecular weight of G98R CRYAA and found that it was shifted to a smaller size range than other CRYAA

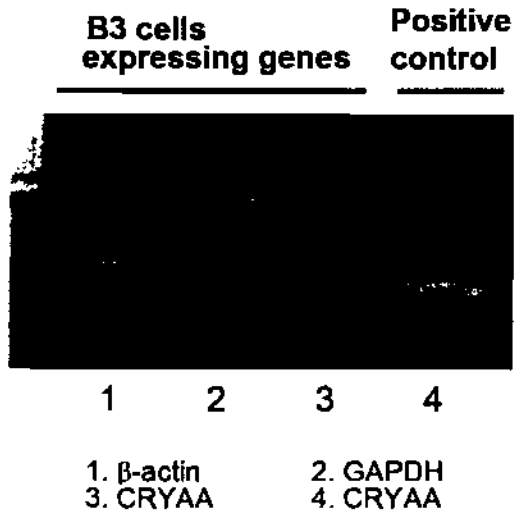

Figure 3.3 Reverse transcription-polymerase chain reaction (RT-PCR) amplification of *β-actin*, *GAPDH* and *CRYAA* in B3 cells. Lane 1, *β-actin* ofB3 cells collected at passage 20; lane 2, *GAPDH* ofB3 cells at passage 20; lane 3, *CRYAA* ofB3 cells at passage 20; lane 4, posivtive control for *CRYAA*.

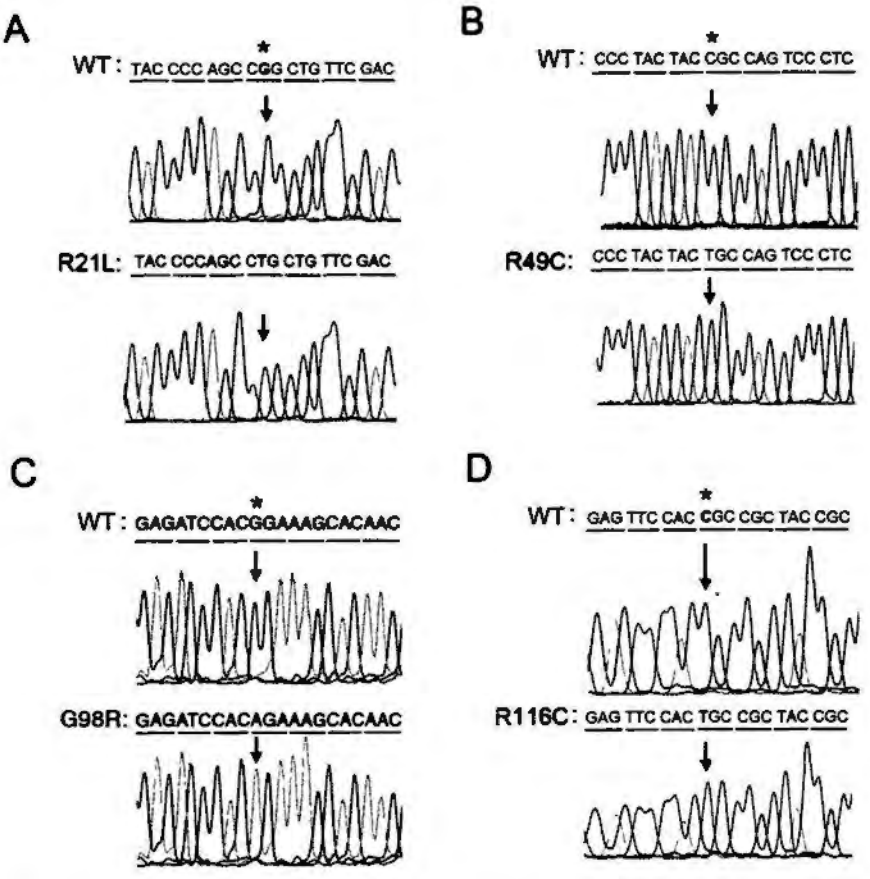

Figure 3.4 Direct sequencing results of CRYAA mutants. Direct sequencing confirmed the base change of **(A)** R21L, c.62G>T (indicated by arrow) for pHis/myc-CRYAA^{R21L}, **(B)** R49C, c.145C>T (indicated by arrow) for pHis/myc-CRYAA^{R49C}, **(C)** G98R, c.292G>A (indicated by arrow) for pHis/myc-CRYAA^{G98R} and **(D)** R116C, c.346C>T (indicated by arrow) for pHis/myc-CRYAA^{R116C}.

mutants (23 kDa of G98R CRYAA compared to 26 kDa of other CRYAA mutants).

When the transfected cells (24 hours after transfection) were collected in 0.5% Tx lysis buffer and fractionated to Tx soluble and insoluble proteins. By western blotting (**Figure 3.5 B**), His/myc-tagged CRYAA mutants carrying R12C, R21L, R49C or R116C were predominantly Tx-soluble but G98R CRYAA was existing more in Tx insoluble fraction. By band densitometry analysis, specific CRYAA bands in both Tx soluble and insoluble fractions from the same protein samples were measured. The average Tx solubilities were 98± 0.876% for WT CRYAA, 95 ± 0.789% for R12C, 96 ± 0.578% for R21C, 68 ± 0.854% for R49C and 96 ± 0.831% for R116C. However, this solubility was tremendously dropped to 1.6 ± 0.239% for G98R CRYAA. This low solubility level was consistently observed upon transfection with different ratios of pHis/myc-CRYAA^{G98R} to Fugene HD reagent. The transfection efficiency was similar among WT and all studied mutants, as verified by immunofluorescence of myc, representing CRYAA (**Figure 3.6**). The efficiency was maintained at about 50% at day 2.

In this experiment, the Tx solubility of G98R CRYAA was substantially reduced when compared to WT and other reported mutants. This suggested that possible folding defects could occur during the biosynthesis of G98R CRYAA in B3 cells.

3.3.2 G98R CRYAA protein expression and localization in B3 cells

Due to the disturbance of G98R CRYAA expression in B3 cells, we further explored more data to reveal the mechanism of this mutant gene resulting in cataract formation.

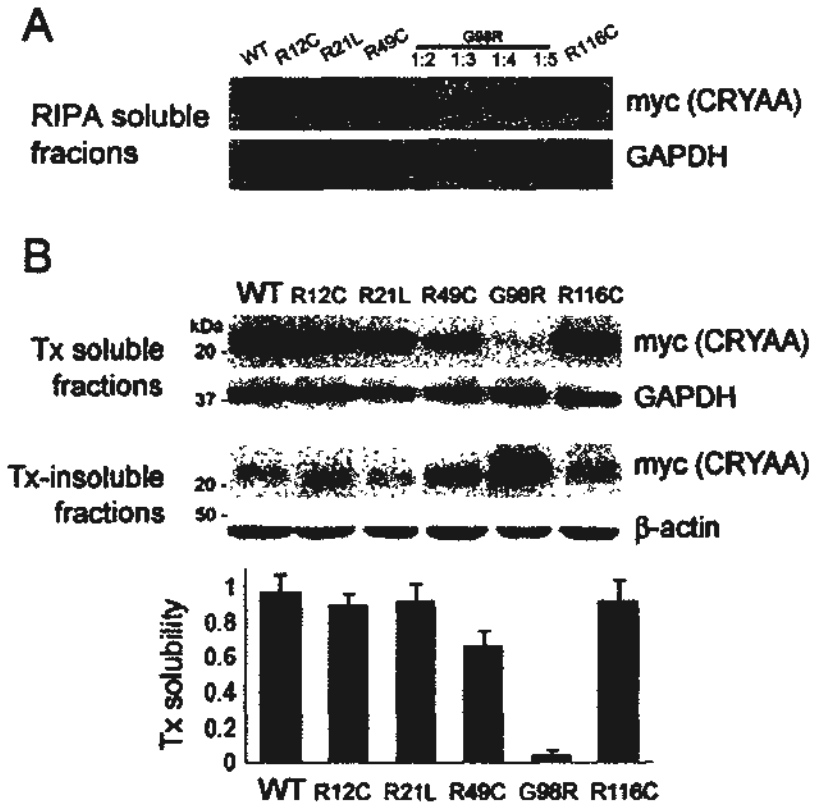

Figure 3.5 Expression of WT and cataract-causing mutant CRYAA in B3 cells. (A) Western blotting of myc detected WT and different mutant CRYAA protein in RIPA buffer. G98R CRYAA had reduced solubility when compared to WT or other mutants. Similar observation was made for different ratios of DNA: Fugene. **(B)** Tx solubility assay of WT and different CRYAA mutants in B3 cells by Western blotting of myc (detecting CRYAA), housekeeping GAPDH and β-actin. The band densitometry analysis showed the drastic reduction of Tx solubility of G98R CRYAA when compared to WT or other mutants.

Figure 3.6 Confocal immunofluorescence images of WT and G98R CRYAA in B3 cells. Distribution of WT and G98R CRYAA was revealed by myc staining (green) in B3 cells by confocal immunofluorescence. Nuclei were stained with DAPI (blue). WT CRYAA was diffusely distributed in cytoplasm, whereas G98R CRYAA formed large intracellular aggregates in the transfected B3 cells.

The construct of pHis/myc-CRYAA^{G98R} were verified by direct sequencing (**Figure 3.4 C**). The transfected cells were extracted with 0.5% Triton X-100 (Tx) followed by fractionation into Tx soluble and insoluble portions. At steady state, His/myc-WT CRYAA was entirely Tx-soluble, however, His/myc-G98R CRYAA was Tx-insoluble (**Figure 3.5**). The average insolubility ratio among four experiments was 3.8± 0.236% for WT CRYAA and 98.4± 0.676% for G98R CRYAA in B3 cells. Only faint Tx soluble G98R CRYAA protein was detectable. These results were consistent with previous study which showed that G98R mutant protein almost exclusively partition into insoluble fractions and form inclusion bodies compared to wild type αA-crystallin when expressed in the bacterial cells (Singh et al., 2006).

Immunofluorescence study showed that pHis/myc-CRYAA^{G98R} (myc staining in green) formed large-sized cytoplasmic aggregates whereas pHis/myc-CRYAA^{WT} was located diffusely in the cytoplasm, nuclei were stained with DAPI (blue) in transfected B3 cells (**Figure 3.6**). To specifically localize the His/myc-G98R CYRAA to any cytoplamic organelles, we performed confocal double immunofluorescence to visualize myc and markers for different organelles. The aggregated G98R CYRAA was intensively co-localized with protein disulfide isomerase (PDI), an ER resident protein (**Figure 3.7**). In contrast, WT CRYAA exhibited mild co-distribution with PDI. We further observed that both WT and G98R CRYAA were not co-localized with Giantin, a Golgi marker (**Figure 3.8**). This demonstrated, for the first time, that mutant CRYAA formed insoluble aggregates in the ER, not in the Golgi apparatus. We suggested that the misfolded mutant G98R CRYAA-induced pre-senile cataract could be an ER storage disease.

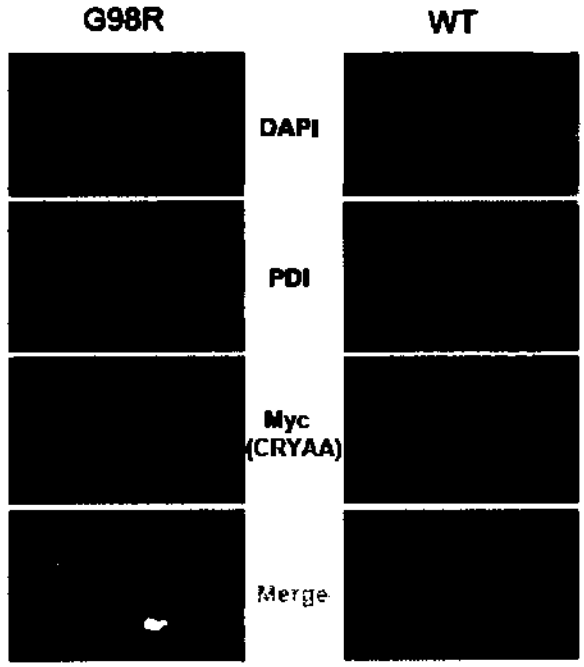

Figure 3.7 Confocal double immunofluorescence images of WT and G98R CRYAA in B3 cells. G98R CRYAA (myc staining in green) formed intracellular aggregates and was intensely codistributed with endoplasmic reticulum (with an ER marker PDI staining in red) in the overlay image (yellow). WT CRYAA (myc staining) was diffusely distributed in the cytoplasm and had only mild codistribution with PDI. Nuclei were stained with DAPI (blue). Scale bars: 10 μm.

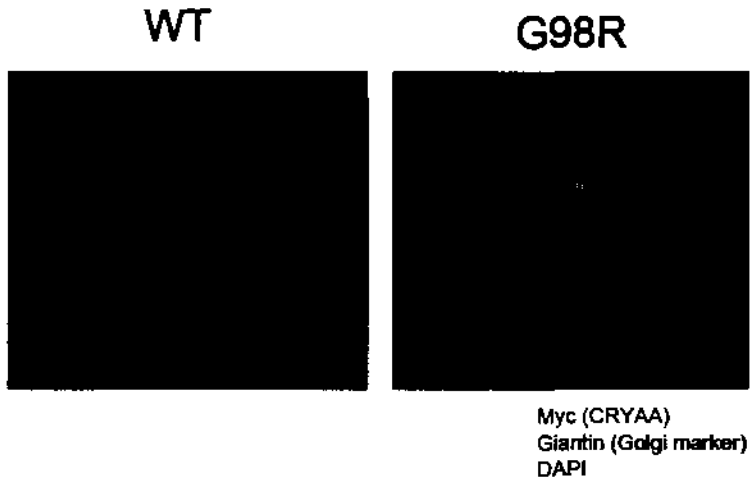

Figure 3.8 Confocal double immunofluorescence images of WT and G98R CRYAA in B3 cells. G98R CRYAA (myc staining in green) and WT CRYAA (myc staining) were not located in Golgi apparatus as marked by giantin (in red) in the overlay image. Nuclei were stained with DAPI (blue).

3.3.3 G98R CRYAA aggregates were reduced by TMAO

We hypothesized that the misfolding of G98R CRYAA with the exposed hydrophobic peptide patches could be rectified by treatment with TMAO, which is an osmolyte with hydrophobic nature and acts as chemical chaperone to stabilize protein with a tightly packed conformation. To authenticate this action, we also tested other small molecule chemicals, 4-PBA, glycerol and DMSO, by virtue of the chaperoning activity reported previously (Brown et al., 1996; Burrows et al., 2000; Ohashi et al., 2003; Ohnishi et al., 2002; Ono et al., 2009; Robben et al., 2006; Yam et al., 2007b). After treatment for 2 days separately with these chemicals, the distribution of transfected CRYAA was examined. Both TMAO and 4-PBA treatments resulted in fewer cells exhibiting large-sized myc-positive aggregates (**Figures 3.9 A and B**), majority of these transfected cells had cytoplasmic punctate staining after treatment (about 50 cells with punctuate staining in total 70 transfected cells). A scoring analysis showed 10% of TMAO-treated mutant cells and 12% of 4-PBA-treated mutant cells with 3+ level of aggregation (**Figure 3.10**). This was highly contrasted to ~75% of mutant cells before treatment (graded as 3+). The staining index, representing the phenotype severity, was also dramatically reduced after TMAO or 4-PBA treatment, approaching to that of WT expressing cells (**Figure 3.10 C**). Treatment with 0.5 or 1% DMSO was ineffective to reduce His/myc-G98R CRYAA aggregates. Also, toxicity was observed in cells treated with 1 or 5% of glycerol.

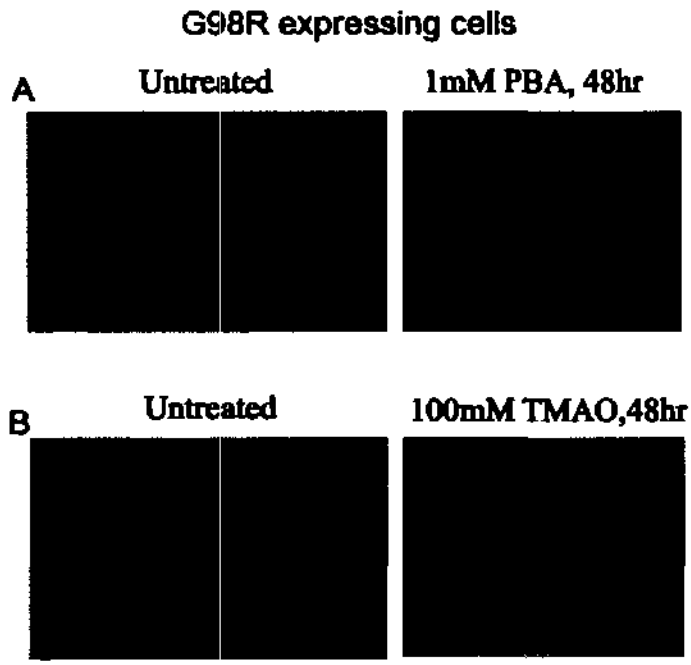

Figure 3.9 Confocal immunofluorescence images of G98R CRYAA in B3 cells treated by small chemicals. **(A, B)** G98R CRYAA was stained with myc (green) in trasnfected B3 cells. Untreated G98R-expressing B3 cells showed aggregated G98R CRYAA, which was reduced after **(A)** 4-PBA (1 mM) and **(B)** TMAO (100 mM) treatments.

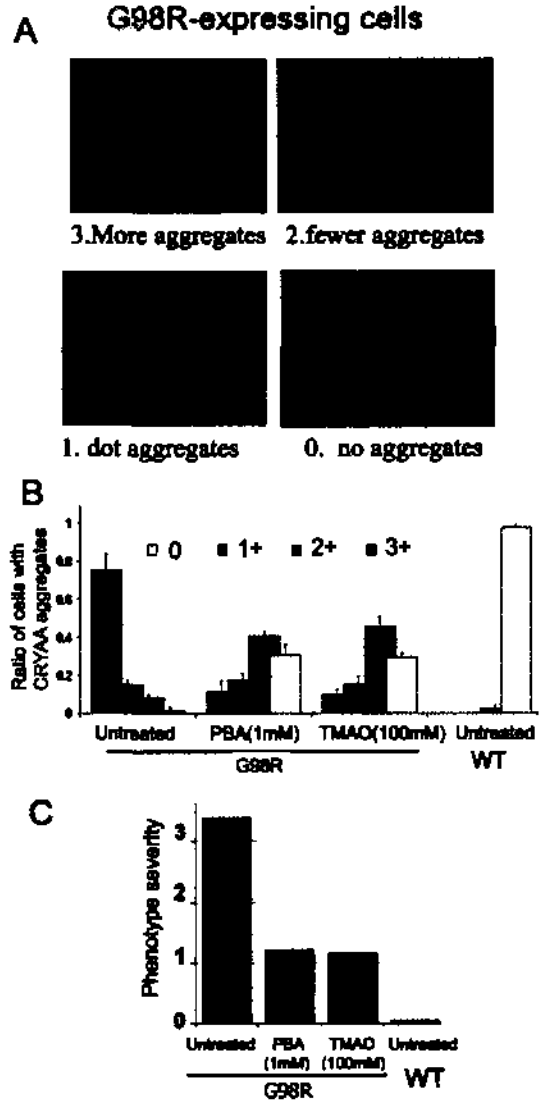

Figure 3.10 Small chemicals reduced G98R CRYAA aggregates in B3 cells. (A) Distribution of G98R CRYAA in trasnfected B3 cells. CRYAA aggregation was graded from 0 to 3+: 0, no aggregate; 1+, few dot-like aggregates; 2+, more dot-like aggregates and 3+, extensive large aggregates. **(B)** Semi-quantitative scoring of intracellular CRYAA aggregates in cells. **(C)** Staining index, representing phenotype severity, showed dramatic reduction after 4-PBA or TMAO treatment.

3.3.4 TMAO reduced Triton X-100-insoluble G98R CRYAA in dose and time dependent manners

Treatment with 100 mM TMAO or 1 mM 4-PBA for 2 days reduced Tx-insoluble His/myc-G98R CRYAA whereas the expression of His/myc-WT CRYAA was unaffected (**Figure 3.11 A**). The percentage of Tx-insoluble mutant protein after TMAO or 4-PBA treatment was similarly decreased to almost one-fourth as that in untreated cells (22 ± 0.764% for TMAO treatment and 28 ± 0.464% for 4-PBA; $p<0.05$, independent Student *t*-test; **Figure 3.11 B**). When examined at 5 days after treatment, 4-PBA-treated cells have notable morphological changes, showing a slender fibroblast-like morphology. Due to these undesirable morphological changes, 4-PBA was not selected in further experiments. Treatment with 0.5 or 1% DMSO was again ineffective in reducing the insoluble His/myc-G98R CRYAA (**Figure 3.11 B**), and 1 or 5% of glycerol killed cells. Hence, DMSO and glycerol were not used in subsequent experiments.

3.3.4.1 TMAO reduced Triton X-100-insoluble G98R CRYAA in dose-dependent manner

A 2-day treatment with TMAO at concentrations from 25 to 300 mM led to a dose-dependent decrease of Tx-insoluble His/myc-G98R CRYAA (**Figure 3.12**). TMAO at 25 mM reduced Tx-insoluble G98R CRYAA to 83 ± 0.464% (compared to 98 ± 0.659% for untreated mutant protein). Tx-insoluble G98R CRYAA was further reduced to 48 ± 0.454% at 50 mM and to 24 ± 0.458% at 100 mM treatment. The reduction was statistically significant ($p<0.05$, independent Student *t*-test). Cell death became prevalent

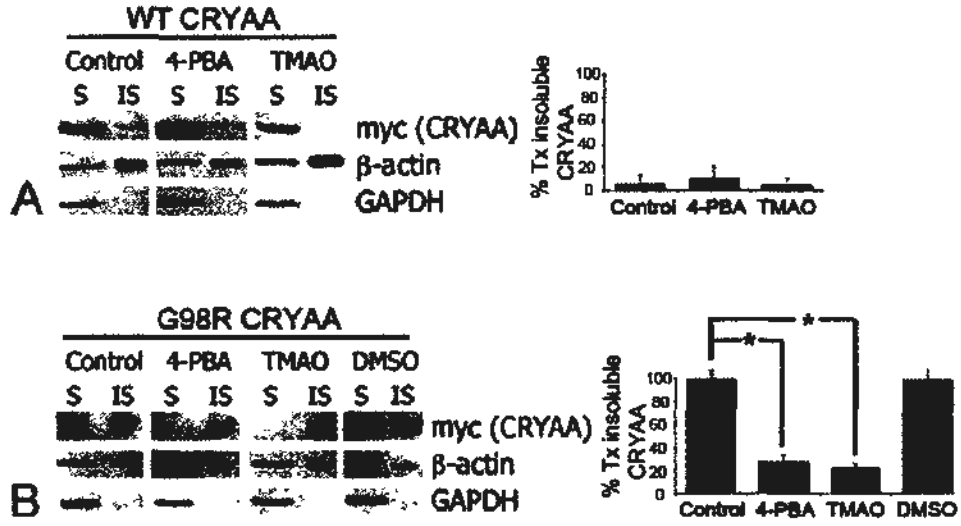

Figure 3.11 The effects of small chemicals on detergent solubility of CRYAA. (A) Western blot analysis of myc (CRYAA) showed that WT was mainly Tx-soluble and not affected by 4-PBA or TMAO treatment. **(B)** Untreated G98R CRYAA was predominantly Tx-insoluble, which was significantly reduced after 4-PBA (1 mM) or TMAO (100 mM) treatment for 2 days. The asterisk (*) indicated a $p<0.05$ by independent Student's *t*-test. DMSO (1%) did not affect mutant insolubility.

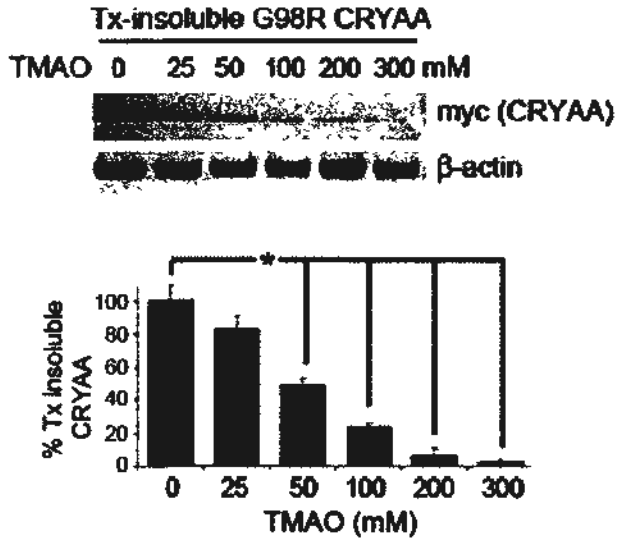

Figure 3.12 TMAO reduced detergent insoluble G98R CRYAA dose-dependently. Treatment with TMAO (25 mM or higher) for 2 days significantly decreased Tx-insoluble G98R CRYAA, compared to the untreated control. The asterisk (*) indicated a $p < 0.05$ by independent Student's t-test.

upon treatment with TMAO at concentrations higher than 200 mM.

3.3.4.2 TMAO reduced Triton X-100-insoluble G98R CRYAA in time-dependent manner

We further observed a time-dependent decrease of Tx-insoluble His/myc-G98R CRYAA when cells were treated with 100 mM TMAO (**Figure 3.13**). At 12 hours after treatment, the expression level of Tx-insoluble mutant protein was decreased to 67 ± 0.434% (compared to 98 ± 0.984% before treatment). It was further reduced to 28 ± 0.844% at 24 hours, 21 ± 0.745% at 48 hours and 3 ± 0.132% at 72 hours, and the reduction was statistically significant ($p<0.05$, independent Student *t*-test). It is notable that while the insoluble G98R CRYAA decreased by TMAO treatment, the level of Tx-soluble G98R protein did not show any changes (always with low expression level in soluble fractions, about 1.6%). It can be postulated that TMAO reduced the detergent insoluble CRYAA mutant peptides through a protein degradation mechanism rather than to refold them.

3.3.5 TMAO induced G98R CRYAA degradation via ubiquitin-proteasome pathway (UPP)

We next investigated how TMAO reduced Tx-insoluble pHis/myc-CRYAA^{G98R} and resolved protein aggregation. Addition of 10 μM MG132, a reversible inhibitor of UPP, in transfected cell culture for 8 hours, a substantial increase of Tx-insoluble His/myc-G98R CRYAA protein was observed (**Figure 3.14**), and the reduced level of Tx-

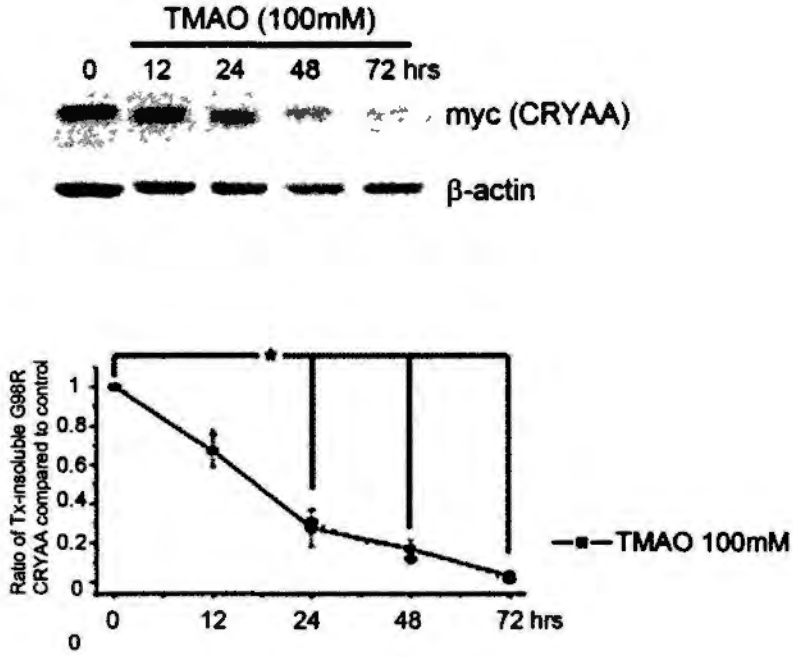

Figure 3.13 TMAO reduced detergent insoluble G98R CRYAA time-dependently. Treatment with TMAO (100mM) for 24 hours or longer time significantly decreased Tx-insoluble G98R CRYAA compared to the untreated control. The asterisk (*) indicated a $p < 0.05$ by independent Student's t-test.

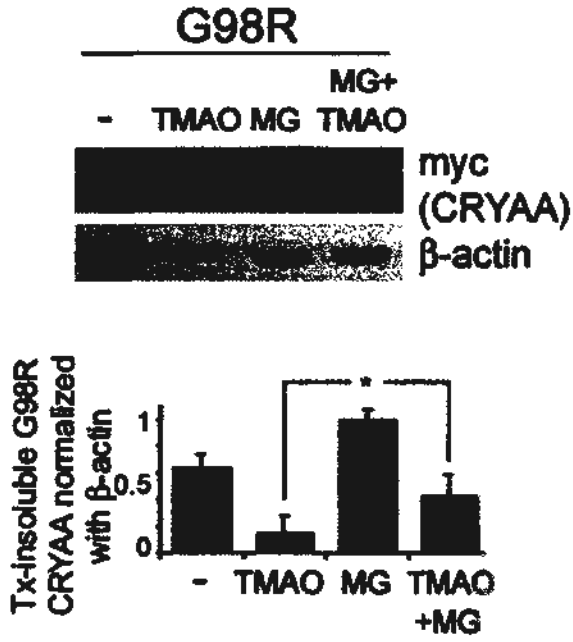

Figure 3.14 The effect of MG132 on the expression of G98R CRYAA. Western blotting showed that reduced level of Tx-insoluble G98R CRYAA after TMAO (100 mM, 2 days) was reversed by MG132 (10 μM, 8 hours) and MG132 alone further increased Tx-insoluble mutant protein. The asterisk (*) indicated a $p < 0.05$ by independent Student *t*-test.

insoluble G98R CRYAA after TMAO (100 mM, 2 days) treatment was reversed by MG132 (10μM, 8 hours). This indicated that G98R CRYAA protein could be degraded via UPP. Blocking of UPP resulted in more Tx-insoluble protein and augmented the mutant CRYAA aggregation in cells, as demonstrated by immunofluorescence, compared to non-MG132-treated G98R cells (**Figure 3.15**). After treatment with 100 mM TMAO for 2 days, a low level of Tx-insoluble mutant was again observed (**Figure 3.15**). The levels were similar as in previous experiments. Further incubation of these TMAO-treated cells with 10 μM MG132 for 8 hours increased Tx-insoluble CRYAA protein. This was not significantly different from the untreated mutant cells. Immunofluorescence showed that His/myc-G98R CRYAA aggregates reappeared inside cells compared to TMAO-treated cells. A semi-quantification of cells with visible intracellular G98R CRYAA aggregates was performed. Nearly all MG132-treated mutant cells showed His/myc-CRYAA aggregates (**Figure 3.15**). The treatment with both TMAO and MG132 resulted in 73% of cells with aggregates, which was similar to the untreated mutant cells (81%). Only TMAO treatment significantly reduced the cells with CRYAA aggregates to 36% ($p<0.05$ when compared to untreated cells or cells with both TMAO and MG132 treatments). On the other hand, treatment with 10 μM 3-methyladenine (3-MA, inhibitor of autophagy) did not show any change of His/myc-G98R CRYAA solubility and subcellular aggregation (**Figure 3.16**), indicating that CRYAA was not a substrate of autophagy.

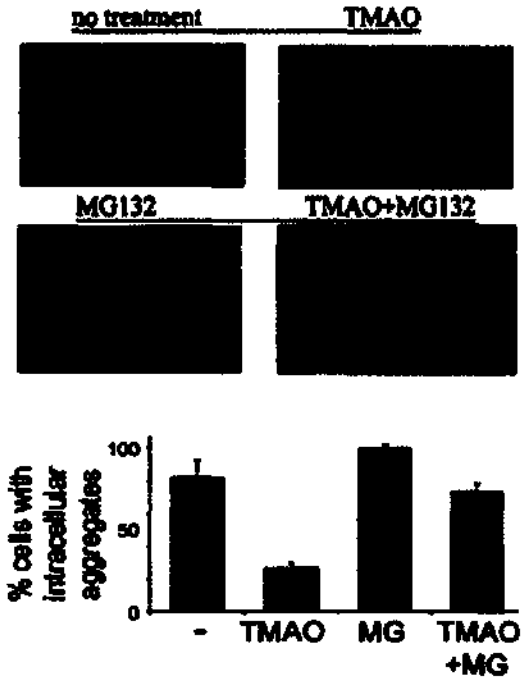

Figure 3.15 The effect of MG132 on the distribution of G98R CRYAA. Confocal immunofluorescence showed reduced level of cytoplasmic G98R CRYAA aggregates after TMAO (100 mM, 2 days) treatment were reversed by MG132 (10 μM, 8 hours) treatment and MG132 alone further increased G98R CRYAA aggregates in transfected B3 cells. The asterisk indicated a $p < 0.05$ by independent Student *t*-test.

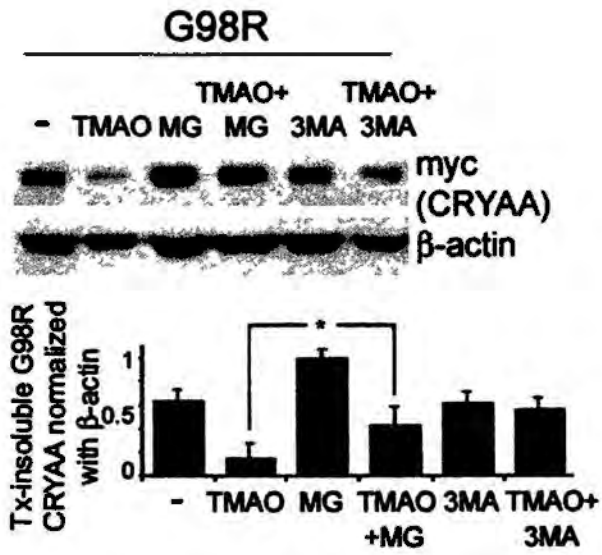

Figure 3.16 The effect of 3-MA on the expression of G98R CRYAA. Western blotting showed no effect of 3-methyladenine (3-MA, inhibitor of autophagy) treatment on Tx-insoluble G98R CRYAA and null changes of Tx-insoluble G98R CRYAA after treatment with 10 μM 3-MA, unlike that of MG132 treatment. The asterisk indicated a $p < 0.05$ by independent Student *t*-test.

3.3.6 ER stress and apoptosis caused by aggregated G98R CRYAA were alleviated by TMAO treatment

We examined if TMAO affected the expression of ER stress-associated proteins, including phosphorylated ER kinase (PERK) and binding immunoglobulin protein (BiP or glucose regulated protein 78, Grp78), in transfected B3 cells. These proteins were upregulated upon His/myc-G98R CRYAA expression when compared to WT CRYAA (**Figure 3.17**). The expressions of PERK and BiP in mutant-expressing cells were increased about two-fold compared with the WT-expressing cells (PERK: from 13 ± 0.153% to 22 ± 0.215% and BiP: from 51 ± 0.542% to 92 ± 0.765%, respectively). B3 cells incubated with transfection Fugene HD reagent had no observable changes in the ER stress-related protein expression. Hence, the induction of ER stress was due to the altered biosynthesis of mutant protein. With TMAO (100 mM) treatment for 2 days, the expression of these ER stress markers was substantially reduced to a level about one-half as that of the untreated cells ($p<0.05$; **Figure 3.17**). The expression of PERK decreased from 22 ± 0.734% to 7 ± 0.212% and BiP was from 92 ± 0.873% to 47 ± 0.983%. $CRYAA^{WT}$-expressing cells were not affected by TMAO treatment, indicating that this chemical chaperone acted on proteins that were not natively folded.

I further explored if the TMAO treatment affect cell apoptosis related with mutant protein expression. Western blot analysis showed that CHOP/GADD153 and caspase-3 were upregulated in pHis/myc-$CRYAA^{G98R}$-expressing B3 cells by nearly two folds compared to pHis/myc-$CRYAA^{WT}$-expressing cells. CHOP expression was 13 ± 0.342%

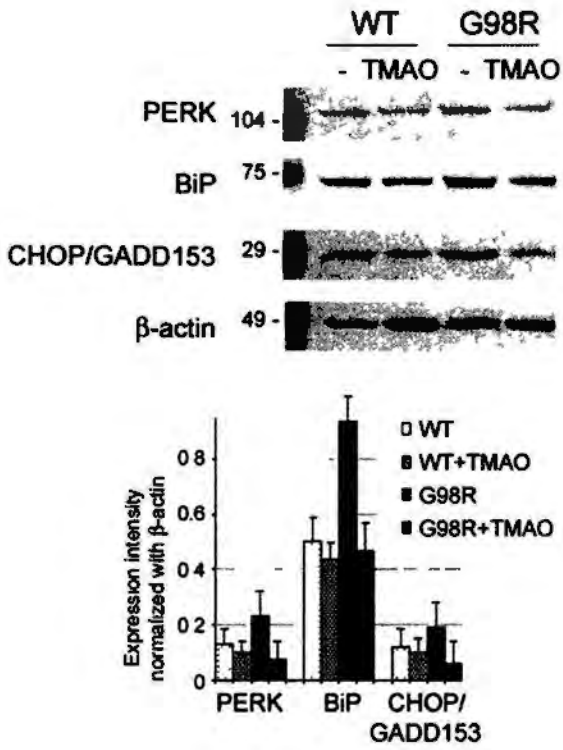

Figure 3.17 TMAO alleviated ER stress of cells expressing G98R CRYAA. TMAO (100 mM, 2 days) reduced expression of ER stress and UPR markers (PERK, BiP, and CHOP/GADD153) that were upregulated in G98R CRYAA-expressing cells. No specific change was observed for WT cells.

compared to GAPDH in WT CRYAA-expressing cell lysate versus 19 ± 0.284% in G98R CRYAA-expressing lysate; caspase-3 was 20 ± 0.531% compared to GAPDH in WT CRYAA-expressing cell lysate versus 29 ± 0.732% in G98R CRYAA-expressing lysate ($p<0.05$, independent Student *t*-test, **Figures 3.17 and 3.18 A**). This was accompanied by increases in percentage of transfected cells undergoing apoptosis which were shown by appearance of fragmented nuclei as revealed by double immunofluorescence of myc (representing CRYAA) and nuclear dye DAPI (apoptosis rate in G98R CRYAA-expressing cells was 22 ± 0.632% versus 6 ± 0.238% for WT CRYA-expressing cells; **Figure 3.18**). Treatment with TMAO (100 mM) for 2 days resulted in reduced expression of both CHOP/GADD153 and caspase-3 ($p<0.05$, independent Student *t*-test; **Figures 3.17 and 3.18 A**). The expression of CHOP normalized with GAPDH was decreased from 19 ± 0.294% to 6 ± 0.198% and caspase-3 was from 2 ± 0.138% to 18 ± 0.328%. Consistent results were obtained in experiments done in triplicate. The suppression of apoptosis-related proteins was supported by a lower percentage of cells showing fragmented nuclei in TMAO-treated G98R CRYAA-expressing cells (13%) (compared to 22% in untreated cells; **Figure 3.18 B**). TMAO treatment on WT CRYAA-expressing cells did not show any expression changes of apoptosis-related protein or in percentage of apoptotic cells (**Figure 3.18 B**).

3.3.7 Effect of TMAO treatment on cell stress signaling

The effect of TMAO on stress signalling was investigated by examining the gene expression involved in heat-shock response, including Hsp70 and 90α and cell stress responses. By semi-quantitative PCR, TMAO treatment (100mM) on G98R CRYAA-

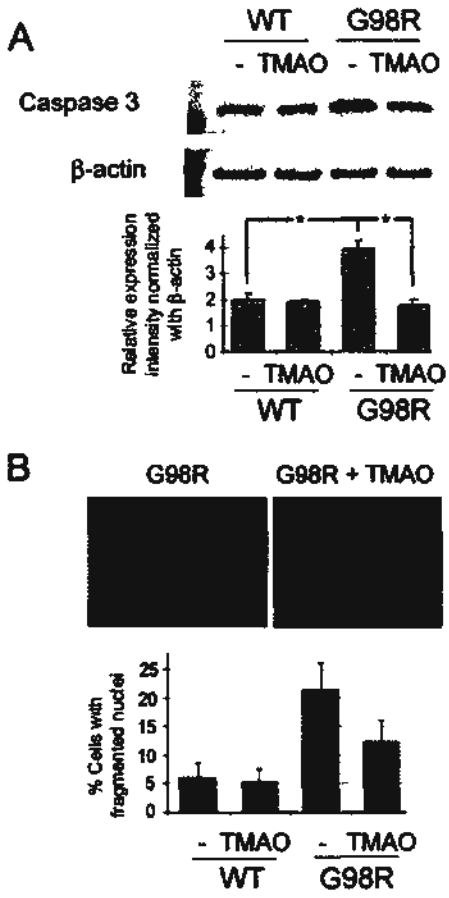

Figure 3.18 Trimethylamine N-oxide alleviated apoptosis of cells expressing G98R CRYAA. (A) Reduced active caspase-3 expression in G98R CRYAA-expressing cells treated with TMAO compared to untreated control. The asterisk indicated a $p < 0.05$ by independent Student *t*-test. **(B)** Fewer G98R CRYAA-expressing cells exhibited fragmented nuclei after TMAO treatment compared to untreated control.

expressing cells 48 hours showed an up-regulation of Hsp70 expression and this was confirmed by using two different pairs of specific primers, Hsp 70(1) and Hsp 70(2) (**Figure 3.19**). No change was observed for Hsp90α expression in G98R CRYAA-expressing cells treated with TMAO. In non-transfected cells, Hsp70 and Hsp90 expression was not altered by TMAO treatment (**Figure 3.19**). On the other hand, gene expression of various cell stress signaling, including superoxide dismutase (SOD) and αB-crystallin (CRYAB) for oxidative stress, metallothionein (MT) for heavy metal-induced stress and interleukin-6 (IL6) for inflammatory-associated stress, was unaffected by TMAO treatment in G98R CRYAA-expressing cells. Therefore, it is suggested here that TMAO treatment on the regulation of Hsp70 expression, which is a molecular chaperone widely expressed in cells and critical for cell survival to modulate cell apoptosis (Polla et al., 1996), could be an underlying mechanism to explain how this small chemical affected the protein folding environment in cells.

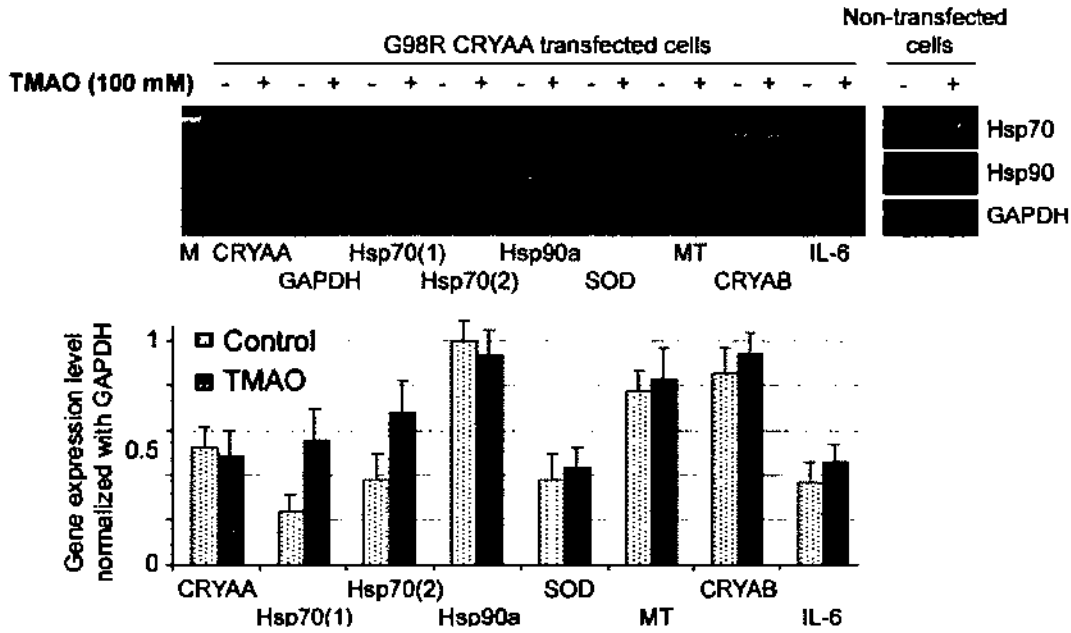

Figure 3.19 Heat shock response and cell stress signalling. Semiquantitative reverse transcription polymerase chain reaction analysis showed specific upregulation of *Hsp70* in G98R CRYAA-expressing cells treated with TMAO, whereas other stress-inducible genes remained unchanged. No changes were found for TMAO treatment on nontransfected cells.

3.4 Discussion

In this study, we expressed the presenile cataract-causing G98R CRYAA in lens epithelial B3 cells by transfection. The mutant protein was found to be insoluble upon Tx extraction and prone to be retained and form aggregates in the ER of cells. This induced the ER stress, and cells underwent apoptosis. This is the first time showing that the misfolded G98R CRYAA-induced presenile cataract could be an ER storage disease. This cellular defect was corrected by the treatment with a chemical chaperone, the natural osmolyte TMAO. Upon treatment, the Tx insolubility was reduced in dose and time-dependent manners, and the cells had less mutant protein aggregates, probably degraded via the ubiquitin proteasome pathway. TMAO treatment alleviated the ER stress and apoptosis. We also showed that TMAO treatment modulated Hsp70 expression, which could be an underlying mechanism to explain how this chemical chaperone affected the protein folding environment in cells.

Unlike WT CRYAA, cataract-causing G98R CRYAA protein was exclusively partitioned to Tx-insoluble fraction and formed inclusion bodies when expressed in bacterial cells (Singh et al., 2006). We extended this observation to human lens epithelial B3 cells and discovered that Tx-insoluble G98R CRYAA mutant protein formed large ER-associated aggregates. The mutation from glycine to arginine induces a gain of positive charge, and the encoded protein is not optimally folded. Bis-ANS binding assay has illustrated that the mutant protein has exposed hydrophobic sites that cause it to become aggregation prone with the formation of very large mixed oligomers with G98R CRYAA (Singh et al., 2006). In my experiment, the aggregation of pHis/myc-

CRYAA^{G98R} further induced the ER stress, as demonstrated by PERK and BiP upregulation. The mutant protein was modestly degradable by UPP. Application of proteasome inhibitor MG132 resulted in an increased level of Tx insoluble mutant protein. The prolonged ER overloading ultimately caused the cells to undergo apoptosis through caspase-3 dependent pathway, in association with increased CHOP/GADD153 expression. This novel observation underlines the aggregation of mutant CRYAA and subsequent cell death as a major pathogenetic factor for the development of lens opacity in cataract. On the other hand, other mutants, except R49C localized in both nuclear and cytoplasmic compartments (Mackay et al., 2003), were mainly restricted in the cytoplasm without aggregate formation (Andley et al., 2002). This delineates the severity of the highly aggregation-prone G98R mutant in the cataract formation, and ways to reduce aggregation could alleviate the disease phenotype.

In recent years chemical chaperoning on misfolded proteins has been shown to prevent or correct protein's non-native conformation, alleviating mistrafficking and the associated cellular defects, which resulted in enhanced cell survival (Kolter and Wendeler, 2003; Leandro and Gomes, 2008; Perlmutter, 2002; Ulloa-Aguirre et al., 2004). Though the exact mechanisms are still undefined, chemical chaperones likely shift the folding equilibrium of substrate proteins to a more native state, reduce nonproductive aggregation, or enhance the resident chaperoning environment, allowing the misfolded proteins to break away from the ER retention and facilitate the transport across intracellular compartments, and resulting in alleviating ER stress and reduction of cell apoptosis (**Figures 3.17 and 3.18**), which means chemical chaperone treatment could help protein

maintain native structure and refold properly. This has been shown in correcting a variety of misfolded proteins associated with pathological conditions and renders the chaperone-assisted protein rescue an appealing strategy to treat protein-folding diseases (Basseri et al., 2009; Ono et al., 2009; Yam et al., 2007b). Removal of aberrant accumulation of misfolded proteins reduced cellular toxicity and enhanced cell survival (Bonapace et al., 2004; Jia et al., 2009c; Ozcan et al., 2006; Yam et al., 2007b).

In this study, TMAO and other small chemicals that have been reported previously for eye-associated proteins were tested in WT or G98R-CRYAA-expressing cells. Despite glycerol and DMSO causing significant cell death, TMAO and 4-PBA at the usage levels were nontoxic, which agreed with previous observation (Bai et al., 1998). However, 4-PBA was not optimal, due to the changes of fibroblastic morphology after long-term incubation. TMAO at optimal concentration of 50-100 mM reduced Tx-insoluble CRYAA and resolved His/myc-G98R CRYAA aggregates in cells. These dosages were similar to our previous report on correcting the mutant myocilin (Jia et al., 2009c). The drug effect was mediated through UPP-associated degradation and was reversed by MG132 inhibition. It has been known that proper UPP function is essential for lens fibre cell differentiation (Marques et al., 2006), in addition to its general regulation in protein quality control, removal of obsolete proteins, cell cycle progression, DNA repair, immune responses and so on (Ye, 2005). Defective UPP leads to abnormal protein degradation, affecting protein biosynthesis and processing, and more severely, causes atypical protein accumulation and stress induction. This has been implicated in different human diseases, such as Parkinson disease, Alzheimer's disease, cancers and so on

(Chiesi et al., 1990; Herrmann et al., 2008), CRYAA is a substrate of UPP, and truncated mutant CRYAA was reported to undergo rapid degradation by UPP to prevent its accumulation in lens cells (Zhang et al., 2007b). However, G98R CRYAA was only moderately degradable by UPP and prone to aggregation (Singh et al., 2006). With TMAO treatment it appeared that TMAO either promoted the degradation of His/myc-G98R mutant through UPP or resolved the protein aggregation in the ER, hence reducing the cellular stress. This was substantiated by reduced expression of ER stress markers, PERK and BiP, as well as pro-apoptotic proteins, caspase-3 and CHOP/GADD153. On the other hand, the non-responsiveness of Tx-insolube G98R CRYAA to 3-MA treatment revealed that G98R CRYAA was not a substrate of autophagy.

TMAO is a naturally occurring osmolyte present in deep water fishes. It is important to counteract the protein destabilizing effect of urea and hydrostatic pressure. Its action on protein folding or stabilization could be due to its hydrophobic nature to push water molecules to the protein surface. This increased hydration affects Gibbs free energy (G) levels along the protein-folding process so that ΔG between native and denatured states becomes larger and drives the equilibrium towards the native state (Alward et al., 1998). The solvent-accessible surface area is reduced and causes a tighter packing of polypeptide or reduces the mobility between protein domains, leading to a more stabilized protein conformation and oligomeric assembly (Shearer and Hampton, 2004). The mutated G98R CRYAA had exposed hydrophobic patches (Singh et al., 2006) which could be modified or removed by TMAO, resulting in a more stabilized conformation, likely recognized by UPP and were being degraded.

In addition, TMAO-initiated cytoprotection pathway was found associated with induced Hsp70 expression, which is critical for cell survival. Hsp70 is a molecular chaperone widely expressed in cells and functions to modulate the engagement and progression of apoptosis induced by various stimuli (Polla et al., 1996). Hsp70 suppresses apoptosis by directly blocking the assembly of functional Apaf-1 apoptosomes (Beere et al., 2000). It also helps proteins to fold through repeated cycles of substrate binding and release. The stress-inducible Hsp70 helps cells cope with the adverse conditions, in part by aiding in the folding of nascent polypeptides or refolding of damaged proteins, preventing or reversal of protein aggregation, or promoting protein trafficking (Brodsky and Chiosis, 2006; Garrido et al., 2006; Mayer and Bukau, 2005; Powers and Workman, 2007). An improvement of mutant cell survival was observed in this study. It appeared either that TMAO stabilized G98R CRYAA and promoted its UPP-associated degradation or it modulated the protein-folding environment and reduces apoptosis through heat-shock response signaling. Here, it cannot be determined if change of Hsp70 expression was directly caused by TMAO treatment, which might involve a change of chaperoning capacity in cells, or a consequence of mutant protein stabilization. In my laboratory, the previous study also identified a delayed Hsp70 expression after heat-shock induction in R12C CRYAA expressing cells (Zhang et al., 2009b). Further work would warrant a better characterization of Hsp70 regulation in cataract pathogenesis and may introduce possible treatment strategies. The effect of TMAO on other cell stress signaling (including metal-induced stress and inflammatory stress) was not observed.

3.5 Conclusion

In conclusion, our study revealed the cellular aggregation and the ER stress induced by misfolded G98R mutant CRYAA in lens epithelial cells, and this caused apoptosis. These defects were alleviated by the natural osmolyte TMAO. Our findings provide a basis for a new chemical-based strategy to alleviate cell stress and improve cell survival.

4 Effects of small chemicals on the folding defects of a structural protein: CRYGD

4.1 Introduction

4.1.1 Structural protein

Structural proteins are those proteins with the primary purpose of producing the essential structural components of the cell. They are the most abundant class of proteins in nature and fulfill a purely structural role, such as collagen, fibronectin and laminin, histone-like proteins and some ribosomal proteins. Normally, the structural protein must fold into a specific three-dimensional structure according to its inherent amino acid sequence to acquire its functionally active and structurally native state. This is assisted by the concentrated milieu of cellular environment and folding machinery, including enzymes, molecular chaperones, pH regulators, ions and transporters as well as input of metabolic energy (Roth J, 2002; Roth et al., 2008; Trombetta ES and Parodi AJ, 2003). The cooperative action allows proteins to be efficiently folded to native state and transported to appropriate targets either intracellularly or extracellularly to function normally. Conversely, proteins may misfold or unfold under stress conditions, including environmental changes due to aging, pH/ion or temperature fluctuation, genetic mutation, or exposure to amino acid analogues. Defective protein features, such as the solubility changes, aggregation and mistrafficking, characterize many human disorders (Aridor M and Hannan LA, 2002; Barral et al., 2004).

4.1.2 γ-crystallins

γ-crystallins belong a super-family of crystalline and are one of the structural proteins in the lens. The γ-crystallin encoding genes are organized as a cluster of five genes (γA to γE-crystallin; gene symbols *CRYGA to CRYGE*) within approximately 50 kb in length and they are all arranged in a head-to-tail orientation. It is known that γ-crystallins is lens fiber cell specific. One of the members, CRYGS, express at significant levels in lens epithelial cells (Wang et al., 2004). By gel-chromatography of total lens proteins, the monomeric γ-crystallins appear as the last peak because of their low molecular mass of about 20 kDa. In mammals, it is the most basic crystallins with isoelectric points ranging from pI 7.1 to 8.6 and contains a high content of free cysteine residues making them highly sensitive to the formation of mixed disulfide bonds during oxidative stress. Besides serving as structural proteins and refractive index gradients, its role in human lens function is yet to be determined. CRYGD is a structural protein essential for lens transparency. Mutations of CRYGD are common genetic lesions causing different types of congenital cataracts. Among the reported families with congenital cataract caused by mutations of crystallin, one-third of them were associated with CRYGD (Graw, 2009).

Cataract is suggested to be a protein folding disease. Being the main structural proteins, the solubility of γ-crystallin is crucial to the lens transparency. Analyzing the mutations in γ-crystallin genes has suggested that there are two molecular mechanisms responsible for the decreased solubility of mutant γ-crystallin proteins. First, the mutation alters the overall conformation of protein leading to the insolubility of protein. Several types of mutations can cause significant structural change on proteins. For example, the mutation

produces a premature STOP codon leading to early truncation, W156X in CRYGD, insertion or deletion of nucleotides which causes frameshifting, such as C42fs in CRYGC; or a single base mutation altering a structurally important residue leading to changes of the secondary and tertiary structure, such as T5P of CRYGC.

4.1.3 Mutant γ-crystallin

Genetic studies have identified mutations of the *γ-crystallin* genes leading to various forms of cataract. The cataract-causing mutations are restricted to human *CRYGC* and *CRYGD* genes as *CRYGE* and *CRYGF* genes are pseudogenes (**Table 4.1**). Similar to other crystallins, the cataract phenotypes caused by *γ-crystallin* mutations are quite varied and there is no specific genotype-phenotype correlation. Moreover, presence of modifier genes might influence the severity of cataract formation. In human, *CRYGD* is mainly affected gene among the γ-crystallin encoding genes. In contrast to *CRYAB* gene, the missense mutations in *CRYGD* affect the two major exons whereas the termination mutations occur only in exon 3 (Graw, 2009). Until now, a total of 12 cataract-causing mutations (UniProt) have been reported including *R15C, P24S, P24T, R37S, R59H, G61C, E107A, Y134X, W156X, G165fsX8, R168W* and *R15S* (Graw, 2009).

4.1.4 Mutant G165fsX8 γD-crystallin

G165fsX8 γD-crystallin (CRYGD) is a novel single base deletion, c.494delG, in exon 3 of the *CRYGD* gene identified in a Chinese family with nuclear type of congenital

Table 4.1 Mutations in human *CRYG* genes.

(Graw, 2009)

nt Position[a]	bp Exchange	aa Position[a]	aa Exchange	Allele symbol (comment)
Human mutations				
CRYGC				
13	A→C	5	Thr→Pro	Coppock-like cataract, dominant
212–222	Duplication GCGGC	59	hybrid protein	Dominant variable zonular pulverulent cataract
327	C→A	109	Cys→stop	Dominant nuclear cataract
502	C→T	168	Arg→Trp	Three independent families with lamellar dominant cataract
CRYGD				
43	C→T	14	Arg→Cys	Dominant progressive juvenile-onset punctuate cataract
70	C→A	24	Pro→Thr	Independent dominant cataracts in 3 families
70	C→T	24	Pro→Ser	Dominant non-nuclear polymorphic congenital cataract
109	C→A	36	Arg→Ser	Dominant symmetric crystal deposition and greyish opacity
176	G→A	58	Arg→His	Aculeiform dominant cataract
181	G→T	61	Gly→Cys	Dominant corraliform cataract
403	C→A	134	Tyr→stop	Dominant cataract
418	C→T	140	Arg→stop	Dominant nuclear cataract
470	G→A	157	Trp→stop	Dominant central nuclear cataract
494	⊿G	165	Frameshift (2 amino acids)	Dominant nuclear cataract
CRYGS				
105	G→T	18	Gly→Val	Polymorphic dominant cortical cataract
116	C→G	39	Ser→Cys	Dominant progressive juvenile-onset cataract

⊿, deletion.

[a] Beginning at coding sequence (start codon ATG).

cataract (Zhang et al., 2007b). This frameshift mutation resulted in a premature termination of protein. When expressed in COS-7 cells, the mutant protein was insoluble upon Triton X-100 extraction. Unlike WT CRYGD, which exists in both the nucleus and cytoplasm (Wang et al., 2007), G165fs mutant was associated with the nuclear envelope as shown by its co-distribution with lamin A/C by confocal double immunofluorescence. This mislocalization together with the reduced solubility could be linked to nuclear changes during lens development, in particular lens fiber cell maturation. These changes could affect nuclear degradation during lens fiber differentiation, thus interfering with lens transparency and leading to opacity formation during lens development. As a whole, G165fs CRYGD causing-cataract could be a protein folding problem. To our knowledge, it is a rare deletion mutation of *CRYGD,* in addition to W156X, found to be disease-causing for autosomal dominant congenital cataract, whereas other reported mutations are single base substitutions.

4.1.5 Effects of small chemicals on defective structural proteins

It is now recognized as a major cause of a large number of protein misfolding or protein conformational disorders with diversified pathologies. Aberrance in protein features, not only confers loss-of-function, but also gain-of-function proteotoxicity or cytotoxicity. Mistrafficking or mislocalization of proteins other than the appropriate target site could also trigger responses at the level of subcellular organelles, leading to organelle instability or even dysfunction. As a whole, protein folding and trafficking defects generate aggregation toxicity leading to cell death, which contributes to disease pathogenesis. Mutations in γ-crystallin are associated with protein aggregation and lens

fiber cell denucleation, as well as self-aggregation of lens protein leading to lens opacification (Talla et al., 2006; Wang et al., 2007).

Many studies on the misfolding and aggregate formation of regulatory proteins have given important links of loss or gain-of-function and aggregation-mediated toxicity to disease pathology (Dohm et al., 2008; Gregersen et al., 2005). They include α1-antitrypsin-associated Mallory-Denk bodies in liver pathology, Parkin/α-synuclein-associated Lewy bodies in Parkinson disease, amyloidosis in neurodegenerative disorders (e.g., Alzheimer's and Huntington's diseases), and myocilin-associated Russell's bodies. Potential measures using molecular or chemical chaperones to rescue the defective proteins have been shown to stabilize them in a more native state, reduce protein-protein aggregation and hence, providing protection against cellular damages and cell loss. In some instances, clinical trials have been initiated to test the therapeutic potential of the chaperone molecules, such as sodium 4-phenylbutyrate (4-PBA) as a chemical chaperone for ΔF508 homozygous cystic fibrosis patients (Rubenstein and Zeitlin, 1998) and pharmacological chaperones for lysosomal storage diseases. Examples of the latter include like AT1001 or 1-deoxygalactonojirimycin to retrieve misfolded α-galactosidase A in Fabry disease (Fan, 2003; Fan and Ishii, 2003; Germain and Fan, 2009) and AT2101 to store destabilized glucocerebrosidase in Gaucher disease (Parenti, 2009; Yam et al., 2006; Yam et al., 2005).

On the other hand, limited information is available for the folding problem of structural proteins and the corrective intervention. Misfolding of type I collagen causes triple helix

disassembly, resulting in a destabilization of matrix formation. In bones and skeletal tissues, collagen misfolding is associated with bone fragility and deformities in skeletal disorders, like osteogenesis imperfecta (Baum and Brodsky, 1999; Byers, 2001; Marini et al., 2007). Conformation alterations of hepatocyte keratin in alcoholic steatohepatitis induce Mallory body formation, which could be a cellular defense to tolerate against toxic stress (Strnad et al., 2008; Zatloukal et al., 2004).

Recently, our group has identified the misfolding of *γD-crystallin (CRYGD)* causing congenital nuclear cataract (Zhang et al., 2007b). CRYGD is a structural protein essential for lens transparency. It is present as monomers with highly symmetric structure with 4 Greek key motifs organized into two highly homologous β-sheet domains connected by a six-residue linker. A premature truncated mutation, G165fsX8, removes the last β-strand of the 4^{th} Greek key motif and affects the interdomain stability leading to protein precipitation and misolocalization to the nuclear envelope. This was suggested to impair the nuclear transfiguration and degradation in lens fiber cell differentiation, leading to opacity formation during lens development. In this study, we tested if the misfolded CRYGD features could be amended by small chemical molecules with known chaperoning activity. To our knowledge, this is the first report showing a potential correction of misfolded structural protein and this can be developed to a novel therapeutic strategy.

4.2 Materials and methods

4.2.1 *WT CRYGD* expression constructs

Total ocular mRNA was extracted from human aborted fetus at week 14 with RNeasy mini kit (Qiagen, Valencia, CA, USA). Reverse transcription was performed with oligo (dT) primer (Roche, Bael, Switzerland) and SuperScript™ III reverse transcriptase (Invitrogen, Carlsbad, CA, USA). Primers with two restriction enzyme cutting sites (CRYGD-WT-F-EcoRI: TGG TGA ATT CC ATG GGG AAG ATC ACC CTC; CRYGD-WT-R-Bgl II: TGG TAG ATC TCC GGA GAA ATC TAT GAC TCT) were designed to amplify the full-length WT cDNA of *CRYGD*. A 545 base-pair *EcoR1/BglII* fragment encompassing the full-length 522 base-pair open reading frame of *CRYGD* was subcloned directionally into the *EcoR1/Bg1II* sites of the plasmid p3XFLAG-myc-CMVTM-26 (Sigma, St Louis, MO, USA) to obtain the construct pFLAG/myc-$CRYGD^{WT}$ (Zhang et al., 2007b).

4.2.2 Site-directed mutagenesis and mutant constructs

G165fsX8 CRYGD, the mutation of c.494delG in *CRYGD*, was also created by the QuikChange II Site-Directed Mutagenesis kit (Stratagene, Lo Jolla, CA) using oligonucleotides: sense 5'- GGG CCA CGA ATG CCA GAG TGG *CT CTC TGA GGA GAG TCA TAG; antisense 5'-CTA TGA CTC TCC TCA GAG AG* CCA CTC TGG CAT TCG TGG CCC (the asterisk indicates the position of the base deletion). Due to the creation of a STOP codon before the myc sequence, the mutant construct was named as pFLAG-$CRYGD^{G165fs}$. Other constructs were made with following oligonucleotides: for pFLAG-$CRYGD^{R15C}$, sense 5'-GAC CGG GGC TTC CAG GGC TGC CAC TAT GAA

TGC AGC; for pFLAG-CRYGD^{R15S}, sense 5′-GAC CGG GGC TTC CAG GGC AGC CAC TAT GAA TGC AGC; for pFLAG-CRYGD^{P24T}, sense 5′-GAA TGC AGC AGC GAC CAC ACC AAC CTG CAG CCC TAC; for pFLAG-CRYGD^{G61C}, sense 5′-TAC TTC CTG CGC CGC TGC GAC TAT GCC GAC (the underline indicates the position of the point mutation). The constructs of *CRYGD* were amplified with the same way as the amplification of *CRYAA* (Refer to Section 3.2.3). Direct sequencing was performed with specific primers for *CRYGD*, including 1F: 5'- ATG AGC AGC CCA ACT ACT CG and 1R: 5'- CCT GAA GAC AGG AGC AGT CC; 2F: 5'- CAG CAG CCC TCC TGC TAT and 2R: 5'-GCT TAT GTG GGG AGC AAA.

4.2.3 Cell culture, transfection and small chemical treatment

COS-7 cells (ATCC) were cultured in Eagle's Minimal Essential medium (MEM, Invitrogen) supplemented with 10% fetal bovine serum (FBS, Invitrogen) and antibiotics (100 units/ml penicillin G and 100 μg/ml streptomycin sulfate, Invitrogen), followed by transfection and small chemical treatment (Refer to Section 3.2.4 and 3.2.5).

4.2.4 Western blotting, immunofluorescence, transcription analysis

The methods for protein analysis by western blotting and immunofluorescence were the same as Section 3.2.6 and 3.2.7. The antibodies used in this part were HRP-conjugated antibodies against FLAG (Sigma) recognizing CRYGD, glyceraldehyde phosphate dehydrogenase (GAPDH; Sigma), and β-actin (Sigma). Transfected cells grown on glass coverslips were detected with a mouse monoclonal anti-FLAG antibody

(recognizing CRYGD, Sigma, 200 ng/ml) followed by appropriate fluorescence conjugated IgG secondary antibody (Alexa Fluor® 488 IgG goat anti-mouse conjugate, Invitrogen, 300 ng/ml) and nuclei counterstained with 4'-6-diamidino-2-phenylindole (DAPI; Sigma, 100 ng/ml). Terminal apoptosis rate was calculated with the same way as that in Section 3.2.9. All the methods of transcription analysis used in this part were followed as Section 3.2.10.

4.3 Results

4.3.1 4-PBA improved the solubility of G165fsX8 CRYGD

The expected molecular size of FLAG/myc-tagged WT CRYGD was ~28 kDa and the size of truncated FLAG-tagged G165fs CRYGD (a shorten peptide and without myc) was ~24 kDa. Our previous finding of the reduced Tx solubility of G165fsX8 CRYGD mutant was confirmed in this study using COS-7 cells (**Figure 4.1**). Western blot analysis of FLAG (representing CRYGD) followed by band densitometry showed that the WT CRYGD protein was predominantly Tx-soluble. More than 95% of WT CRYGD protein (at 28 kDa by molecular mass) was present in the Tx-soluble fraction and a very faint FLAG-immunoreactive band existed after resolving the Tx-insoluble proteins by small chemical treatment (**Figure 4.2 A**). This was not observed for the G165fsX8 mutant protein, which was found to be mainly Tx-insoluble. About 83% of this premature truncated protein (at 24 kDa by molecular mass) was present as Tx-insoluble. At 1 day after transfection, the cells were treated with different small chemicals, including 4-PBA (with treatment doses from 0.25 to 3 mM) for another 2 days. The cells were collected for Tx solubility assay. A dose-dependent change of Tx solubility of G165fsX8 mutant was observed (**Figures 4.1 A and B**). Treatment with 4-PBA of concentration ranging from 1 to 3 mM caused a significant reduction of Tx insolubility from 83 ± 0.869% (untreatment) to 37 ± 0.549% (for 1 mM 4-PBA treatment), 15 ± 0.462% (2 mM 4-PBA treatment) and 10 ± 0.384% (3 mM 4-PBA treatment). The reduction of insoluble protein was significant when analyzed by independent Student's *t*-test ($p<0.05$). Simultaneously, 4-PBA

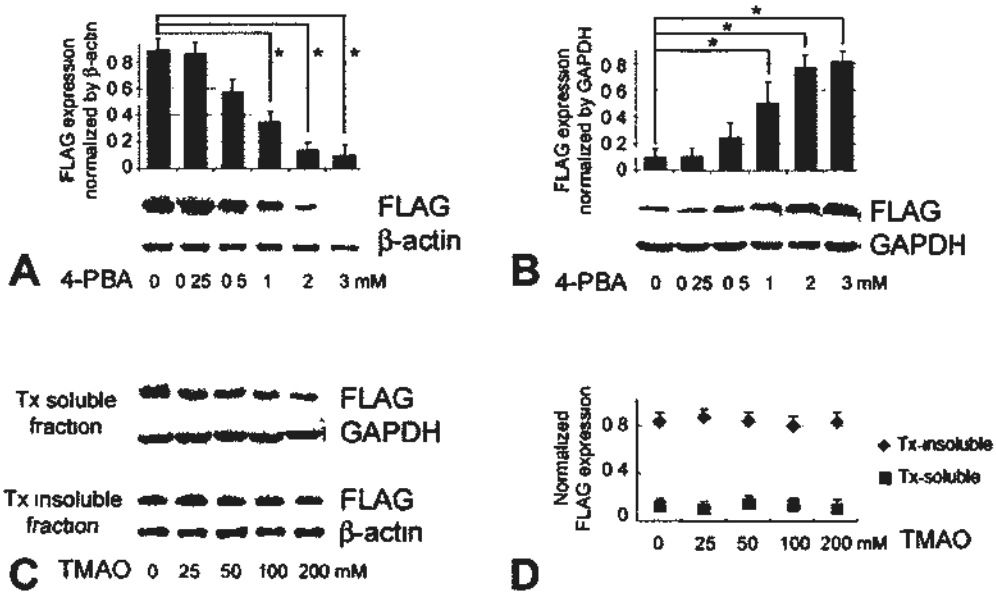

Figure 4.1 Chemical chaperone 4-PBA improved Tx solubility of G165fsX8 CRYGD expressing in COS-7 cells. Cells were treated with 4-PBA (0 to 3 mM) for 2 days followed by western blotting for FLAG-tagged CRYGD and band densitometry (represented by histogram). **(A)** Tx insoluble fractions; **(B)** Tx soluble fractions. β-Actin and GAPDH were the housekeeping proteins of Tx-insoluble and soluble fractions, respectively. **(C)** Treatment of cells with TMAO (0 to 300 mM) for 2 days followed by Tx solubility test for FLAG-tagged CRYGD expression. **(D)** Band densitometry analysis showed that TMAO did not affect the mutant protein solubility.

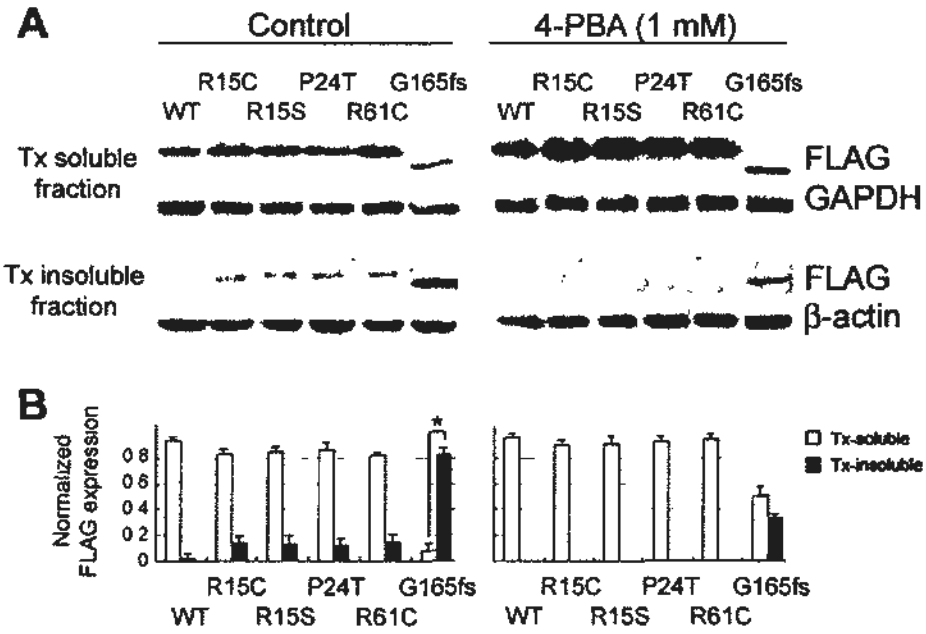

Figure 4.2 4-PBA improved the solubility of various cataract-causing CRYGD mutants expressing in COS-7 cells. (A) Western blotting of FLAG and housekeeping proteins in Tx soluble and insoluble fractions from cells expressing WT, R15C, R15S, P24T, R61C or G165fsX8 CRYGD treated (right) or not (left) with 1 mM 4-PBA for 2 days. **(B)** Band densitometry of FLAG-tagged CRYGD normalized with housekeeping proteins in cells from A.

treatment improved the solubility of mutant protein in the same G165fsX8 CRYGD-expressing COS-7 cells (**Figure 4.1 B**).

Other reported small chemicals were also tested for their effect on G165fsX8 CRYGD protein solubility. Treatment with TMAO (25 to 200 mM) for 2 days did not result in any obvious change of Tx solubility (**Figures 4.2 C and D**). There were always about 83% of Tx-insoluble G165fs CRYGD protein in the G165fs CRYGD-expressing cells treated or not with TMAO, and the soluble proteins also maintained around 15% during TMAO treatment (25 to 200 mM) for 2 days. Treatment with DMSO (0.5 to 1%) or glycerol (1 to 5%) was also ineffective to improve mutant protein solubility and cytotoxicity was observed. DMSO almost had the same effect as TMAO on the G165fs CRYGD-expressing cells, and it did not show any improvement of solubility of G165fs CRYGD protein. During glycerol treatment on the cells transfected with G165fs CRYGD, there were more floating cells at 24 hours after treatment, and more cells tended to be dying as well as had obvious morphological changes on the face of transfected cells, which were difficult to be harvested for protein solubility analysis. Therefore, these three chemicals were not used in the following study.

4.3.2 4-PBA improved the solubility of different CRYGD mutants

In addition to *WT* and *G165fsX8 CRYGD*, recombinant FLAG/myc-tagged *CRYGD* mutants *(R15C, R15S, P24T and R61C)* were created by PCR-based site-directed mutagenesis and constructs were confirmed by direct sequencing. These missense mutants with FLAG and myc tagging have expected molecular size of ~28 kDa. When

cell lysate were fractionated into Tx-soluble and Tx-insoluble fraction and analyzed by western blotting of FLAG (representing CRYGD), the mutant proteins were moderately Tx-insoluble. The amount of R15C CRYGD to be Tx-insoluble was 17 ± 0.235%, R15S was 15 ± 0.145%, P24T was 14 ± 0.241% and R61C was 19 ± 0.159%. This was much lowered than G165fsX8 mutant (about 83% protein was Tx-insoluble) (**Figure 4.2 A**). The cells were treated with 4-PBA (1 mM) treatment for 2 days and cells were collected again for Tx solubility test. Irrespective to the mutation, the Tx-insoluble mutant protein were greatly reduced and they again became Tx-soluble after 4-PBA treatment (**Figure 4.2**).

4.3.3 4-PBA relocalized G165fsX8 CRYGD from nuclear envelope

When expressed in COS-7 cells, FLAG-tagged G165fsX8 CRYGD was redistributed as a ring-shaped structure on the nuclear periphery (**Figure 4.3 C**). Minimal staining in the cytoplasm and inner nucleus was observed. By using confocal microscopy, our team had identified its colocalization with lamin A/C in the nuclear envelope (Zhang et al., 2007b). In contrast, FLAG-tagged WT CRYGD was located in both nuclear and cytoplasmic regions (**Figure 4.3 A**). This was different to the reported cytoplasmic staining of normal CRYGD and this could be due to the protein over-expression by cytomegalovirus (CMV) promoter. We focused our observation on the defective nuclear envelope staining of mutant CRYGD. Treatment with 4-PBA for 48 hours successfully reduced the amount of mutant cells with CRYGD staying on the nuclear envelope. Instead, most treated cells exhibited a nuclear and faint cytoplasmic G165fsX8 CRYGD staining (**Figure 4.3 D**). A quantitative analysis showed that about 20% of mutant cells

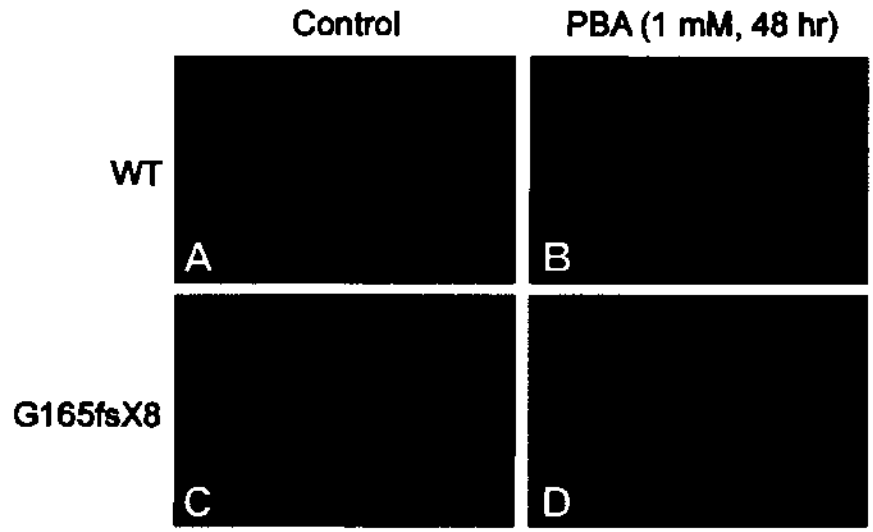

Figure 4.3 The corrective effect of 4-PBA on G165fsX8-expressing cells. 4-PBA corrected the mislocalization of G165fs CRYGD as shown by confocal immunofluorescence. **(A)** Untreated WT cells, **(B)** WT cells treated with 1 mM PBA for 2 days, **(C)** untreated G165fs CRYGD cells and **(D)** G165fs CRYGD cells treated with 1 mM PBA for 2 days.

had nuclear G165fsX8 CRYGD after 0.5 mM 4-PBA treatment and about 60% nuclear staining after 1 mM 4-PBA treatment. No change was observed for WT cells treated or not with 4-PBA (**Figures 4.3 A and B**).

4.3.4 4-PBA treatment rescued G165fsX8 mutant cells from apoptosis

In the same cell preparation and treatment, the apoptosis rate was determined as the percentage of G165fsX8 CRYGD-transfected cells showing fragmented nuclei. In untreated mutant cells, the apoptosis rate was about 13%, which were 3 folds higher than that of WT cells (4%) ($p<0.05$, independent Student *t*-test) (**Figure 4.4**). Treatment of mutant cells with 1 mM PBA for 2 days significantly reduced the apoptosis rate to about 6% ($p<0.05$, independent Student *t*-test). There was no clear difference in the apoptosis rate of WT cells with or without 4-PBA treatment.

4.3.5 4-PBA treatment up-regulated Hsp70 expression

The correction of G165fsX8 CRYGD protein for becoming more Tx soluble by 4-PBA could be mediated through heat-shock responses. By RT-PCR analysis, the steady state RNA expression of Hsp70 and Hsp90 was investigated. Each experiment was done in triplicate and the amplification of GAPDH in the same sample was used as housekeeping control. An up-regulated Hsp70 expression was detected in mutant cells after 4-PBA treatment (**Figure 4.5**), but no changes of Hsp90 expression was observed. Cells expressing WT CRYGD had no detectable changes of Hsp70 and Hsp90 expression caused by 4-PBA treatment.

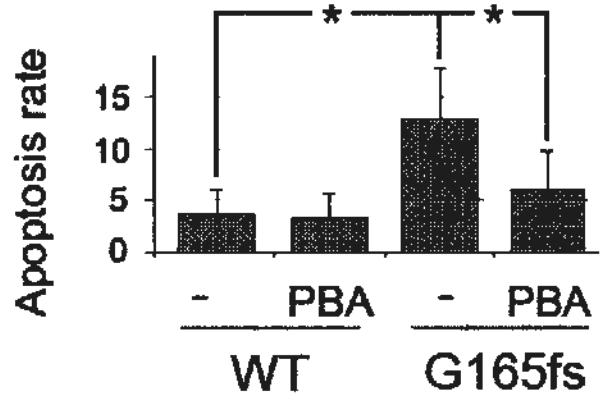

Figure 4.4 Apoptosis rate of cells with nuclear fragmentation. 4-PBA reduced apoptosis of mutant cells with nuclear fragmentation.

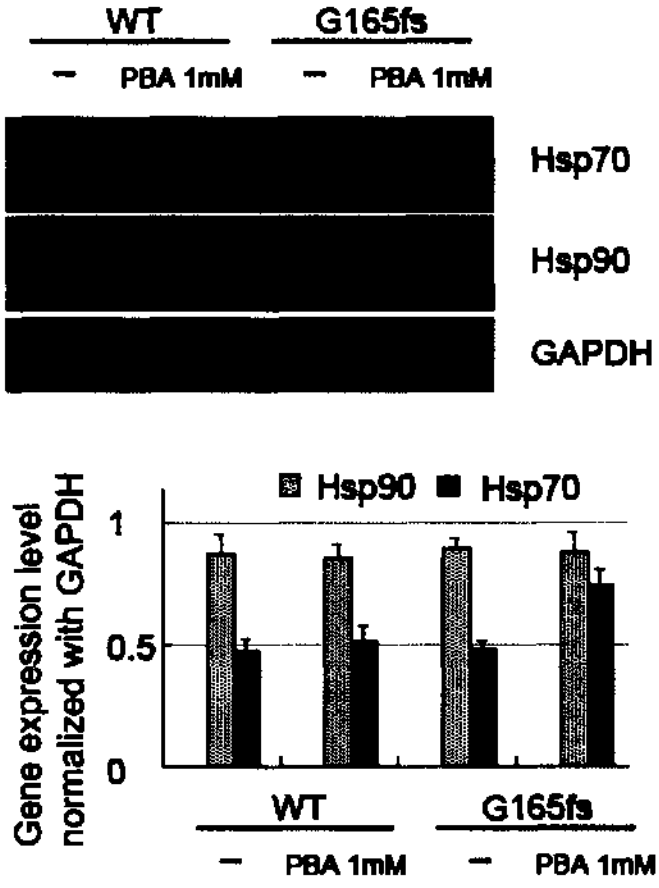

Figure 4.5 Semi-quantitative RT-PCR analysis of gene expression level. 4-PBA caused specific up-regulation of Hsp70 in G165fsX8 CRYGD cells. No change was found for Hsp90.

4.4 Discussion

γD-Crystallin (CRYGD) is a structural protein essential for lens transparency. Mutations of CRYGD are known as common genetic lesions causing different types of congenital cataracts (Devi et al., 2008; Li et al., 2008; Plotnikova et al., 2007; Zhang et al., 2009a; Zhang et al., 2007b; Zhu et al., 1997). Functional changes and alteration of crystallin properties could cause breakdown of lens microstructure resulting in changes of refractive index and light scattering. In this study, different cataract-causing CRYGD mutants was characterized *in vitro* and the disrupted features were attempted to rescue by treatment with small chemical molecules with protein chaperoning activity. While WT and most reported CRYGD mutants were mildly insoluble upon Tx extraction, G165fsX8 mutant causing nuclear type of congenital cataract demonstrated significant Tx insolubility in transfected COS-7 cells, with the same distribution in B3 cells (Zhang et al., 2009a). Moreover, unlike WT CRYGD existing predominantly in cell nucleus (different from reported cytoplasmic staining, possibly due to the overexpression by CMV promoter in the plasmid), G165fsX8 was mislocalized to the nuclear envelope, consistent with our previous finding of its co-localization with lamin A/C (Zhang et al., 2007b). This could lead to impaired nuclear transfiguration and degradation process during lens fiber cell differentiation, thus resulting in opacity formation. The present result showed that the protein defect was alleviated by small chemical molecule, 4-PBA. Tx insolubility was dose-dependently reduced and mutant protein was relocalized to the nucleus, similar as that for WT CRYGD. This correction resulted in reduced apoptosis, and it could be associated with Hsp70 up-regulation in treated cells.

Aggregopathies, or diseases due to aggregation of disease-specific proteins, are usually manifested with altered intracellular pathways involved in protein refolding, aggregation and/or degradation (Corboy MJ et al., 2005; Dobson, 2006; Markossian KA and Kurganov BI, 2004). Protein refolding is often arbitrated by the chaperone and enzyme-mediated protein quality control machinery, including heat shock proteins (e.g. Hsp70 family) and ER lectins, whereas protein degradation involves the ubiquitin-proteasome system (UPS) or autophagy. Limited information has been known for the refolding of structural proteins. In some instance, the traditional view of chaperone molecules binding to unfolded polypeptide chains to prevent aggregation and promote native folding remains controversial. Pro-type I collagen triple helix did not fold properly at temperature higher than 34°C, even in an environment with ER-like molecular crowding (Makareeva and Leikin, 2007). The binding of ER chaperones to unfolded procollagen C-propeptides destabilized the triple helix, unless the chaperone binding was made to folded peptides with native conformation. Keratin aggregation forming Mallory-Denk bodies involved abnormal keratin cross-linking via transglutaminase. Presence of UPS inhibitors accelerated the aggregate formation, which was attenuated by autophagy (Strnad et al., 2008). These reported findings characterize the biological significance of the structural protein misfolding in the disease pathogenesis, however no corrective intervention has been known to alleviate the defective features.

My study reveals, for the first time, a proof-of-principle correction of misfolded structural protein to regain proper biological features by small molecules exhibiting protein chaperoning activity. This can be developed to a novel therapeutic strategy for the

prevention of, in our case congenital cataract or, aggregopathies involving the defective structural proteins. Chemical chaperoning on misfolded proteins has been shown experimentally to prevent or correct protein's non-native conformation, alleviate the mistrafficking and the associated cellular defects, resulting in better cell survival (Kolter T and Wendeler M, 2003; Leandro and Gomes, 2008; Perlmutter DH, 2002; Ulloa-Aguirre A et al., 2004). Though the exact mechanisms are still to be delineated, chemical chaperones likely shift the folding equilibrium towards a more native state, reduce non-productive aggregation or enhance the resident chaperoning environment. This relieves the ER-retention and facilitates the transport of client proteins across the intracellular compartments. Ultimately, the cells will have better survival. Increasing evidence of its correction on different misfolded proteins associated with disease pathology has rendered the chaperone-assisted protein rescue an appealing strategy to treat protein folding diseases (Basseri et al., 2009; Ono et al., 2009; Singh et al., 2008; Yam GHF et al., 2006; Yam GHF et al., 2007b). Removal of aberrant accumulation of misfolded proteins by chemical chaperone could reduce cellular toxicity and enhanced cell survival (Datta et al., 2009; de Almeida et al., 2007; Hanada et al., 2007; Jafarnejad et al., 2008; Kubota et al., 2006), and they could also alleviate ER stress and apoptosis in lysosomal storage diseases (Wei et al., 2008; Ozcan et al., 2006; Pratt et al., 2009).

4-PBA has several known functions on cells. It acts as a peroxisome proliferator and histone deacetylase inhibitor to affect transcription. It has been approved for clinical use to restore chloride conductance in cystic fibrosis patients and treat the urea cycle disorders (Collins et al., 1995; Maestri et al., 1991; Rubenstein RC and Zeitlin PL, 1998).

No drug-induced toxicity was encountered by patients. Functions as a chemical chaperone, it significantly improves the folding of many proteins, including α1-antitrypsin, nephrin, myocilin, Pael receptor and, in this case, CRYGD, and restores the protein localization, contributing to better cell viability (Burrows JA et al., 2000; Kubota et al., 2006; Liu XL et al., 2004; Yam GHF et al., 2007b). The molecular mechanism of how this small chemical molecule causes protein recovery appears inconclusive. Though it has been reported as a transcriptional regulator, no significant gene changes was observed for the ER unfolded protein response (Wright et al., 2004). On the other hand, a down-regulation of constitutive Hsp70 protein caused by the decreased stability of mRNA was observed, indicating a mode of action different from that of inhibiting deacetylase activity (Rubenstein and Lyons, 2001). In my assay, an inducible Hsp70 expression was detected after 4-PBA treatment. This could be beneficial for protein disaggregation, protein refolding and complex remodeling, trafficking and regulation of heat-shock responses (Choo-Kang and Zeitlin, 2001; Liberek et al., 2008; Teter et al., 1999; Zhang et al., 2001; Zietkiewicz et al., 2006). However, the role of Hsp70 in folding of structural proteins is unknown, except the co-staining of Hsp70 with misfolded keratin in Mallory bodies (Fausther et al., 2004). Interaction of small Hsp47 with type I collagen was important for the Golgi transport (Makareeva and Leikin, 2007; Zerangue et al., 1999). Moreover, Hsp70 is anti-apoptotic by directly associating with Apaf-1, by antagonism of apoptosis-inducing factor, or through direct suppression of downstream caspases (Beere et al., 2000; Komarova et al., 2004; Ravagnan et al., 2001). Inhibition of its function is sufficient to induce cell death in some tumors (Brodsky and Chiosis, 2006).

In Zebrafish lens development, inducible Hsp70 is a vital regulator for lens fiber cell differentiation (Blechinger et al., 2002; Evans et al., 2005).

4.5 Conclusion

In conclusion, 4-PBA reversed the defective protein features of G165fsX8 CRYGD and reduced the apoptosis possibly through Hsp70 signaling. Hsp70 up-regulation may be directly caused by 4-PBA or change of chaperoning capacity in the cells. This could lead to mutant protein stabilization. Further work warrants a better characterization of Hsp70 regulation in cataractogenesis and for potential therapeutic strategies.

5 Effects of small chemicals on the glaucoma-causing mutant myocilin

5.1 Introduction

5.1.1 Glaucoma

Glaucoma is a blinding disease associated with optic neuropathy caused by a characteristic progressive degeneration of optic nerve and loss of retinal ganglion cells (Morrison et al., 2005). It is a leading cause of irreversible blindness affecting more than 70 million people worldwide. There are many different sub-types of glaucoma. Raised intraocular pressure (IOP) is a significant risk factor for developing glaucoma (above 22 mmHg or 2.9 kPa). One person may develop nerve damage at a relatively low pressure, while another person may have high eye pressure for years and yet never develop damage. Untreated glaucoma leads to permanent damage of the optic nerve and resultant visual field loss, which can progress to blindness.

Glaucoma can be divided roughly into two main categories, "open angle" and "closed angle" glaucoma. Open angle, chronic glaucoma tends to progress more slowly and the patient may not notice that they have lost vision until the disease has progressed significantly. Closed angle glaucoma can appear suddenly and is often painful; visual loss can progress quickly but the discomfort often leads patients to seek medical attention before permanent damage occurs.

5.1.1.1 Primary open-angle glaucoma (POAG)

Primary open-angle glaucoma (POAG), the most common form of glaucoma by far, is expected to reach 45 million cases by 2010 (Sieving and Collins, 2007). Because POAG is usually painless, people with POAG can remain unaware of the condition until damage to the optic nerve has already occurred. Risk factors for POAG include older age (in general over age 60, but over 40 for blacks), race, Hispanic ethnicity, family history of glaucoma, elevated IOP, thin central cornea, and increased cup-disk ratio (Friedman et al., 2004). Some cupping of optic disk is normal if it is stable; any change in cupping ratio can indicate pathology. The cup-disk ratio compares the diameter of the cupped portion of the disk to its overall diameter. Other risk factors include peripheral vasospasm, systemic hypertension, cardiovascular disease, diabetes, hypothyroidism and other thyroid disorders, myopia, migraine, smoking, long-term steroid use, and heavy computer use by those with refractive errors, such as astigmatism, myopia, or hyperopia (Tatemichi et al., 2004; Weinreb and Khaw, 2004). Mutations of myocilin (*MYOC*) gene are also associated with high IOP resulting in POAG.

There are usually two types of open angle glaucoma: primary and juvenile-onset open-angle glaucoma (POAG and JOAG, respectively). The first one (POAG) is a common form, accounting for more than half of all cases (Klein et al., 1992). JOAG appears early in life (before 40 years old) and is transmitted in an autosomal-dominant inheritance fashion (Johnson et al., 1996). Numerous disease-causing *MYOC* mutations have now been identified, and additional loci on other chromosomes have been linked to JOAG (Avisar et al., 2009).

5.1.1.2 Primary angle closure glaucoma (PACG)

This is a closed angle type of glaucoma, i.e. the iris is found to block the drainage of the eye through the trabecular meshwork. It is a primary glaucoma because there is unknown cause relating to another condition, although the problem itself is clearly visible and related to the depth of the drainage angle of the eye (which is shallow). It includes chronic angle closure glaucoma and acute angle closure glaucoma (previously called acute glaucoma) (Sihota et al., 2004).

In PACG, the drainage angle is 'narrow', with signs that the iris has pressed against the trabecular meshwork and damages it, or the drainage angle is 'closed', with the iris stuck to the surface of the trabecular meshwork. In most eyes with this sort of glaucoma, the IOP is constantly higher than 'normal' because there is a blockage of, or damage to, the trabecular meshwork (TM). In some eyes, the pressure is intermittently higher than normal because the iris blocks the TM only some of the time. Sometimes angle closure results in an episode of very severe pain in the eye with short-term loss of vision. This is called acute angle closure glaucoma (previously called acute glaucoma).

5.1.1.3 Other types of glaucoma

In addition to open-angle and closed-angle glaucoma mentioned above, there are also developmental categories, which are further divided into primary and secondary types. Examples of secondary open-angle glaucomas include those associated with exfoliation or pigment-dispersion syndrome. Closed-angle glaucoma can be primary (e.g., pupillary block) or secondary (e.g., inflammatory or neovascular causes). Developmental forms of

glaucoma include primary congenital glaucoma and glaucoma associated with syndromes (e.g., aniridia or the Axenfeld-Rieger syndrome). Primary open-angle glaucoma, the predominant form of glaucoma in western countries, comprises of several clinically indistinguishable diseases.

5.1.2 POAG-causing genes

5.1.2.1 Genes associated with POAG

It is increasingly clear that POAG, in most cases, is inherited as a complex trait, where the disease results from the interaction of multiple genes and environmental factors (Sieving and Collins, 2007). This is agreeable to the complex phenotype of glaucoma, resulting from diverse pathological processes that involve changes in the aqueous humor outflow pathway, the retina and optic nerve, and even, as suggested recently, cerebrospinal fluid dynamics (Berdahl et al., 2008). So far, three genes have been identified to associate with glaucoma among the 14 known chromosomal loci. These genes are *myocilin/TIGR* (in GLC1A locus), *optineurin* (in GLC1E), and *WDR36* (in GLC1G). They are identified through family-based studies with glaucoma inherited as a Mendelian trait, where the altered function of a single gene is sufficient to cause the disease.

5.1.2.2 Myocilin

Approximately 4% of cases of adult-onset POAG and more than 10% of juvenile-onset cases are associated with *MYOC* mutations (Aldred et al., 2004). *MYOC* was identified by Stone and co-workers in GLC1A locus, which was the first reported locus for POAG

located on chromosome 1 (Morissette et al., 1995; Sheffield et al., 1993; Stone et al., 1997). The MYOC protein was previously known as trabecular meshwork inducible-glucocorticoid response protein or TIGR (Polansky et al., 1997). This genetic form of glaucoma is typically associated with high IOP and frequently requires surgical intervention for disease control. In adult POAG populations, the prevalence of *MYOC* mutations in POAG cases varies between 3 and 5% making it the most common form of inherited glaucoma currently known (Aldred et al., 2004; Baird et al., 2005; Chakrabarti et al., 2005; Libby et al., 2005). MYOC protein is a signal peptide secretary protein (Hebert and Molinari, 2007; Ponnambalam and Baldwin, 2003). It has both intracellular and intercellular functions (Ueda et al., 2002; Ueda and Yue, 2003) and can be found in various organelles such as the endoplasmic reticulum (ER), Golgi apparatus, and mitochondria (O'Brien et al., 2000; Ueda et al., 2000).

5.1.2.3 MYOC mutations

So far, more than 90 glaucoma-causing mutations have been identified in *MYOC*. These mutations are found in 3.86% (155/4107) of Caucasian probands with POAG (including normal tension glaucoma) or ocular hypertension, 3.3% (18/545) of probands of African descendants (including African Americans and black residents in Africa) and 4.44% (36/810) of Asian probands (Gong et al., 2004). Among them, many of which (such as *C245Y, Q368X, P370L, R422H, C433R, Y437H, I477N, I477S* and *N480K*) are aggressive mutants causing high IOP-associated juvenile-onset POAG; some (*R82C, T377M, D380A* and *R422C*) showed low LOD score (<3.0, θ=0) in linkage studies. Many of them are located in the olfactomedin-like domain of the encoded MYOC protein. Four

changes (R82C, C245Y, R422C and C433R) involve cysteine residues, which might affect the secondary structure of protein. Three mutations (*G252R, G367R* and *P370L*) were found in Asians and Caucasians, and three (*T293K, T377M* and *E352K*) in Africans and Caucasians. *Y371D* is a latest novel myocilin mutation which causes an aggressive form of JOAG in a Caucasian family from the Middle-East (Avisar et al., 2009).

5.1.2.4 MYOC mutations causing protein folding diseases

Many glaucoma-causing MYOC mutants have folding problem. They have been shown to be misfolded, more detergent-insoluble, and aggregation-prone than the wildtype (WT) protein. Some are detected being retained intracellularly (Jacobson et al., 2001; Joe et al., 2003; Yam et al., 2007a). Despite WT MYOC, which does not have a proven function, the mutants may cause glaucoma by a pathologic gain of function. Reports showed that several missense and truncated MYOC mutants (such as P370L, Q368X and K423E form hetero-oligomeric complexes with WT MYOC and aggregate intracellularly, resulting in secretion blockade (Gobeil et al., 2004; Liu and Vollrath, 2004). For mutants like C245Y, P370L and Y437H, formation of inclusion bodies typical of Russell bodies in the ER proved the intracellular localization and trafficking defects, which induces unfolded protein response (UPR) and result in apoptosis (Yam et al., 2007a). Reduction in TM cell population has been reported in glaucoma patients (Alvarado et al., 1984). The phagocytic capacity of TM would be compromised and the remaining TM population is insufficient for the effective cleaning of aqueous humor, thus leading to elevation of IOP (Matsumoto and Johnson, 1997). Moreover, the misfolded mutants are recognized by the protein quality control machinery in the ER, leading to the

formation of ER aggregation bodies typical of Russell's bodies and become trafficking defective (Haargaard et al., 2004; Yam et al., 2007a; Yam et al., 2007b). Besides the reported clinical evidence (Lam et al., 2000; Morissette et al., 1998), heterozygous expression of mutant MYOC caused WT MYOC to be retained intracellularly and form aggregation-prone complexes with mutant protein (Gobeil et al., 2004; Gould et al., 2006; Yam et al., 2007a). This could induce cellular stress and alter the cell morphology, which became prone to apoptosis (Joe et al., 2003; Yam et al., 2007a).

This cell apoptosis could explain the reduction of TM cells in patients with *MYOC*-caused glaucoma (Liu and Vollrath, 2004; Rohen et al., 1993). These glaucoma-associated MYOC mutants are also known to be secretion defective (Fan et al., 2006; Liu and Vollrath, 2004). Impaired MYOC secretion may lead to an altered extracellular matrix (ECM) at the TM cells that impedes aqueous humor outflow. Hence, *MYOC*-caused glaucoma is a protein folding disease and it is necessary to further understand the pathologic gain-of-function mechanism of these diseases induced by glaucoma-associated *MYOC* mutations. In our laboratory, the mutated D384N MYOC was found to be aggregation-prone and had protein trafficking problem, resulting in activation of ER stress and cell apoptosis.

5.1.3 The effect of small chemicals on MYOC mutations

The success of chemicals to correct a variety of misfolded proteins associated with pathologic conditions has made the chaperone-assisted therapy an appealing therapeutic approach for protein-folding diseases. It was shown that 4-phenylbutyric acid (4-PBA)

corrected ER-retained aggregated MYOC mutants (C245Y, P370L, and Y437H) for intracellular trafficking and this action rescued the affected cells from apoptosis (Yam et al., 2007b). In my study, I further tested the effect of small chemicals a battery of mutant MYOC and elucidated the generality of this therapeutic strategy for MYOC-caused POAG.

5.1.4 Selected MYOC mutations

MYOC variants were chosen by virtue of their proven contribution to glaucoma onset and pathogenesis (Vollrath and Liu, 2006). *D384N MYOC*, reported by our group earlier (Jia et al., 2009a) was the major variant studied in this part. It was a novel mutation causing a substitution of Asp with Asn at the 384 amino acid position and it caused juvenile-onset open-angle glaucoma in a Chinese JOAG family. In my study, the mechanism how D384N MYOC caused the onset and pathogenesis glaucoma was also investigated. The other 13 variants including nine aggressive mutants causing high IOP-associated juvenile-onset POAG (C245Y, Q368X, P370L, R422H, C433R, Y437H, I477N, I477S and N480K) and four ambiguous or mild variants (R82C, T377M, D380A and R422C), were examined for their changes upon small chemical treatments.

5.2 Materials and methods

5.2.1 Expression constructs, mutagenesis, and transfection

Full-length WT *MYOC* cDNA from human skeletal muscle was cloned to p3xFLAG-myc-CMV-25 (Sigma-Aldrich, St. Louis, MO) to generate pFLAG-myc-MYOC^{WT} (Yam et al., 2007b). Single base change was introduced by site-directed mutagenesis (QuikChange II; Stratagene, La Jolla, CA) with specific oligonucleotides (listed in **Table 5.1**) and the constructs were verified by direct sequencing. Human trabecular meshwork (HTM) cells (Yam et al., 2007b) were transfected with 1 μg plasmid DNA using 1 μl FuGene HD reagent (Roche Diagnostics, Basel, Switzerland).

5.2.2 Low temperature or chemical treatments

Transfected cells were incubated at 37°C or 30°C, 1 mM 4-PBA (triButyrate, Triple Crown America, Inc., Perkasie, PA) or 25 to 200 mM TMAO (Sigma-Aldrich) for 48 hours. 4-PBA (1 mM, triButyrate, Triple Crown America, Inc., Perkasie, PA), 25 to 200 mM TMAO (Sigma-Aldrich) or D_2O-based culture media was added to transfected cells for different time intervals.

5.2.3 MYOC secretion and solubility

Culture medium was immunoprecipitated with rabbit polyclonal antibody against myc (Santa Cruz Biotech, Santa Cruz, CA) bound to protein A beads (Dynabead; Dynal-Invitrogen, Carlsbad, CA) and analyzed by western blot analysis for FLAG. After PBS

Table 5.1 Glaucoma-causing mutants of myocilin and specific oligonucleotides for mutagenesis.

Sequence change	Exon	Suspected change	POAG onset	IOP (mmHg)	Mutagenesis oligos (sense strand from 5', bold and underlined is base change)
R82C[60]	1	Change in charge & disulfide bond	Adult	Not available	GAGAGACAGCAGCACCCAA**T**GCT-TAGACCTGGAGGCCACCA
C245Y[18]	3	Change in charge & disulfide bond	Juvenile	19-26	GGAGTGGAGAGGGAGACACCGG-AT**A**TGGAGAACTAGTTTGGGTAGG
Q368Stop[58]	3	Premature termination	Juvenile	21-56	GGAGCTGGCTACCACGGA**T**AGTT-CCCGTATTCTTGGGGTGG
P370L[59, 62]	3	Change in β-sheet	Juvenile	38	CTGGCTACCACGGACAGTTCC**T**G-TATTCTTGGGGTGGCTACAC
T377M[60]	3	Change in polarity	Juvenile	20-50	GTATTCTTGGGGTGGCTACA**T**GGA-CATTGACTTGGCTGTGG
D380A[64]	3	Unknown	Juvenile	Not available	GGGGTGGCTACACGGACATT**G**CC-TTGGCTGTGGATGAAGCAG
R422C[60]	3	Change in charge	Normal subject	Normal	AACCTGGGAGACAAACATC**T**GTA-AGCAGTCAGTCGCCAATG
R422H[60]	3	Change in charge	Juvenile	Not available	AACCTGGGAGACAAACATCC**A**TA-AGCAGTCAGTCGCCAATG
C433R[63]	3	Change in charge & disulfide bond	Juvenile	30	GTCGCCAAGCCTTCATCATC**C**GTG-GCACCTTGTACACCGTCAG
Y437H[60]	3	Change in charge	Juvenile	14-77	CATCATCTGTGGCACCTTG**C**ACAC-CGTCAGCAGCTACACC
I477S[59, 77]	3	Change in phosphorylation	Juvenile	high	GCTATAAGTACAGCAGCATGA**A**T-GACTACAACCCCCTGGAGA
I477N[61]	3	Change in glycosylation	Juvenile	20-52	GCTATAAGTACAGCAGCATGA**G**T-GACTACAACCCCCTGGAGA
N480K[59]	3	Change in glycosylation	Juvenile	28-48	CAGCAGCATGATTGACTACAA**A**C-CCCTGGAGAAGAAGCTCTT

washes, the cells were lysed in Triton X-100 (Tx) lysis buffer at 5 x10^6 cells/mL for 2 minutes on ice (Yam et al., 2007b; Zhou and Vollrath, 1999). After centrifugation, Tx-soluble and insoluble fractions were analyzed by western blot analysis using mouse monoclonal anti-GAPDH-horseradish peroxidase (HRP) conjugate (Sigma-Aldrich), anti-β-actin-HRP conjugate (Sigma-Aldrich) and anti-FLAG-HRP conjugate for MYOC (Sigma-Aldrich), followed by enhanced chemiluminescence (Amersham, Bucks, UK). Band intensity was then analyzed with image-analysis software (Quantity One Image Analysis; BioRad, Hercules, CA). MYOC expression was normalized with GAPDH for Tx-soluble protein or β-actin for Tx-insoluble protein.

5.2.4 MYOC transcription

Total RNA was obtained by a RNA purification kit (RNeasy kit; Qiagen, Valencia, CA) and an on-column DNase digestion kit (RNase-free DNase kit; Qiagen). Complementary DNA from 1 μg RNA, 10 ng/mL random hexanucleotide primer (Invitrogen) and reverse transcriptase (SuperScript III; Invitrogen) was amplified for *MYOC* and *GAPDH* (Yam et al., 2007b). All the methods of transcription analysis used in this part were followed as Section 3.2.10.

5.2.5 Immunofluorescence and apoptosis assay

Cells were fixed and stained with a monoclonal antibody against FLAG (Sigma-Aldrich) and red X-conjugated secondary antibody (Jackson Immuno Research Laboratory, West Grove, PA). Nuclei were stained with DAPI. Samples were examined

by fluorescence microscopy (DMRB; Leica, Wetzlar, Germany) equipped with a color imaging system (Spot RT; Diagnostic Instruments, Sterling Heights, MI). The apoptosis rate was represented as the percentage of cells with fragmented nuclei. For each experiment (n= 3), 10 random images (x40 objective) were analyzed.

5.2.6 Density gradient and protein analysis

Stable transfectant were selected by 800 μg/ml geneticin (Geneticin 418; Invitrogen) for 10 days. Cells treated with small chemicals for 2 days were collected in 250 mM sucrose buffer containing 10 mM HEPES-NaOH (pH 7.4), 1 mM EDTA.Na2 and protease inhibitor Complete™ , homogenized and spun at 1500g to remove the nuclei (Dounce; Bellco Glass Co., Vineland, NJ). The supernatant was further spun at 65,000g for an hour. The clear supernatant contained cytoplasmic soluble protein (see Figure 5.7, fraction 1). Pellet containing cytoplasmic organelles was layered on top of a density gradient (Optiprep 2.5%-30%; Nycomed, Oslo, Norway) and spun at 100,000g for 2 hours. Fractions 2 to 8 (according to Optiprep density) were analyzed by western blot analysis with anti-FLAG-HRP, monoclonal anti-calnexin (BD Bioscience), polyclonal anti-GM130 antibody (Santa Cruz Biotechnology), and detected by ECL.

5.3 Results

5.3.1 Solubility of MYOC mutants

In this study, a total of 14 glaucoma-causing variants of *MYOC* were examined. When expressed in HTM cells, we confirmed the reduced Tx solubility of these MYOC mutants. Approximately 85% of D384N MYOC mutant protein was resistant to 0.5% Tx extraction compared with about 25% of WT MYOC. Similarly reduced Tx solubility was found for C245Y, P370L, and Y437H mutants (**Figure 5.1**). The average Tx solubilities were 23 ± 0.325% for C245Y, 32 ± 0.415% for P370L, 33 ± 0.565% for Y437H MYOC in HTM cells. Other mutants of MYOC, such as Q368X, R422H, C433R, I477N, I477S and N480K MYOC were also highly Tx-insoluble (**Figure 5.2**), whereas those with T377M or R422C mutation had not more than 25% solubility, R82C and D380A MYOC were less than 50% Tx-soluble (**Figure 5.3**). In earlier studies, similar Tx solubility changes was obtained when FLAG-tagged or GFP-tagged MYOC fusion proteins (WT, C245Y, P370L and Y437H) were expressed in CHO-K1, HepG2 and HTM cells (Yam GHF et al., 2007b). Hence, altered Tx solubility exhibited by MYOC variants was not cell-type specific.

5.3.2 Chemical treatment on the solubility of MYOC mutants

When the transfected cells were treated with small chemical molecules (1 mM 4-PBA, 100 mM TMAO or D_2O-based medium) for 2 days, most tested variants had improved Tx solubility, as shown by the western blotting of FLAG epitope followed by band densitometry (**Figures 5. 2 and 5.3**). These treatments also reduced most of Tx-insoluble

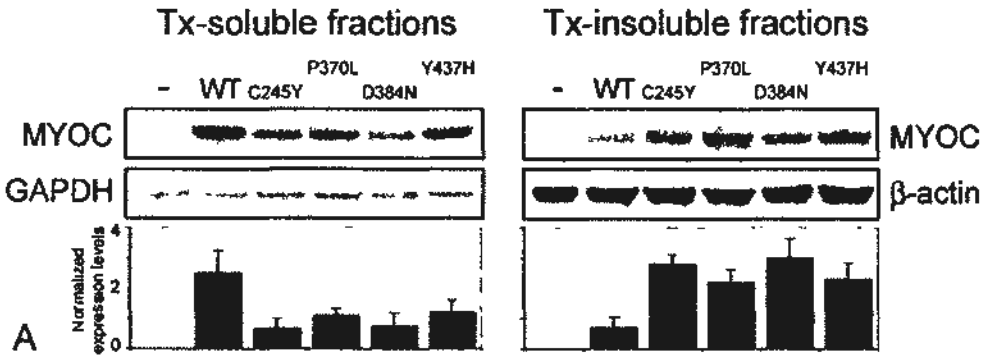

Figure 5.1 Detergent solubility test of MYOC mutants. Western blot analysis of FLAG showed reduced Tx solubility of D384N MYOC. The solubility change was similar to C245Y, P370L, and Y437H MYOC. GAPDH and β-actin were the housekeeping genes in the Tx-soluble and -insoluble fractions, respectively. Quantification by band densitometry indicated the predominant expression of Tx-insoluble mutant MYOC. WT, cells transfected with WT MYOC; -, cells transfected with vector only.

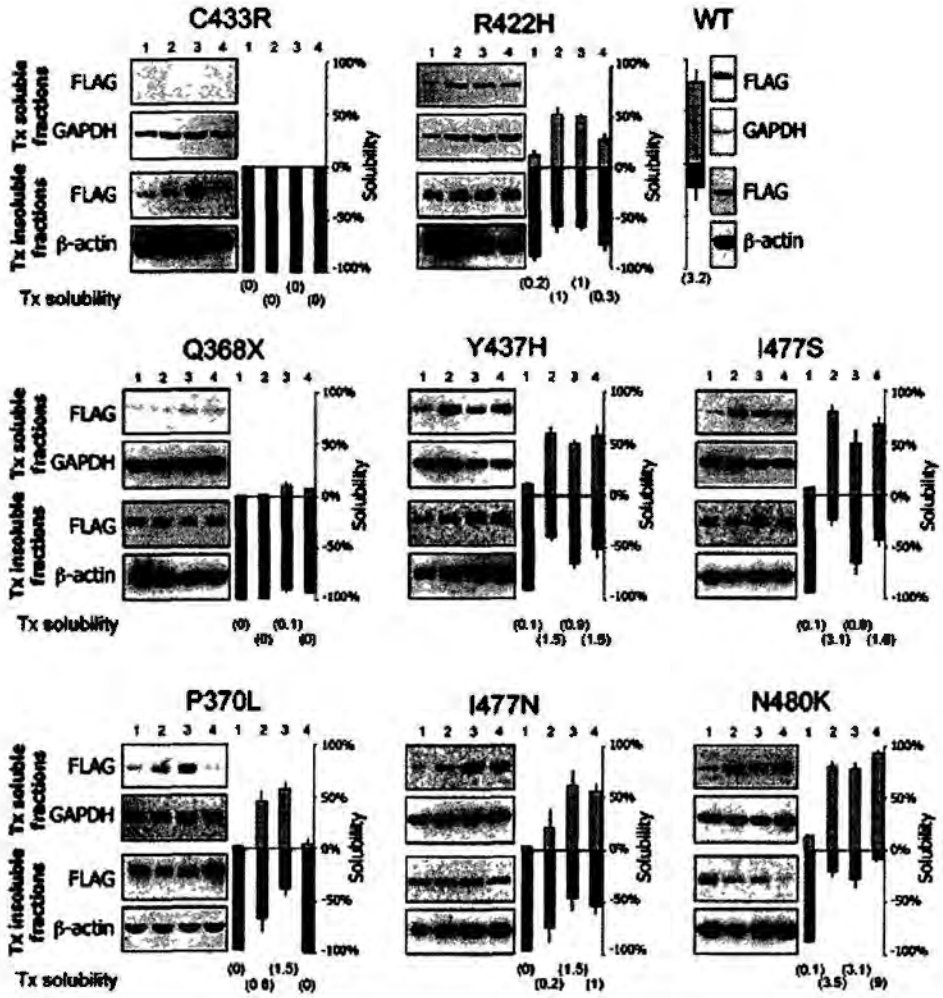

Figure 5.2 Effect of small chemicals on Tx solubility of aggressive MYOC variants. Expression of FLAG representing MYOC in Tx-soluble and Tx-insoluble fractions were quantified and normalized with the respective GAPDH (for Tx-soluble fractions) or β-actin (for Tx-insoluble fractions) expression. Experiment was done in triplicate and representative western blot pictures were presented in this figure. The Tx solubility was the percentage of total protein (sum of Tx-soluble and Tx-insoluble MYOC) and plotted as bar chart. Results were similar in triplicated experiments. 1, untreated; 2, 1 mM 4-PBA; 3, 100 mM TMAO; 4, D_2O-based medium. WT, wild-type.

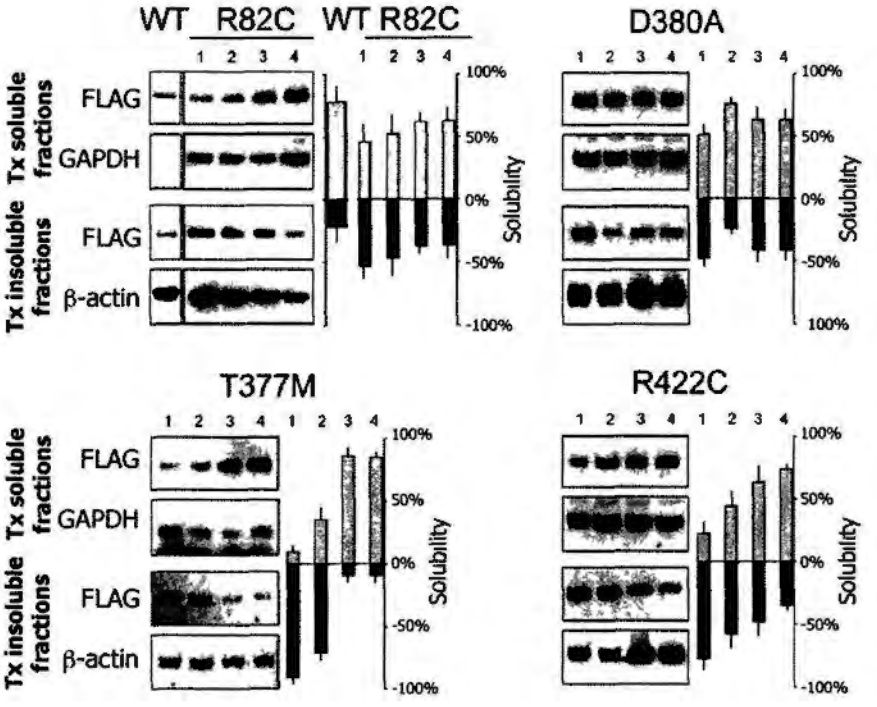

Figure 5.3 Small chemicals improved the Tx solubility of mild or ambiguous glaucoma-causing MYOC variants. Western blot analysis of FLAG showed reduced Tx solubility of R82C, D380A, T377M, R422C MYOC. 1, untreated; 2, 1 mM 4-PBA; 3, 100 mM TMAO; 4, D_2O-based medium. WT, wild-type.

MYOC mutans whereas the expression of WT MYOC was unaffected. Q368X and C433R MYOC remained Tx insoluble before or after small chemical treatments. Q368X mutant was only faintly detectable in Tx-soluble fractions after TMAO or D_2O treatment and C433R had no changes at all. The percentage of Tx-insoluble C245Y mutant after TMAO, 4-PBA or D_2O treatment was similarly decreased to more than 50% as that in untreated cells (46 ± 0.345% of Tx-insoluble C245Y mutant for PBA treatment, 23 ± 0.255% for TMAO treatment, 26 ± 0.185% for D_2O treatment, compared to 82 ± 0.935% for untreatment; $p<0.05$, independent Student *t*-test; **Figure 5.2**). The Tx solubility ratio (calculated as percentage of Tx-soluble MYOC compared to percentage of Tx-insoluble MYOC) of C245Y mutant is 1.7 for PBA treatment, 2.6 for TMAO treatment, 2.4 for D_2O treatment, and 0.021 for untreatment (**Figure 5.2**). Changes of Tx solubility ratio for the other mutants were listed in **Table 5.2**.

D384N MYOC, a novel mutation identified in a Chinese family, was also transfected in HTM cells. The transfected cells were incubated in a lower temperature to test if the folding defect can be corrected by condition enhancing refolding. It is hypothetized that low temperature can help the refolding of proteins, which have inherent folding disorders. When cells expressing D384N MYOC were incubated at 30°C for 2 days, the expression of Tx-soluble D384N MYOC was increased (**Figure 5.4**). In the further treatment with small chemicals, the same increase was detected when cells were treated with 1 mM 4-PBA or 50 mM TMAO. A faint doublet of soluble MYOC seen at 37°C became strongly expressed. Among the treatments, TMAO gave the highest level of Tx-soluble D384N MYOC (~6.2-fold that of the untreated mutant) and approached a level closed to that of

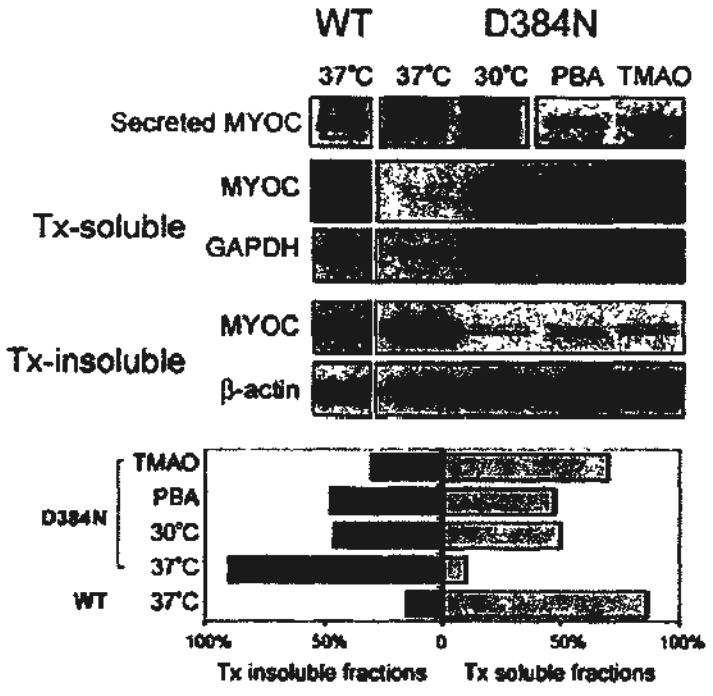

Figure 5.4 Improvement of secretion and Tx solubility of D384N MYOC. D384N-transfected cells were incubated at 30°C or treated with small chemicals (1 mM 4-PBA and 50 mM TMAO) for 2 days. By combined immunoprecipitation-Western blot analysis, D384N MYOC was detectable in the culture medium after TMAO and 4-PBA treatments. Incubation at 30°C did not show MYOC secretion. Increased expression of the Tx-soluble mutant MYOC was found after treatments. Results were compared to untreated cells expressing mutant or WT MYOC.

Table 5.2 Triton X-100 solubility ratios* of MYOC variants upon small chemical treatments.

	Treatments			
	Untreated	**4-PBA**	**TMAO**	**D_2O**
Wildtype	3.2	-	-	-
(A) Aggressive mutants				
C245Y	0.021	1.7	2.6	2.4
Q368X	0	0	0.1	0
P370L	0	0.6	1.5	0
R422H	0.2	1	1	0.3
Y437H	0.1	1.5	0.9	1.5
I477N	0	0.2	1.5	1
I477S	0.1	3.1	0.9	1.6
N480K	0.1	3.5	3.1	9
(B) Mild / ambiguous variants				
R82C	0.7	1	1.7	1.7
T377M	0.1	0.4	9	9
D380A	1	3.1	1.7	1.7
R422C	0.3	0.7	1.4	2.1

* Tx solubility ratio was calculated as percentage of Tx-soluble MYOC compared to percentage of Tx-insoluble MYOC.

the WT. Incubation at 30°C or with 1 mM 4-PBA caused approximately a threefold increase of Tx solubility. When the cells treated with both PBA and TMAO simultaneously, they had the same effect on the cells as TMAO treatment only. Results were reproducible in three different experiments.

The MYOC variants responded differently to small chemicals. For T377M mutant, the corrected level after 4-PBA treatment was about one-half as that of TMAO or D_2O. For I477N mutant, 4-PBA-treated level was about one-third as that of TMAO or D_2O. Nevertheless, P370L MYOC did not respond to D_2O treatment and remained Tx-insoluble (**Figures 5.2 and 5.3**).

In conclusion, TMAO treatment seemed to cause a better correct effect on mutant MYOC than other treatment. And also, TMAO-treated cells had no notable morphological changes, compared to PBA-treated cells when examined at two more days. Therefore, TMAO was selected in further experiments.

5.3.3 Dose-responsive effect of chemical treatment on D384N MYOC solubility and secretion

In this study, the mutant D384N MYOC was selected for a detailed investigation to verify the effect of small chemicals on correcting folding defects of MYOC and the consequent cell changes. To examine the MYOC secretion, a combined immunoprecipitation (IP) of media from cultures with the same number of cells and with excessive anti-myc antibody bound to protein A magnetic beads followed by immunoblot

analysis with excessive anti-FLAG HRP antibody was performed. In contrast to incubation at 30°C with a very minor secretion of D384N MYOC (**Figure 5.4**), more MYOC secretion was found after treatment with small chemicals (PBA and TMAO).

When applied at concentrations higher than 25 mM, TMAO enhanced D384N MYOC solubility, with the highest level at the 100 mM concentration (**Figure. 5.5 A**). The secretion was also improved with treatment at this drug concentration. From 5 x 10^6 cells, incubation with TMAO at 25 mM or higher caused mutant MYOC secretion. The peak secretion level was attained with 50 to 100 mM TMAO (**Figure. 5.5 B**). TMAO at 200 mM did not induce more secretion. In further experiments, a lower dose of TMAO (50 mM) with sufficient corrective ability to the secretion defect of D384N MYOC was used.

Semi-quantitative RT-PCR analysis did not reveal any changes in the steady state *MYOC* expression when cells were treated with up to 200 mM TMAO (**Figure 5.5 C**). Similar expression level of D384N MYOC was observed before and after TMAO treatment. This illustrated that TMAO treatment did not promote MYOC expression but altered the solubility of mutant protein for better trafficking and secretion.

5.3.4 Chemical treatment on apoptosis of D384N MYOC

Previous studies have demonstrated that glaucoma-associated MYOC mutants act through a pathological gain-of-function by inducing aggregate formation and the ER stress, which ultimately resulted in apoptotic cell death (Joe MK et al., 2003; Liu Y and Vollrath D, 2004; Yam GHF et al., 2007a; Yam GHF et al., 2007b). To study the cellular

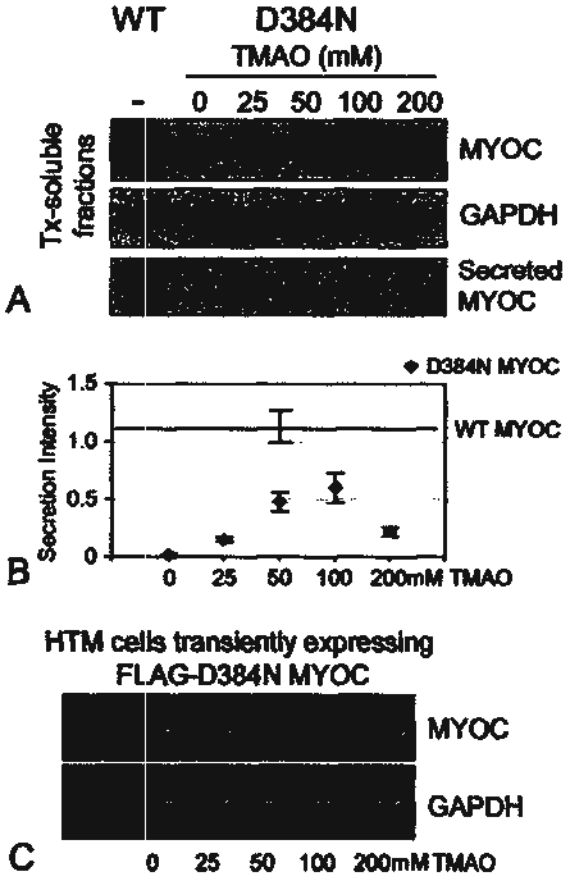

Figure 5.5 TMAO improved Tx solubility and secretion of D384N MYOC. (**A**) HTM cells (2x 10^6 cells) transiently expressing FLAG/myc-WT or D384N MYOC were treated with different doses of TMAO (0-200 mM) for 2 days. Tx-soluble fractions were assayed for FLAG (MYOC) and GAPDH. Untreated WT-expressing cells were used as the control. Culture media were collected and IP for myc, followed by Western blot analysis for FLAG for MYOC secretion. (**B**) Band densitometry showed that 50 to 100 mM TMAO improved the secretion of D384N MYOC to a level about half of WT MYOC. (**C**) RT-PCR analysis showed no transcriptional changes of MYOC by TMAO treatment (0-200 mM). GAPDH expression served as the internal control for sample loading.

changes casued by D384N MYOC, immunofluorescence study was performed on transfected HTM cells. D384N MYOC formed cellular aggregates (**Figure 5.6 B**), whereas WT had a diffuse vesicular distribution (Figure 5.6 A). More D384N cells (78 ± 14%) had intracellular MYOC aggregates than WT cells did (1.4 ± 0.1%; $p < 0.05$, paired Student's *t*-test). FLAG/myc-tagged MYOC expressing HTM cells showing fragmented nuclei by DAPI staining was quantified. An examination of the percentage of FLAG-positive cells with fragmented nuclei showed that D384N MYOC-expressing cells had an apoptosis rate of 31 ± 3.3%, whereas the apoptosis rate was 9 ± 1.5% in cells expressing WT MYOC (Figure 5.6 C). After the cells incubated with 50 mM TMAO for 2 days, the rate was reduced to 15.5 ± 2.5% in D384N MYOC-expressing cells (**Figure 5.6 D**). Treatment with 1 mM PBA mildly reduced the apoptosis rate to 20.5 ± 1.5% and low-temperature (30°C) treatment maintained the apoptosis rate at 28.7 ± 2.3% in D384N MYOC-expressing cells. The rate for untreated mock-transfected HTM cells was 2 ± 0.5%.

5.3.5 TMAO action on subcellular distribution of D384N MYOC

HTM cells stably expressing FLAG/myc-MYOC (WT or D384N) were treated with 50 mM TMAO for 2 days, followed by separation of cytoplasmic fractions by density gradient (0-30% Optiprep; Nycomed). Collected fractions were immunoblotted for FLAG (representing MYOC), ER lectin calnexin, and Golgi protein GM130. The D384N mutant was restricted to fractions immunoreactive to calnexin and was not in fractions with GM130 (**Figure 5.7**), whereas WT MYOC was distributed in a broader pattern along the gradient that was positive for calnexin and GM130. Moreover, the D384N mutant was

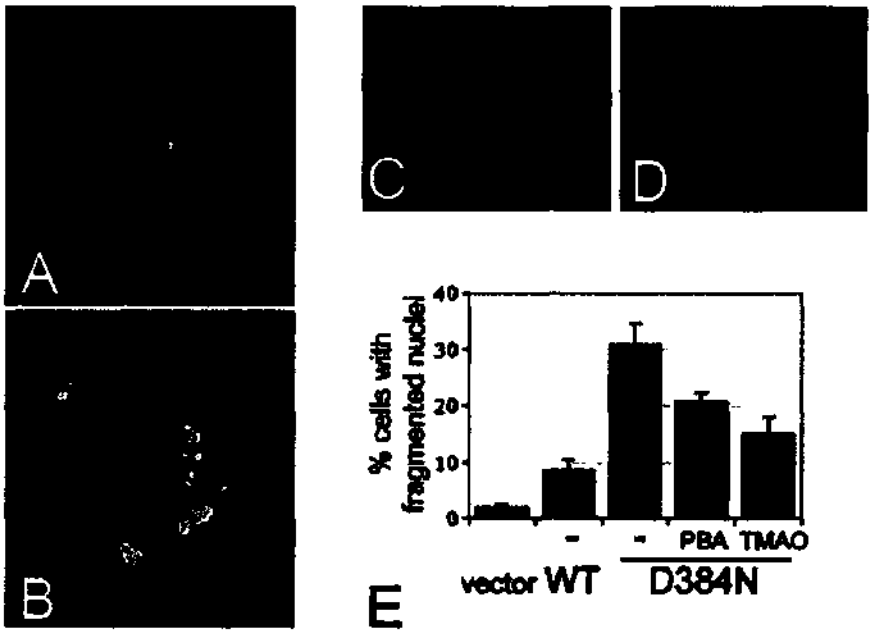

Figure 5.6 Immunofluorescence of FLAG/myc-WT and mutant D384N MYOC in HTM cells. **(A)** WT MYOC and **(B)** D384N MYOC-expressing cells. Scale bar: 10 μm. **(C)** Untreated D384N cells and **(D)** TMAO-treated D384N cells. Scale bar: 5 μm. **(E)** Apoptosis rates determined by the percentage of cells with fragmented nuclei. TMAO treatment for 2 days resulted in more of a reduction of apoptosis than did 4-PBA.

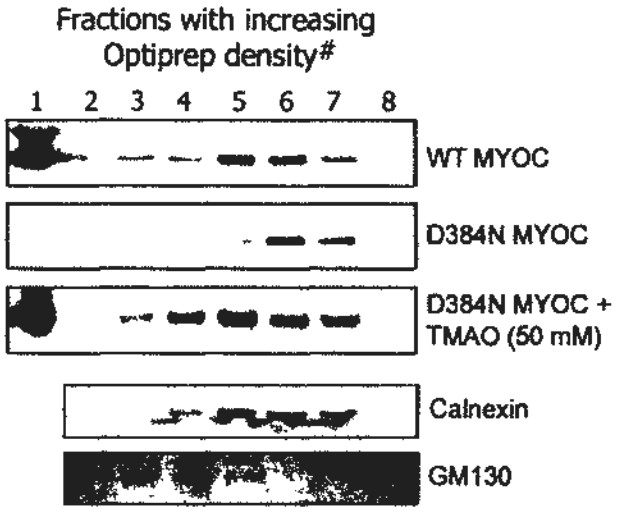

Figure 5.7 TMAO altered the subcellular distribution of D384N MYOC. Unlike WT MYOC with broad distribution and presence in the cytosolic fraction (*lane 1*), untreated D384N mutant mainly co-migrated with calnexin (*lanes 4-7*). No immunoreactivity was detected in GM130-positive fractions (*lanes 2-4*). TMAO-treated mutant MYOC was redistributed in both ER and Golgi-enriched fractions and cytosolic fraction, similar to WT MYOC.

not detectable in the cytoplasmic soluble protein (fraction 1), which showed intense immunoreactivity for WT MYOC. Treatment with 50 mM TMAO for 2 days resulted in a redistribution of the D384N mutant resembling that of WT. Mutant protein was co-distributed in GM130-positive fractions and reappeared in the cytoplasmic soluble fraction.

5.4 Discussion

Many mutations do not cause disease through impaired synthesis of polypeptide, but produce protein that cannot fold properly (Dobson, 2006; Gregersen, 2006; Outeiro and Tetzlaff, 2007) and thus lead to a disruption of normal functions. Inside cells, there exists stringent protein quality control in the ER-Golgi region to monitor the folding of secretory and membrane proteins (Moremen and Molinari, 2006; Roth, 2002). In addition to molecular chaperones and enzymes aiding the folding of peptides (Barral et al., 2004; Fewell et al., 2001), various machinery proteins are involved in the recognition and retention of aberrant proteins (Bukau et al., 2006; Helenius and Aebi, 2004; McClellan et al., 2005).

In this study, three small molecule compounds, 4-PBA, D_2O and TMAO, could act as chemical chaperones to correct the detergent insolubility and mistrafficking of glaucoma-causing MYOC variants and consequently, rescued the affected cells from apoptosis. Among the 14 MYOC variants studied, only Q368X and C433R mutant proteins were insensitive to treatment by any of the three chemicals. Other variants demonstrated improved detergent solubility and extracellular secretion. This indicated a mutation-dependent chemical chaperoning profile, likely due to variations in effects of the mutations on the protein properties or structure. Incubation of cells at 30°C or with small chemicals, 4-PBA (1 mM) or TMAO (50 mM), improved Tx solubility of D384N MYOC. Furthermore, small chemical treatment restored its secretion. D384N MYOC was mostly non-secreted, which may contribute to the severity of IOP elevation and early disease onset. Vollrath and Liu (2006) reported that the degree of mutant secretion at 30°C is

inversely related to the severity of the associated glaucoma phenotype. However, D384N MYOC remained non-secreted at low temperature incubation. In contrast, small chemicals should be good facilitators of folding of temperature-sensitive mutants. Among the chaperone molecules, TMAO engendered a redistribution of mutant MYOC from the ER. D384N protein was restricted to the density gradient fractions immunoreactive for calnexin, an ER resident protein, whereas WT MYOC was detected in a broader distribution and was not limited to calnexin-positive fractions. With TMAO treatment, D384N mutant was relocalized from the ER-enriched to Golgi-enriched fractions (GM130 positive) and was highly indicative of a reduced ER retention. The shortened ER retention and activation of UPR could rescue the affected cells from apoptosis (Jia et al., 2009a). As indicated in Figure 5.6, D384N MYOC-expressing cells had a higher apoptosis rate than that of WT-expressing cells, whereas the apoptosis rate of D384N MYOC-expressing cells was reduced after TMAO treatment.

Setting up a favorable environment for the refolding of improperly folded proteins to their native state has been proposed as a new therapeutic avenue for treating protein-folding diseases (Cohen and Kelly, 2003; Loo and Clarke, 2007). Although low temperature can improve protein folding and alleviate abnormal morphology and cell killing induced by misfolded protein expression (Liu and Vollrath, 2004; Rennolds et al., 2008; Vollrath and Liu, 2006), application of low temperature to tissue cells is practically very difficult. Delivery of drugs to target tissue sites is more feasible. Many studies have described the use of cell-permeable small molecules with chaperoning activity to reverse the mislocalization or reduce the aggregation of proteins associated with human diseases

(Bennion et al., 2004; Bonapace et al., 2004; Burrows et al., 2000; Jafarnejad et al., 2008; Mu et al., 2008; Ozcan et al., 2006; Yam et al., 2007b). They include 4-PBA, polyols such as glycerol, trimethylamines such as TMAO, enzyme antagonists, and chemical ligands. The mechanisms of action may involve the stabilization of proteins, prevention of undesirable interactions between proteins, reduction of aggregate formation, and alteration of folding environment or endogenous chaperone activity (Loo and Clarke, 2007; Papp and Csermely, 2006). This gives more efficient transport of client proteins to the intracellular or extracellular destinations. Beside the loss of activity, abnormal protein folding and aggregation can contribute to gain-of-function cytotoxicity (de Almeida et al., 2007; Gregersen, 2006; Yam et al., 2007a). Hence, correction of protein misfolding or mistrafficking is of critical importance to rescue the damaged cells and relieve the disease severity. Recent reports have substantiated the efficacy of chemical chaperones in alleviating ER stress and apoptosis in lysosomal storage diseases (Wei et al., 2008; Yam et al., 2006; Yam et al., 2005).

TMAO acts as a protein stabilizer to protect ligand binding and polymerization against pressure inhibition (Yancey, 2005). It improves folding and assembly of different proteins (Banks and Gloss, 2004; Kumar et al., 2005; Tamarappoo and Verkman, 1998). It is hydrophobic and is capable of forcing water molecules out of solution onto the protein surface. This unique hydrophobic feature makes TMAO more effective than 4-PBA in correcting MYOC folding (Yam et al., 2007b). Misfolded MYOC may exist in partially denatured or aggregated states. 4-PBA may act by stabilizing the thermolabile mutant MYOC and thus salvage them from denaturation. In the presence of TMAO,

driving out water molecules from molten globule structure favors folding into a more native conformation and tighter packing. The mutant amino acid asparagine may lay deep in the protein conformation and is less solvent accessible. Thus, increased hydrostatic pressure caused by TMAO shifts the equilibrium from the improperly folded state to a more native state. This action was evidenced by the correction of aquaporin-2 mutants for functional water channelling activity in mice (Tamarappoo and Verkman, 1998), formation of histone tetramers (Banks and Gloss, 2004), cell surface expression of the functional chloride conductance transporter F508 CFTR (Fischer et al., 2001), and recovery of trypsin activity (Kumar et al., 2005).

5.5 Conclusion

Mechanism of chemical chaperoning is yet to be fully understood, it is likely that they stabilize the incorrect folding to reduce aggregation and prevent non-productive interactions with resident proteins or chaperones, thereby facilitate transport across intracellular compartments. In this study, osmolytes PBA, D_2O and TMAO showed different corrective effect on the detergent solubility and secretion among the curable mutants. Especially for TMAO, it reduced the ER retention and improved the secretion of D384N mutant MYOC. This rescued cells from apoptosis of D384N expressed cells. In conclusion, small chemicals with chaperone activity possess the potential to treat MYOC-caused POAG and that topical administration should be tested for their therapeutic effects in glaucoma.

6 General conclusions

There are many people woldwide suffer from blindness caused by different kinds of eye diseases, such as cataract, glaucoma, age-related macular degeneration (AMD), retinitis pigmentosa (RP). In my project, extensive investigations have been conducted *in vitro* to characterize two cataract-causing genes, *CRYAA (αA-crystallin)* and *CRYGD (γD-crystallin)* and a high tension primary open-angle glaucoma-causing gene, *MYOC (myocillin)*.

In the study about G98R CRYAA, *mutant CRYAA* was expressed in cultured human lens epithelial B3 cells and their solubility, aggregation, localization in organelles, and apoptotic effects were studied. I showed that G98R CRYAA induced the ER stress, and the affected cells underwent apoptosis. This is the first time to show that presenile cataract that caused by the misfolded G98R CRYAA, could be an ER storage disease. This cellular defect was corrected by the treatment with chemical chaperone, natural osmolyte TMAO. I also showed that TMAO treatment modulated Hsp70 expression, which could be an underlying mechanism how this chemical chaperone affected the protein folding environment in cells.

Furthermore, *mutant G165fsX8 CRYGD* was also studied. I expressed *mutant CRYGD* in COS-7 cells and tested that the altered protein properties could be resolved by treatment with chemical osmolyte. My results showed improvement of protein solubility and reduction of cell apoptosis in mutant expressing cells treated with sodium 4-phenylbutyrate, 4-PBA.

I also investigated myocilin-casued glaucoma that could be caused by disruptive protein folding. In culture, I transfected different *MYOC variants*, including *D384N MYOC*, to human trabecular meshwork cells followed by treatment with small and natural osmolyte molecule, TMAO. The treatment reduced the ER retention and improved the secretion of D384N mutant MYOC. This alleviated the ER stress and rescued cells from apoptosis, likely according to the chemical chaperone activity of TMAO.

In summary, I have characterized the altered protein properties caused by three mutant genes and shown that the disrupted protein functions could be resolved by treatment with small chemical molecules, such as TMAO and 4-PBA, by virtue of their chaperoning capabilities. My results illustrated the biological mechanism of chaperone action in the correction of these misfolded proteins. Given that these chemicals are cell-permeable and small in size, they should be tested in animal studies on their biological effects to lens opacity or elevated intraocular pressure.

7 Future perspectives

Recently, a group of exogenous small molecules that are freely diffusible in cells and with chaperoning activity (collectively termed as chemical chaperones) has successfully corrected a variety of misfolded proteins and the associated cellular defects or protein folding abnormalities (Janovick et al., 2009; Jiang et al., 2009; Tveten et al., 2007). The mechanism of their chemical chaperoning, though not fully understood, may involve an improvement and stabilization of protein folding environment, prevention of non-productive protein interactions, reduction of aggregate formation and alteration of endogenous chaperone activity.

Given the fundamental interplay between small molecules and misfolded proteins in maintaining their native structure, it is likely that numerous classes of compounds will be found that function as chemical chaperones to ameliorate diseases of proteostasis deficiency. And also, the exact mechanism of these small molecules' action on dispruted proteisn should be explored to examine the changes of protein structure after correction by small chemical molecules. Meanwhile, these small molecules should be tested in animal studies on their biological effects to determine whether they could be potential therapeutic and applicable for the treatment of ocular diseases through topical administration in the future study.

Therefore, I propose that such therapeutic strategies, including combination therapies, represent a new approach for treating a range of diverse human diseases, especially protein folding diseases in the eye.

8 References

Aldred, M. A., Baumber, L., Hill, A., Schwalbe, E. C., Goh, K., Karwatowski, W., and Trembath, R. C. (2004). Low prevalence of MYOC mutations in UK primary open-angle glaucoma patients limits the utility of genetic testing. Hum Genet *115*, 428-431.

Alvarado, J., Murphy, C., and Juster, R. (1984). Trabecular meshwork cellularity in primary open-angle glaucoma and nonglaucomatous normals. Ophthalmology *91*, 564-579.

Alward, W. L., Fingert, J. H., Coote, M. A., Johnson, A. T., Lerner, S. F., Junqua, D., Durcan, F. J., McCartney, P. J., Mackey, D. A., Sheffield, V. C., and Stone, E. M. (1998). Clinical features associated with mutations in the chromosome 1 open-angle glaucoma gene (GLC1A). N Engl J Med *338*, 1022-1027.

Andley, U. P. (2007). Crystallins in the eye: Function and pathology. Prog Retin Eye Res *26*, 78-98.

Andley, U. P. (2009). AlphaA-crystallin R49Cneo mutation influences the architecture of lens fiber cell membranes and causes posterior and nuclear cataracts in mice. BMC Ophthalmol *9*, 4.

Andley, U. P., Patel, H. C., and Xi, J. H. (2002). The R116C mutation in alpha A-crystallin diminishes its protective ability against stress-induced lens epithelial cell apoptosis. J Biol Chem *277*, 10178-10186.

Andley, U. P., Song, Z., Wawrousek, E. F., Fleming, T. P., and Bassnett, S. (2000). Differential protective activity of alpha A- and alphaB-crystallin in lens epithelial cells. J Biol Chem *275*, 36823-36831.

Araki-Sasaki, K., Ando, Y., Nakamura, M., Kitagawa, K., Ikemizu, S., Kawaji, T., Yamashita, T., Ueda, M., Hirano, K., Yamada, M., *et al.* (2005). Lactoferrin Glu561Asp facilitates secondary amyloidosis in the cornea. Br J Ophthalmol *89*, 684-688.

Argon, Y., and Simen, B. B. (1999). GRP94, an ER chaperone with protein and peptide binding properties. Semin Cell Dev Biol *10*, 495-505.

Aridor M, and Hannan LA (2002). Traffic jams II: an update of diseases of intracellular transport. Traffic *3*, 781-790.

Aroca-Aguilar, J. D., Sanchez-Sanchez, F., Martinez-Redondo, F., Coca-Prados, M., and Escribano, J. (2008). Heterozygous expression of myocilin glaucoma mutants increases secretion of the mutant forms and reduces extracellular processed myocilin. Mol Vis *14*, 2097-2108.

Augusteyn, R. C. (2004). alpha-crystallin: a review of its structure and function. Clin Exp Optom *87*, 356-366.

Augusteyn, R. C. (2007). Growth of the human eye lens. Mol Vis *13*, 252-257.

Avisar, I., Lusky, M., Robinson, A., Shohat, M., Dubois, S., Raymond, V., and Gaton, D. D. (2009). The novel Y371D myocilin mutation causes an aggressive form of juvenile open-angle glaucoma in a Caucasian family from the Middle-East. Mol Vis *15*, 1945-1950.

Bai, C., Biwersi, J., Verkman, A. S., and Matthay, M. A. (1998). A mouse model to test the in vivo efficacy of chemical chaperones. J Pharmacol Toxicol Methods *40*, 39-45.

Baird, P. N., Richardson, A. J., Craig, J. E., Rochtchina, E., Mackey, D. A., and Mitchell, P. (2005). The Q368STOP myocilin mutation in a population-based cohort: the Blue Mountains Eye Study. Am J Ophthalmol *139*, 1125-1126.

Balch, W. E., Morimoto, R. I., Dillin, A., and Kelly, J. W. (2008). Adapting proteostasis for disease intervention. Science *319*, 916-919.

Banks, D. D., and Gloss, L. M. (2004). Folding mechanism of the (H3-H4)2 histone tetramer of the core nucleosome. Protein Sci *13*, 1304-1316.

Barral, J. M., Broadley, S. A., Schaffar, G., and Hartl, F. U. (2004). Roles of molecular chaperones in protein misfolding diseases. Semin Cell Dev Biol *15*, 17-29.

Basseri, S., Lhotak, S., Sharma, A. M., and Austin, R. C. (2009). The chemical chaperone 4-phenylbutyrate inhibits adipogenesis by modulating the unfolded protein response. J Lipid Res *50*, 2486-24501.

Baum, J., and Brodsky, B. (1999). Folding of peptide models of collagen and misfolding in disease. Curr Opin Struct Biol *9*, 122-128.

Beby, F., Commeaux, C., Bozon, M., Denis, P., Edery, P., and Morle, L. (2007). New phenotype associated with an Arg116Cys mutation in the CRYAA gene: nuclear cataract, iris coloboma, and microphthalmia. Arch Ophthalmol *125*, 213-216.

Beere, H. M., Wolf, B. B., Cain, K., Mosser, D. D., Mahboubi, A., Kuwana, T., Tailor, P., Morimoto, R. I., Cohen, G. M., and Green, D. R. (2000). Heat-shock protein 70 inhibits apoptosis by preventing recruitment of procaspase-9 to the Apaf-1 apoptosome. Nat Cell Biol *2*, 469-475.

Bennion, B. J., DeMarco, M. L., and Daggett, V. (2004). Preventing misfolding of the prion protein by trimethylamine N-oxide. Biochemistry *43*, 12955-12963.

Berdahl, J. P., Allingham, R. R., and Johnson, D. H. (2008). Cerebrospinal fluid pressure is decreased in primary open-angle glaucoma. Ophthalmology *115*, 763-768.

Bergamini, E. (2006). Autophagy: a cell repair mechanism that retards ageing and age-associated diseases and can be intensified pharmacologically. Mol Aspects Med *27*, 403-410.

Bian, Q., Fernandes, A. F., Taylor, A., Wu, M., Pereira, P., and Shang, F. (2008). Expression of K6W-ubiquitin in lens epithelial cells leads to upregulation of a broad spectrum of molecular chaperones. Mol Vis *14*, 403-412.

Bichet, D., Cornet, V., Geib, S., Carlier, E., Volsen, S., Hoshi, T., Mori, Y., and De Waard, M. (2000). The I-II loop of the Ca2+ channel alpha1 subunit contains an endoplasmic reticulum retention signal antagonized by the beta subunit. Neuron *25*, 177-190.

Blechinger, S. R., Evans, T. G., Tang, P. T., Kuwada, J. Y., Warren, J. T., Jr., and Krone, P. H. (2002). The heat-inducible zebrafish hsp70 gene is expressed during normal lens development under non-stress conditions. Mech Dev *112*, 213-215.

Bloemendal, H., and de Jong, W. W. (1991). Lens proteins and their genes. Prog Nucleic Acid Res Mol Biol *41*, 259-281.

Bonapace, G., Waheed, A., Shah, G. N., and Sly, W. S. (2004). Chemical chaperones protect from effects of apoptosis-inducing mutation in carbonic anhydrase IV identified in retinitis pigmentosa 17. Proc Natl Acad Sci U S A *101*, 12300-12305.

Bonilla, M., and Cunningham, K. W. (2003). Mitogen-activated protein kinase stimulation of Ca(2+) signaling is required for survival of endoplasmic reticulum stress in yeast. Mol Biol Cell *14*, 4296-4305.

Booth, D. R., Sunde, M., Bellotti, V., Robinson, C. V., Hutchinson, W. L., Fraser, P. E., Hawkins, P. N., Dobson, C. M., Radford, S. E., Blake, C. C., and Pepys, M. B. (1997). Instability, unfolding and aggregation of human lysozyme variants underlying amyloid fibrillogenesis. Nature *385*, 787-793.

Bornheim, R., Muller, M., Reuter, U., Herrmann, H., Bussow, H., and Magin, T. M. (2008). A dominant vimentin mutant upregulates Hsp70 and the activity of the ubiquitin-proteasome system, and causes posterior cataracts in transgenic mice. J Cell Sci *121*, 3737-3746.

Brady, J. P., Garland, D., Duglas-Tabor, Y., Robison, W. G., Jr., Groome, A., and Wawrousek, E. F. (1997). Targeted disruption of the mouse alpha A-crystallin gene induces cataract and cytoplasmic inclusion bodies containing the small heat shock protein alpha B-crystallin. Proc Natl Acad Sci U S A *94*, 884-889.

Brian, G., and Taylor, H. (2001). Cataract blindness--challenges for the 21st century. Bull World Health Organ *79*, 249-256.

Brodsky, J. L., and Chiosis, G. (2006). Hsp70 molecular chaperones: emerging roles in human disease and identification of small molecule modulators. Curr Top Med Chem *6*, 1215-1225.

Brown, A. J., Sun, L., Feramisco, J. D., Brown, M. S., and Goldstein, J. L. (2002). Cholesterol addition to ER membranes alters conformation of SCAP, the SREBP escort protein that regulates cholesterol metabolism. Mol Cell *10*, 237-245.

Bukau, B., Weissman, J., and Horwich, A. (2006). Molecular chaperones and protein quality control. Cell *125*, 443-451.

Burrows, J. A., Willis, L. K., and Perlmutter, D. H. (2000). Chemical chaperones mediate increased secretion of mutant alpha 1-antitrypsin (alpha 1-AT) Z: A potential pharmacological strategy for prevention of liver injury and emphysema in alpha 1-AT deficiency. Proc Natl Acad Sci U S A *97*, 1796-1801.

Byers, P. H. (2001). Folding defects in fibrillar collagens. Philos Trans R Soc Lond B Biol Sci *356*, 151-157; discussion 157-158.

Caciotti, A., Donati, M. A., d'Azzo, A., Salvioli, R., Guerrini, R., Zammarchi, E., and Morrone, A. (2009). The potential action of galactose as a "chemical chaperone": increase of beta galactosidase activity in fibroblasts from an adult GM1-gangliosidosis patient. Eur J Paediatr Neurol *13*, 160-164.

Carbone, M. A., Ayroles, J. F., Yamamoto, A., Morozova, T. V., West, S. A., Magwire, M. M., Mackay, T. F., and Anholt, R. R. (2009). Overexpression of myocilin in the Drosophila eye activates the unfolded protein response: implications for glaucoma. PLoS One *4*, e4216.

Chakrabarti, S., Kaur, K., Komatireddy, S., Acharya, M., Devi, K. R., Mukhopadhyay, A., Mandal, A. K., Hasnain, S. E., Chandrasekhar, G., Thomas, R., and Ray, K. (2005). Gln48His is the prevalent myocilin mutation in primary open angle and primary congenital glaucoma phenotypes in India. Mol Vis *11*, 111-113.

Chambers, C., and Russell, P. (1991). Deletion mutation in an eye lens beta-crystallin. An animal model for inherited cataracts. J Biol Chem *266*, 6742-6746.

Chan, H. S., and Dill, K. A. (1998). Protein folding in the landscape perspective: chevron plots and non-Arrhenius kinetics. Proteins *30*, 2-33.

Chapple, J. P., and Cheetham, M. E. (2003). The chaperone environment at the cytoplasmic face of the endoplasmic reticulum can modulate rhodopsin processing and inclusion formation. J Biol Chem *278*, 19087-19094.

Chapple, J. P., Grayson, C., Hardcastle, A. J., Saliba, R. S., van der Spuy, J., and Cheetham, M. E. (2001). Unfolding retinal dystrophies: a role for molecular chaperones? Trends Mol Med *7*, 414-421.

Chen, Y. C., Reid, G. E., Simpson, R. J., and Truscott, R. J. (1997). Molecular evidence for the involvement of alpha crystallin in the colouration/crosslinking of crystallins in age-related nuclear cataract. Exp Eye Res *65*, 835-840.

Cheong, H. I., Cho, H. Y., Park, H. W., Ha, I. S., and Choi, Y. (2007). Molecular genetic study of congenital nephrogenic diabetes insipidus and rescue of mutant vasopressin V2 receptor by chemical chaperones. Nephrology (Carlton) *12*, 113-117.

Chiesi, M., Longoni, S., and Limbruno, U. (1990). Cardiac alpha-crystallin. III. Involvement during heart ischemia. Mol Cell Biochem *97*, 129-136.

Choo-Kang, L. R., and Zeitlin, P. L. (2001). Induction of HSP70 promotes DeltaF508 CFTR trafficking. Am J Physiol Lung Cell Mol Physiol *281*, L58-68.

Cid, V. J., Duran, A., del Rey, F., Snyder, M. P., Nombela, C., and Sanchez, M. (1995). Molecular basis of cell integrity and morphogenesis in Saccharomyces cerevisiae. Microbiol Rev *59*, 345-386.

Cochella, L., and Green, R. (2005). Fidelity in protein synthesis. Curr Biol *15*, R536-540.
Cohen, F. E., and Kelly, J. W. (2003). Therapeutic approaches to protein-misfolding diseases. Nature *426*, 905-909.

Collins, A. F., Pearson, H. A., Giardina, P., McDonagh, K. T., Brusilow, S. W., and Dover, G. J. (1995). Oral sodium phenylbutyrate therapy in homozygous beta thalassemia: a clinical trial. Blood *85*, 43-49.

Corboy MJ, Thomas PJ, and Wigley WC (2005). Aggresome formation. Methods Mol Biol *301*, 305-327.

Datta, R., Waheed, A., Bonapace, G., Shah, G. N., and Sly, W. S. (2009). Pathogenesis of retinitis pigmentosa associated with apoptosis-inducing mutations in carbonic anhydrase IV. Proc Natl Acad Sci U S A *106*, 3437-3442.

de Almeida, S. F., Picarote, G., Fleming, J. V., Carmo-Fonseca, M., Azevedo, J. E., and de Sousa, M. (2007). Chemical chaperones reduce endoplasmic reticulum stress and prevent mutant HFE aggregate formation. J Biol Chem *282*, 27905-27912.

de Jong, W. W., Caspers, G. J., and Leunissen, J. A. (1998). Genealogy of the alpha-crystallin--small heat-shock protein superfamily. Int J Biol Macromol *22*, 151-162.

Delcourt, C., Dupuy, A. M., Carriere, I., Lacroux, A., and Cristol, J. P. (2005). Albumin and transthyretin as risk factors for cataract: the POLA study. Arch Ophthalmol *123*, 225-232.

Deocaris, C. C., Takano, S., Priyandoko, D., Kaul, Z., Yaguchi, T., Kraft, D. C., Yamasaki, K., Kaul, S. C., and Wadhwa, R. (2008). Glycerol stimulates innate chaperoning, proteasomal and stress-resistance functions: implications for gerontomanipulation. Biogerontology *9*, 269-282.

Derham, B. K., and Harding, J. J. (1999). Alpha-crystallin as a molecular chaperone. Prog Retin Eye Res *18*, 463-509.

Devi, R. R., Yao, W., Vijayalakshmi, P., Sergeev, Y. V., Sundaresan, P., and Hejtmancik, J. F. (2008). Crystallin gene mutations in Indian families with inherited pediatric cataract. Mol Vis *14*, 1157-1170.

Dice, J. F. (2007). Chaperone-mediated autophagy. Autophagy *3*, 295-299.

Dice, J. F., and Terlecky, S. R. (1990). Targeting of cytosolic proteins to lysosomes for degradation. Crit Rev Ther Drug Carrier Syst *7*, 211-233.

Ding, J. D., Lin, J., Mace, B. E., Herrmann, R., Sullivan, P., and Bowes Rickman, C. (2008). Targeting age-related macular degeneration with Alzheimer's disease based immunotherapies: anti-amyloid-beta antibody attenuates pathologies in an age-related macular degeneration mouse model. Vision Res *48*, 339-345.

Dobson, C. M. (2001). The structural basis of protein folding and its links with human disease. Philos Trans R Soc Lond B Biol Sci *356*, 133-145.

Dobson, C. M. (2003). Protein folding and misfolding. Nature *426*, 884-890.

Dobson, C. M. (2006). Protein aggregation and its consequences for human disease. Protein Pept Lett *13*, 219-227.

Dobson, C. M., and Ellis, R. J. (1998). Protein folding and misfolding inside and outside the cell. Embo J *17*, 5251-5254.

Dohm, C. P., Kermer, P., and Bahr, M. (2008). Aggregopathy in neurodegenerative diseases: mechanisms and therapeutic implication. Neurodegener Dis *5*, 321-338.

Dube, D. H., and Bertozzi, C. R. (2005). Glycans in cancer and inflammation--potential for therapeutics and diagnostics. Nat Rev Drug Discov *4*, 477-488.

Ecroyd, H., and Carver, J. A. (2009). Crystallin proteins and amyloid fibrils. Cell Mol Life Sci *66*, 62-81.

Ellgaard, L., Molinari, M., and Helenius, A. (1999). Setting the standards: quality control in the secretory pathway. Science *286*, 1882-1888.

Ellis, R. J. (2001a). Macromolecular crowding: an important but neglected aspect of the intracellular environment. Curr Opin Struct Biol *11*, 114-119.

Ellis, R. J. (2001b). Molecular chaperones: inside and outside the Anfinsen cage. Curr Biol *11*, R1038-1040.

Evans, T. G., Yamamoto, Y., Jeffery, W. R., and Krone, P. H. (2005). Zebrafish Hsp70 is required for embryonic lens formation. Cell Stress Chaperones *10*, 66-78.

Fan, B. J., Leung, D. Y., Wang, D. Y., Gobeil, S., Raymond, V., Tam, P. O., Lam, D. S., and Pang, C. P. (2006). Novel myocilin mutation in a Chinese family with juvenile-onset open-angle glaucoma. Arch Ophthalmol *124*, 102-106.

Fan, J., Fariss, R. N., Purkiss, A. G., Slingsby, C., Sandilands, A., Quinlan, R., Wistow, G., and Chepelinsky, A. B. (2005). Specific interaction between lens MIP/Aquaporin-0 and two members of the gamma-crystallin family. Mol Vis *11*, 76-87.

Fan, J. Q. (2003). A contradictory treatment for lysosomal storage disorders: inhibitors enhance mutant enzyme activity. Trends Pharmacol Sci *24*, 355-360.

Fan, J. Q., and Ishii S (2003). Cell-based screening of active-site specific chaperone for the treatment of Fabry disease. Methods Enzymol *363*, 412-420.

Fausther, M., Villeneuve, L., and Cadrin, M. (2004). Heat shock protein 70 expression, keratin phosphorylation and Mallory body formation in hepatocytes from griseofulvin-intoxicated mice. Comp Hepatol *3*, 5.

Ferrufino-Ponce, Z. K., and Henderson, B. A. (2006). Radiotherapy and cataract formation. Semin Ophthalmol *21*, 171-180.

Fewell, S. W., Travers, K. J., Weissman, J. S., and Brodsky, J. L. (2001). The action of molecular chaperones in the early secretory pathway. Annu Rev Genet *35*, 149-191.

Fingert, J. H., Stone, E. M., Sheffield, V. C., and Alward, W. L. (2002). Myocilin glaucoma. Surv Ophthalmol *47*, 547-561.

Fischer, H., Fukuda, N., Barbry, P., Illek, B., Sartori, C., and Matthay, M. A. (2001). Partial restoration of defective chloride conductance in DeltaF508 CF mice by trimethylamine oxide. Am J Physiol Lung Cell Mol Physiol *281*, L52-57.

Fleming, T. P., Song, Z., and Andley, U. P. (1998). Expression of growth control and differentiation genes in human lens epithelial cells with extended life span. Invest Ophthalmol Vis Sci *39*, 1387-1398.

Freeze, H. H. (2007). Congenital Disorders of Glycosylation: CDG-I, CDG-II, and beyond. Curr Mol Med *7*, 389-396.

Friedman, D. S., Wilson, M. R., Liebmann, J. M., Fechtner, R. D., and Weinreb, R. N. (2004). An evidence-based assessment of risk factors for the progression of ocular hypertension and glaucoma. Am J Ophthalmol *138*, S19-31.

Fu, L., and Liang, J. J. (2003). Alteration of protein-protein interactions of congenital cataract crystallin mutants. Invest Ophthalmol Vis Sci *44*, 1155-1159.

Fukuda, M. (1991). Leukosialin, a major O-glycan-containing sialoglycoprotein defining leukocyte differentiation and malignancy. Glycobiology *1*, 347-356.

Garrido, C., Brunet, M., Didelot, C., Zermati, Y., Schmitt, E., and Kroemer, G. (2006). Heat shock proteins 27 and 70: anti-apoptotic proteins with tumorigenic properties. Cell Cycle *5*, 2592-2601.

Germain, D. P., and Fan, J. Q. (2009). Pharmacological chaperone therapy by active-site-specific chaperones in Fabry disease: in vitro and preclinical studies. Int J Clin Pharmacol Ther *47 Suppl 1*, S111-117.

Gilbert, C., and Foster, A. (2001). Childhood blindness in the context of VISION 2020--the right to sight. Bull World Health Organ *79*, 227-232.

Glickman, M. H., and Ciechanover, A. (2002). The ubiquitin-proteasome proteolytic pathway: destruction for the sake of construction. Physiol Rev *82*, 373-428.

Gobeil, S., Rodrigue, M. A., Moisan, S., Nguyen, T. D., Polansky, J. R., Morissette, J., and Raymond, V. (2004). Intracellular sequestration of hetero-oligomers formed by wild-type and glaucoma-causing myocilin mutants. Invest Ophthalmol Vis Sci *45*, 3560-3567.

Gong, B., Zhang, L. Y., Pang, C. P., Lam, D. S., and Yam, G. H. (2009). Trimethylamine N-oxide alleviates the severe aggregation and ER stress caused by G98R alphaA-crystallin. Mol Vis *15*, 2829-2840.

Gong, G., Kosoko-Lasaki, O., Haynatzki, G. R., and Wilson, M. R. (2004). Genetic dissection of myocilin glaucoma. Hum Mol Genet *13 Spec No 1*, R91-102.

Gould, D. B., Reedy, M., Wilson, L. A., Smith, R. S., Johnson, R. L., and John, S. W. (2006). Mutant myocilin nonsecretion in vivo is not sufficient to cause glaucoma. Mol Cell Biol *26*, 8427-8436.

Graw, J. (1999). Cataract mutations and lens development. Prog Retin Eye Res *18*, 235-267.

Graw, J. (2004). Congenital hereditary cataracts. Int J Dev Biol *48*, 1031-1044.

Graw, J. (2009). Genetics of crystallins: cataract and beyond. Exp Eye Res *88*, 173-189.

Gregersen, N. (2006). Protein misfolding disorders: pathogenesis and intervention. J Inherit Metab Dis *29*, 456-470.

Gregersen N, Bolund L, and Bross P (2005). Protein misfolding, aggregation, and degradation in disease. Mol Biotechnol *31*, 141-150.

Haargaard, B., Wohlfahrt, J., Fledelius, H. C., Rosenberg, T., and Melbye, M. (2004). A nationwide Danish study of 1027 cases of congenital/infantile cataracts: etiological and clinical classifications. Ophthalmology *111*, 2292-2298.

Haezebrouck, P., Joniau, M., Van Dael, H., Hooke, S. D., Woodruff, N. D., and Dobson, C. M. (1995). An equilibrium partially folded state of human lysozyme at low pH. J Mol Biol *246*, 382-387.

Hanada, S., Harada, M., Kumemura, H., Bishr Omary, M., Koga, H., Kawaguchi, T., Taniguchi, E., Yoshida, T., Hisamoto, T., Yanagimoto, C., *et al.* (2007). Oxidative stress induces the endoplasmic reticulum stress and facilitates inclusion formation in cultured cells. J Hepatol *47*, 93-102.

Harding, H. P., Novoa, I., Zhang, Y., Zeng, H., Wek, R., Schapira, M., and Ron, D. (2000a). Regulated translation initiation controls stress-induced gene expression in mammalian cells. Mol Cell *6*, 1099-1108.

Harding, H. P., Zhang, Y., Bertolotti, A., Zeng, H., and Ron, D. (2000b). Perk is essential for translational regulation and cell survival during the unfolded protein response. Mol Cell *5*, 897-904.

Harding, H. P., Zhang, Y., and Ron, D. (1999). Protein translation and folding are coupled by an endoplasmic-reticulum-resident kinase. Nature *397*, 271-274.

Hartl, F. U. (1996). Molecular chaperones in cellular protein folding. Nature *381*, 571-579.

Hebert, D. N., and Molinari, M. (2007). In and out of the ER: protein folding, quality control, degradation, and related human diseases. Physiol Rev *87*, 1377-1408.

Hegde, A. N. (2004). Ubiquitin-proteasome-mediated local protein degradation and synaptic plasticity. Prog Neurobiol *73*, 311-357.

Helenius, A., and Aebi, M. (2004). Roles of N-linked glycans in the endoplasmic reticulum. Annu Rev Biochem *73*, 1019-1049.

Herrmann, J., Soares, S. M., Lerman, L. O., and Lerman, A. (2008). Potential role of the ubiquitin-proteasome system in atherosclerosis: aspects of a protein quality disease. J Am Coll Cardiol *51*, 2003-2010.

Horwich, A. (2002). Protein aggregation in disease: a role for folding intermediates forming specific multimeric interactions. J Clin Invest *110*, 1221-1232.

Hossler, P., Mulukutla, B. C., and Hu, W. S. (2007). Systems analysis of N-glycan processing in mammalian cells. PLoS One *2*, e713.

Hung, J. Y., Hsu, Y. L., Ni, W. C., Tsai, Y. M., Yang, C. J., Kuo, P. L., and Huang, M. S. (2009). Oxidative and endoplasmic reticulum stress signaling are involved in dehydrocostuslactone-mediated apoptosis in human non-small cell lung cancer cells. Lung Cancer *68*, 355-365.

Hurley, J. H., Dean, A. M., Sohl, J. L., Koshland, D. E., Jr., and Stroud, R. M. (1990). Regulation of an enzyme by phosphorylation at the active site. Science *249*, 1012-1016.

Hurtley, S. M., and Helenius, A. (1989). Protein oligomerization in the endoplasmic reticulum. Annu Rev Cell Biol *5*, 277-307.

Ibba, M., and Soll, D. (1999). Quality control mechanisms during translation. Science *286*, 1893-1897.

Jacobson, N., Andrews, M., Shepard, A. R., Nishimura, D., Searby, C., Fingert, J. H., Hageman, G., Mullins, R., Davidson, B. L., Kwon, Y. H., *et al.* (2001). Non-secretion of mutant proteins of the glaucoma gene myocilin in cultured trabecular meshwork cells and in aqueous humor. Hum Mol Genet *10*, 117-125.

Jaenicke, R., and Slingsby, C. (2001). Lens crystallins and their microbial homologs: structure, stability, and function. Crit Rev Biochem Mol Biol *36*, 435-499.

Jafarnejad, A., Bathaie, S. Z., Nakhjavani, M., Hassan, M. Z., and Banasadegh, S. (2008). The improvement effect of L-Lys as a chemical chaperone on STZ-induced diabetic rats, protein structure and function. Diabetes Metab Res Rev *24*, 64-73.

Jakubowski, H., and Goldman, E. (1992). Editing of errors in selection of amino acids for protein synthesis. Microbiol Rev *56*, 412-429.

Janovick, J. A., Maya-Nunez, G., Ulloa-Aguirre, A., Huhtaniemi, I. T., Dias, J. A., Verbost, P., and Conn, P. M. (2009). Increased plasma membrane expression of human follicle-stimulating hormone receptor by a small molecule thienopyr(im)idine. Mol Cell Endocrinol *298*, 84-88.

Jia, L. Y., Gong, B., Pang, C. P., Huang, Y., Lam, D. S., Wang, N., and Yam, G. H. (2009). Correction of the disease phenotype of myocilin-causing glaucoma by a natural osmolyte. Invest Ophthalmol Vis Sci *50*, 3743-3749.

Jiang, C. C., Wroblewski, D., Yang, F., Hersey, P., and Zhang, X. D. (2009). Human melanoma cells under endoplasmic reticulum stress are more susceptible to apoptosis induced by the BH3 mimetic obatoclax. Neoplasia *11*, 945-955.

Joe, M. K., Sohn, S., Hur, W., Moon, Y., Choi, Y. R., and Kee, C. (2003). Accumulation of mutant myocilins in ER leads to ER stress and potential cytotoxicity in human trabecular meshwork cells. Biochem Biophys Res Commun *312*, 592-600.

Johnson, A. T., Richards, J. E., Boehnke, M., Stringham, H. M., Herman, S. B., Wong, D. J., and Lichter, P. R. (1996). Clinical phenotype of juvenile-onset primary open-angle glaucoma linked to chromosome 1q. Ophthalmology *103*, 808-814.

Johnson, L. N., and Barford, D. (1993). The effects of phosphorylation on the structure and function of proteins. Annu Rev Biophys Biomol Struct *22*, 199-232.

Johnson, L. N., and Lewis, R. J. (2001). Structural basis for control by phosphorylation. Chem Rev *101*, 2209-2242.

Jung, J., Byeon, I. J., Wang, Y., King, J., and Gronenborn, A. M. (2009). The structure of the cataract-causing P23T mutant of human gammaD-crystallin exhibits distinctive local conformational and dynamic changes. Biochemistry *48*, 2597-2609.

Kanki, K., Kawamura, T., and Watanabe, Y. (2009). Control of ER stress by a chemical chaperone counteracts apoptotic signals in IFN-gamma-treated murine hepatocytes. Apoptosis *14*, 309-319.

Kantorow, M., and Piatigorsky, J. (1998). Phosphorylations of alpha A- and alpha B-crystallin. Int J Biol Macromol *22*, 307-314.

Kaushal, S., and Khorana, H. G. (1994). Structure and function in rhodopsin. 7. Point mutations associated with autosomal dominant retinitis pigmentosa. Biochemistry *33*, 6121-6128.

Kelly, J. W. (1998). The alternative conformations of amyloidogenic proteins and their multi-step assembly pathways. Curr Opin Struct Biol *8*, 101-106.

Kim, P. S., and Arvan, P. (1998). Endocrinopathies in the family of endoplasmic reticulum (ER) storage diseases: disorders of protein trafficking and the role of ER molecular chaperones. Endocr Rev *19*, 173-202.

Kivela, T., Tarkkanen, A., Frangione, B., Ghiso, J., and Haltia, M. (1994). Ocular amyloid deposition in familial amyloidosis, Finnish: an analysis of native and variant gelsolin in Meretoja's syndrome. Invest Ophthalmol Vis Sci *35*, 3759-3769.

Klein, B. E., Klein, R., Sponsel, W. E., Franke, T., Cantor, L. B., Martone, J., and Menage, M. J. (1992). Prevalence of glaucoma. The Beaver Dam Eye Study. Ophthalmology *99*, 1499-1504.

Klionsky, D. J. (2005). The molecular machinery of autophagy: unanswered questions. J Cell Sci *118*, 7-18.

Kolter, T., and Wendeler, M. (2003). Chemical chaperones--a new concept in drug research. Chembiochem *4*, 260-264.

Komarova, E. Y., Afanasyeva, E. A., Bulatova, M. M., Cheetham, M. E., Margulis, B. A., and Guzhova, I. V. (2004). Downstream caspases are novel targets for the antiapoptotic activity of the molecular chaperone hsp70. Cell Stress Chaperones *9*, 265-275.

Kontsekova, E., Ivanovova, N., Handzusova, M., and Novak, M. (2009). Chaperone-like antibodies in neurodegenerative tauopathies: implication for immunotherapy. Cell Mol Neurobiol *29*, 793-798.

Kosmaoglou, M., Schwarz, N., Bett, J. S., and Cheetham, M. E. (2008). Molecular chaperones and photoreceptor function. Prog Retin Eye Res *27*, 434-449.

Kozutsumi, Y., Segal, M., Normington, K., Gething, M. J., and Sambrook, J. (1988). The presence of malfolded proteins in the endoplasmic reticulum signals the induction of glucose-regulated proteins. Nature *332*, 462-464.

Kubota, K., Niinuma, Y., Kaneko, M., Okuma, Y., Sugai, M., Omura, T., Uesugi, M., Uehara, T., Hosoi, T., and Nomura, Y. (2006). Suppressive effects of 4-phenylbutyrate on the aggregation of Pael receptors and endoplasmic reticulum stress. J Neurochem *97*, 1259-1268.

Kumar, R., Serrette, J. M., and Thompson, E. B. (2005). Osmolyte-induced folding enhances tryptic enzyme activity. Arch Biochem Biophys *436*, 78-82.

Kundu, M., and Thompson, C. B. (2008). Autophagy: basic principles and relevance to disease. Annu Rev Pathol *3*, 427-455.

Lam, D. S., Leung, Y. F., Chua, J. K., Baum, L., Fan, D. S., Choy, K. W., and Pang, C. P. (2000). Truncations in the TIGR gene in individuals with and without primary open-angle glaucoma. Invest Ophthalmol Vis Sci *41*, 1386-1391.

Lampi, K. J., Shih, M., Ueda, Y., Shearer, T. R., and David, L. L. (2002). Lens proteomics: analysis of rat crystallin sequences and two-dimensional electrophoresis map. Invest Ophthalmol Vis Sci *43*, 216-224.

Landry, Y., and Gies, J. P. (2008). Drugs and their molecular targets: an updated overview. Fundam Clin Pharmacol *22*, 1-18.

Lapko, V. N., Smith, D. L., and Smith, J. B. (2003). Expression of betaA2-crystallin in human lenses. Exp Eye Res *77*, 383-385.

Leandro, P., and Gomes, C. M. (2008). Protein misfolding in conformational disorders: rescue of folding defects and chemical chaperoning. Mini Rev Med Chem *8*, 901-911.

Lee, J. W., Beebe, K., Nangle, L. A., Jang, J., Longo-Guess, C. M., Cook, S. A., Davisson, M. T., Sundberg, J. P., Schimmel, P., and Ackerman, S. L. (2006). Editing-defective tRNA synthetase causes protein misfolding and neurodegeneration. Nature *443*, 50-55.

Lee, K., Tirasophon, W., Shen, X., Michalak, M., Prywes, R., Okada, T., Yoshida, H., Mori, K., and Kaufman, R. J. (2002). IRE1-mediated unconventional mRNA splicing and S2P-mediated ATF6 cleavage merge to regulate XBP1 in signaling the unfolded protein response. Genes Dev *16*, 452-466.

Levine, B., and Klionsky, D. J. (2004). Development by self-digestion: molecular mechanisms and biological functions of autophagy. Dev Cell *6*, 463-477.

Li, F., Wang, S., Gao, C., Liu, S., Zhao, B., Zhang, M., Huang, S., Zhu, S., and Ma, X. (2008). Mutation G61C in the CRYGD gene causing autosomal dominant congenital coralliform cataracts. Mol Vis *14*, 378-386.

Li, M., Baumeister, P., Roy, B., Phan, T., Foti, D., Luo, S., and Lee, A. S. (2000). ATF6 as a transcription activator of the endoplasmic reticulum stress element: thapsigargin stress-induced changes and synergistic interactions with NF-Y and YY1. Mol Cell Biol *20*, 5096-5106.

Libby, R. T., Gould, D. B., Anderson, M. G., and John, S. W. (2005). Complex genetics of glaucoma susceptibility. Annu Rev Genomics Hum Genet *6*, 15-44.

Liberek, K., Lewandowska, A., and Zietkiewicz, S. (2008). Chaperones in control of protein disaggregation. Embo J *27*, 328-335.

Lin, H. Y., Masso-Welch, P., Di, Y. P., Cai, J. W., Shen, J. W., and Subjeck, J. R. (1993). The 170-kDa glucose-regulated stress protein is an endoplasmic reticulum protein that binds immunoglobulin. Mol Biol Cell *4*, 1109-1119.

Litt, M., Kramer, P., LaMorticella, D. M., Murphey, W., Lovrien, E. W., and Weleber, R. G. (1998). Autosomal dominant congenital cataract associated with a missense mutation in the human alpha crystallin gene CRYAA. Hum Mol Genet *7*, 471-474.

Liu, C. Y., Schroder, M., and Kaufman, R. J. (2000). Ligand-independent dimerization activates the stress response kinases IRE1 and PERK in the lumen of the endoplasmic reticulum. J Biol Chem *275*, 24881-24885.

Liu, C. Y., Wong, H. N., Schauerte, J. A., and Kaufman, R. J. (2002). The protein kinase/endoribonuclease IRE1alpha that signals the unfolded protein response has a luminal N-terminal ligand-independent dimerization domain. J Biol Chem *277*, 18346-18356.

Liu, X. L., Done, S. C., Yan, K., Kilpelainen, P., Pikkarainen, T., and Tryggvason, K. (2004). Defective trafficking of nephrin missense mutants rescued by a chemical chaperone. J Am Soc Nephrol *15*, 1731-1738.

Liu, Y., and Vollrath, D. (2004). Reversal of mutant myocilin non-secretion and cell killing: implications for glaucoma. Hum Mol Genet *13*, 1193-1204.

Loo, T. W., and Clarke, D. M. (2007). Chemical and pharmacological chaperones as new therapeutic agents. Expert Rev Mol Med *9*, 1-18.

Luibl, V., Isas, J. M., Kayed, R., Glabe, C. G., Langen, R., and Chen, J. (2006). Drusen deposits associated with aging and age-related macular degeneration contain nonfibrillar amyloid oligomers. J Clin Invest *116*, 378-385.

Mackay, D. S., Andley, U. P., and Shiels, A. (2003). Cell death triggered by a novel mutation in the alphaA-crystallin gene underlies autosomal dominant cataract linked to chromosome 21q. Eur J Hum Genet *11*, 784-793.

Maestri, N. E., Hauser, E. R., Bartholomew, D., and Brusilow, S. W. (1991). Prospective treatment of urea cycle disorders. J Pediatr *119*, 923-928.

Makareeva, E., and Leikin, S. (2007). Procollagen triple helix assembly: an unconventional chaperone-assisted folding paradigm. PLoS One *2*, e1029.

Malhotra, J. D., and Kaufman, R. J. (2007). The endoplasmic reticulum and the unfolded protein response. Semin Cell Dev Biol *18*, 716-731.

Mandic, A., Hansson, J., Linder, S., and Shoshan, M. C. (2003). Cisplatin induces endoplasmic reticulum stress and nucleus-independent apoptotic signaling. J Biol Chem *278*, 9100-9106.

Marini, J. C., Forlino, A., Cabral, W. A., Barnes, A. M., San Antonio, J. D., Milgrom, S., Hyland, J. C., Korkko, J., Prockop, D. J., De Paepe, A., *et al.* (2007). Consortium for

osteogenesis imperfecta mutations in the helical domain of type I collagen: regions rich in lethal mutations align with collagen binding sites for integrins and proteoglycans. Hum Mutat *28*, 209-221.

Markossian, K. A., and Kurganov, B. I. (2004). Protein folding, misfolding, and aggregation. Formation of inclusion bodies and aggresomes. Biochemistry (Mosc) *69*, 971-984.

Marques, C., Guo, W., Pereira, P., Taylor, A., Patterson, C., Evans, P. C., and Shang, F. (2006). The triage of damaged proteins: degradation by the ubiquitin-proteasome pathway or repair by molecular chaperones. Faseb J *20*, 741-743.

Martin, S., and Randal, J. K. (2005). ER stress and the unfolded protein response. Mutation Research *569*, 29-63.

Matsumoto, Y., and Johnson, D. H. (1997). Trabecular meshwork phagocytosis in glaucomatous eyes. Ophthalmologica *211*, 147-152.

Mayer, M. P., and Bukau, B. (2005). Hsp70 chaperones: cellular functions and molecular mechanism. Cell Mol Life Sci *62*, 670-684.

Mayor, U., Guydosh, N. R., Johnson, C. M., Grossmann, J. G., Sato, S., Jas, G. S., Freund, S. M., Alonso, D. O., Daggett, V., and Fersht, A. R. (2003). The complete folding pathway of a protein from nanoseconds to microseconds. Nature *421*, 863-867.

McClellan, A. J., Tam, S., Kaganovich, D., and Frydman, J. (2005). Protein quality control: chaperones culling corrupt conformations. Nat Cell Biol *7*, 736-741.

McCullough, K. D., Martindale, J. L., Klotz, L. O., Aw, T. Y., and Holbrook, N. J. (2001). Gadd153 sensitizes cells to endoplasmic reticulum stress by down-regulating Bcl2 and perturbing the cellular redox state. Mol Cell Biol *21*, 1249-1259.

Meehan, S., Berry, Y., Luisi, B., Dobson, C. M., Carver, J. A., and MacPhee, C. E. (2004). Amyloid fibril formation by lens crystallin proteins and its implications for cataract formation. J Biol Chem *279*, 3413-3419.

Melnick, J., Dul, J. L., and Argon, Y. (1994). Sequential interaction of the chaperones BiP and GRP94 with immunoglobulin chains in the endoplasmic reticulum. Nature *370*, 373-375.

Meusser, B., Hirsch, C., Jarosch, E., and Sommer, T. (2005). ERAD: the long road to destruction. Nat Cell Biol *7*, 766-772.

Mezzacasa, A., and Helenius, A. (2002). The transitional ER defines a boundary for quality control in the secretion of tsO45 VSV glycoprotein. Traffic *3*, 833-849.

Miyazawa, T., Kubo, E., Takamura, Y., and Akagi, Y. (2007). Up-regulation of P-glycoprotein expression by osmotic stress in rat sugar cataract. Exp Eye Res *84*, 246-253.

Mizushima, N., Levine, B., Cuervo, A. M., and Klionsky, D. J. (2008). Autophagy fights disease through cellular self-digestion. Nature *451*, 1069-1075.

Moremen, K. W., and Molinari, M. (2006). N-linked glycan recognition and processing: the molecular basis of endoplasmic reticulum quality control. Curr Opin Struct Biol *16*, 592-599.

Morissette, J., Clepet, C., Moisan, S., Dubois, S., Winstall, E., Vermeeren, D., Nguyen, T. D., Polansky, J. R., Cote, G., Anctil, J. L., *et al.* (1998). Homozygotes carrying an autosomal dominant TIGR mutation do not manifest glaucoma. Nat Genet *19*, 319-321.

Morissette, J., Cote, G., Anctil, J. L., Plante, M., Amyot, M., Heon, E., Trope, G. E., Weissenbach, J., and Raymond, V. (1995). A common gene for juvenile and adult-onset primary open-angle glaucomas confined on chromosome 1q. Am J Hum Genet *56*, 1431-1442.

Morrison, J. C., Johnson, E. C., Cepurna, W., and Jia, L. (2005). Understanding mechanisms of pressure-induced optic nerve damage. Prog Retin Eye Res *24*, 217-240.

Mu, T. W., Ong, D. S., Wang, Y. J., Balch, W. E., Yates, J. R., 3rd, Segatori, L., and Kelly, J. W. (2008). Chemical and biological approaches synergize to ameliorate protein-folding diseases. Cell *134*, 769-781.

Mulhern, M. L., Madson, C. J., Kador, P. F., Randazzo, J., and Shinohara, T. (2007). Cellular osmolytes reduce lens epithelial cell death and alleviate cataract formation in galactosemic rats. Mol Vis *13*, 1397-1405.

Murugesan, R., Santhoshkumar, P., and Sharma, K. K. (2007). Cataract-causing alphaAG98R mutant shows substrate-dependent chaperone activity. Mol Vis *13*, 2301-2309.

Narberhaus, F. (2002). Alpha-crystallin-type heat shock proteins: socializing minichaperones in the context of a multichaperone network. Microbiol Mol Biol Rev *66*, 64-93.

Naujokat, C., and Hoffmann, S. (2002). Role and function of the 26S proteasome in proliferation and apoptosis. Lab Invest *82*, 965-980.

Nikawa, J., Akiyoshi, M., Hirata, S., and Fukuda, T. (1996). Saccharomyces cerevisiae IRE2/HAC1 is involved in IRE1-mediated KAR2 expression. Nucleic Acids Res *24*, 4222-4226.

Nikawa, J., and Yamashita, S. (1992). IRE1 encodes a putative protein kinase containing a membrane-spanning domain and is required for inositol phototrophy in Saccharomyces cerevisiae. Mol Microbiol *6*, 1441-1446.

Nixon, R. A. (2003). The calpains in aging and aging-related diseases. Ageing Res Rev *2*, 407-418.

Noorwez, S. M., Kuksa, V., Imanishi, Y., Zhu, L., Filipek, S., Palczewski, K., and Kaushal, S. (2003). Pharmacological chaperone-mediated in vivo folding and stabilization of the P23H-opsin mutant associated with autosomal dominant retinitis pigmentosa. J Biol Chem *278*, 14442-14450.

O'Brien, E. T., Ren, X., and Wang, Y. (2000). Localization of myocilin to the golgi apparatus in Schlemm's canal cells. Invest Ophthalmol Vis Sci *41*, 3842-3849.

Oda, Y., Hosokawa, N., Wada, I., and Nagata, K. (2003). EDEM as an acceptor of terminally misfolded glycoproteins released from calnexin. Science *299*, 1394-1397.

Ohashi, T., Uchida, K., Uchida, S., Sasaki, S., and Nihei, H. (2003). Intracellular mislocalization of mutant podocin and correction by chemical chaperones. Histochem Cell Biol *119*, 257-264.

Ohnishi, K., Ota, I., Yane, K., Takahashi, A., Yuki, K., Emoto, M., Hosoi, H., and Ohnishi, T. (2002). Glycerol as a chemical chaperone enhances radiation-induced apoptosis in anaplastic thyroid carcinoma cells. Mol Cancer *1*, 4.

Ono, K., Ikemoto, M., Kawarabayashi, T., Ikeda, M., Nishinakagawa, T., Hosokawa, M., Shoji, M., Takahashi, M., and Nakashima, M. (2009). A chemical chaperone, sodium 4-phenylbutyric acid, attenuates the pathogenic potency in human alpha-synuclein A30P+A53T transgenic mice. Parkinsonism Relat Disord.

Onodera, J., and Ohsumi, Y. (2005). Autophagy is required for maintenance of amino acid levels and protein synthesis under nitrogen starvation. J Biol Chem *280*, 31582-31586.

Orrenius, S., Zhivotovsky, B., and Nicotera, P. (2003). Regulation of cell death: the calcium-apoptosis link. Nat Rev Mol Cell Biol *4*, 552-565.

Outeiro, T. F., and Tetzlaff, J. (2007). Mechanisms of disease II: cellular protein quality control. Semin Pediatr Neurol *14*, 15-25.

Ozcan, U., Yilmaz, E., Ozcan, L., Furuhashi, M., Vaillancourt, E., Smith, R. O., Gorgun, C. Z., and Hotamisligil, G. S. (2006). Chemical chaperones reduce ER stress and restore glucose homeostasis in a mouse model of type 2 diabetes. Science *313*, 1137-1140.

Papa, F. R., Zhang, C., Shokat, K., and Walter, P. (2003). Bypassing a kinase activity with an ATP-competitive drug. Science *302*, 1533-1537.

Papp, E., and Csermely, P. (2006). Chemical chaperones: mechanisms of action and potential use. Handb Exp Pharmacol, 405-416.

Parenti, G. (2009). Treating lysosomal storage diseases with pharmacological chaperones: from concept to clinics. EMBO Mol Med *1*, 268-279.

Perlmutter, D. H. (2002). Chemical chaperones: a pharmacological strategy for disorders of protein folding and trafficking. Pediatr Res *52*, 832-836.

Peschek, J., Braun, N., Franzmann, T. M., Georgalis, Y., Haslbeck, M., Weinkauf, S., and Buchner, J. (2009). The eye lens chaperone alpha-crystallin forms defined globular assemblies. Proc Natl Acad Sci U S A *106*, 13272-13277.

Plotnikova, O. V., Kondrashov, F. A., Vlasov, P. K., Grigorenko, A. P., Ginter, E. K., and Rogaev, E. I. (2007). Conversion and compensatory evolution of the gamma-crystallin genes and identification of a cataractogenic mutation that reverses the sequence of the human CRYGD gene to an ancestral state. Am J Hum Genet *81*, 32-43.

Polansky, J. R., Fauss, D. J., Chen, P., Chen, H., Lutjen-Drecoll, E., Johnson, D., Kurtz, R. M., Ma, Z. D., Bloom, E., and Nguyen, T. D. (1997). Cellular pharmacology and molecular biology of the trabecular meshwork inducible glucocorticoid response gene product. Ophthalmologica *211*, 126-139.

Polla, B. S., Kantengwa, S., Francois, D., Salvioli, S., Franceschi, C., Marsac, C., and Cossarizza, A. (1996). Mitochondria are selective targets for the protective effects of heat shock against oxidative injury. Proc Natl Acad Sci U S A *93*, 6458-6463.

Ponnambalam, S., and Baldwin, S. A. (2003). Constitutive protein secretion from the trans-Golgi network to the plasma membrane. Mol Membr Biol *20*, 129-139.

Powers, E. T., Morimoto, R. I., Dillin, A., Kelly, J. W., and Balch, W. E. (2009). Biological and chemical approaches to diseases of proteostasis deficiency. Annu Rev Biochem *78*, 959-991.

Powers, M. V., and Workman, P. (2007). Inhibitors of the heat shock response: biology and pharmacology. FEBS Lett *581*, 3758-3769.

Pras, E., Frydman, M., Levy-Nissenbaum, E., Bakhan, T., Raz, J., Assia, E. I., Goldman, B., and Pras, E. (2000). A nonsense mutation (W9X) in CRYAA causes autosomal recessive cataract in an inbred Jewish Persian family. Invest Ophthalmol Vis Sci *41*, 3511-3515.

Pratt, E. B., Yan, F. F., Gay, J. W., Stanley, C. A., and Shyng, S. L. (2009). Sulfonylurea receptor 1 mutations that cause opposite insulin secretion defects with chemical chaperone exposure. J Biol Chem *284*, 7951-7959.

Radford, S. E., and Dobson, C. M. (1999). From computer simulations to human disease: emerging themes in protein folding. Cell *97*, 291-298.

Raguenez, G., Muhlethaler-Mottet, A., Meier, R., Duros, C., Benard, J., and Gross, N. (2009). Fenretinide-induced caspase-8 activation and apoptosis in an established model of metastatic neuroblastoma. BMC Cancer *9*, 97.

Rahi, J. S., and Dezateux, C. (2000). Congenital and infantile cataract in the United Kingdom: underlying or associated factors. British Congenital Cataract Interest Group. Invest Ophthalmol Vis Sci *41*, 2108-2114.

Ravagnan, L., Gurbuxani, S., Susin, S. A., Maisse, C., Daugas, E., Zamzami, N., Mak, T., Jaattela, M., Penninger, J. M., Garrido, C., and Kroemer, G. (2001). Heat-shock protein 70 antagonizes apoptosis-inducing factor. Nat Cell Biol *3*, 839-843.

Rennolds, J., Boyaka, P. N., Bellis, S. L., and Cormet-Boyaka, E. (2008). Low temperature induces the delivery of mature and immature CFTR to the plasma membrane. Biochem Biophys Res Commun *366*, 1025-1029.

Resnikoff, S., Pascolini, D., Etya'ale, D., Kocur, I., Pararajasegaram, R., Pokharel, G. P., and Mariotti, S. P. (2004). Global data on visual impairment in the year 2002. Bull World Health Organ *82*, 844-851.

Robben, J. H., Sze, M., Knoers, N. V., and Deen, P. M. (2006). Rescue of vasopressin V2 receptor mutants by chemical chaperones: specificity and mechanism. Mol Biol Cell *17*, 379-386.

Rohen, J. W., Lutjen-Drecoll, E., Flugel, C., Meyer, M., and Grierson, I. (1993). Ultrastructure of the trabecular meshwork in untreated cases of primary open-angle glaucoma (POAG). Exp Eye Res *56*, 683-692.

Roof, D. J., Adamian, M., and Hayes, A. (1994). Rhodopsin accumulation at abnormal sites in retinas of mice with a human P23H rhodopsin transgene. Invest Ophthalmol Vis Sci *35*, 4049-4062.

Roth, J. (2002). Protein N-glycosylation along the secretory pathway: relationship to organelle topography and function, protein quality control, and cell interactions. Chem Rev *102*, 285-303.

Roth, J., Yam, G. H., Fan, J., Hirano, K., Gaplovska-Kysela, K., Le Fourn, V., Guhl, B., Santimaria, R., Torossi, T., Ziak, M., and Zuber, C. (2008). Protein quality control: the who's who, the where's and therapeutic escapes. Histochem Cell Biol *129*, 163-177.

Rubenstein RC, and Zeitlin PL (1998). A pilot clinical trial of oral sodium 4-phenylbutyrate (Buphenyl) in deltaF508-homozygous cystic fibrosis patients: partial restoration of nasal epithelial CFTR function. Am J Respir Crit Care Med *157*, 484-490.

Rubenstein, R. C., and Lyons, B. M. (2001). Sodium 4-phenylbutyrate downregulates HSC70 expression by facilitating mRNA degradation. Am J Physiol Lung Cell Mol Physiol *281*, L43-51.

Russo, A. A., Jeffrey, P. D., and Pavletich, N. P. (1996). Structural basis of cyclin-dependent kinase activation by phosphorylation. Nat Struct Biol *3*, 696-700.

Santhiya, S. T., Soker, T., Klopp, N., Illig, T., Prakash, M. V., Selvaraj, B., Gopinath, P. M., and Graw, J. (2006). Identification of a novel, putative cataract-causing allele in CRYAA (G98R) in an Indian family. Mol Vis *12*, 768-773.

Santhoshkumar, P., and Sharma, K. K. (2004). Inhibition of amyloid fibrillogenesis and toxicity by a peptide chaperone. Mol Cell Biochem *267*, 147-155.

Shamu, C. E., and Walter, P. (1996). Oligomerization and phosphorylation of the Ire1p kinase during intracellular signaling from the endoplasmic reticulum to the nucleus. Embo J *15*, 3028-3039.

Shearer, A. G., and Hampton, R. Y. (2004). Structural control of endoplasmic reticulum-associated degradation: effect of chemical chaperones on 3-hydroxy-3-methylglutaryl-CoA reductase. J Biol Chem *279*, 188-196.

Sheffield, V. C., Stone, E. M., Alward, W. L., Drack, A. V., Johnson, A. T., Streb, L. M., and Nichols, B. E. (1993). Genetic linkage of familial open angle glaucoma to chromosome 1q21-q31. Nat Genet *4*, 47-50.

Shi, Y., An, J., Liang, J., Hayes, S. E., Sandusky, G. E., Stramm, L. E., and Yang, N. N. (1999). Characterization of a mutant pancreatic eIF-2alpha kinase, PEK, and co-localization with somatostatin in islet delta cells. J Biol Chem *274*, 5723-5730.

Sieving, P. A., and Collins, F. S. (2007). Genetic ophthalmology and the era of clinical care. Jama *297*, 733-736.

Sihota, R., Sood, A., Gupta, V., Dada, T., and Agarwal, H. C. (2004). A prospective longterm study of primary chronic angle closure glaucoma. Acta Ophthalmol Scand *82*, 209-213.

Singh, D., Raman, B., Ramakrishna, T., and Rao Ch, M. (2006). The cataract-causing mutation G98R in human alphaA-crystallin leads to folding defects and loss of chaperone activity. Mol Vis *12*, 1372-1379.

Singh, D., Raman, B., Ramakrishna, T., and Rao Ch, M. (2007). Mixed oligomer formation between human alphaA-crystallin and its cataract-causing G98R mutant: structural, stability and functional differences. J Mol Biol *373*, 1293-1304.

Singh, O. V., Pollard, H. B., and Zeitlin, P. L. (2008). Chemical rescue of deltaF508-CFTR mimics genetic repair in cystic fibrosis bronchial epithelial cells. Mol Cell Proteomics *7*, 1099-1110.

Snow, C. D., Nguyen, H., Pande, V. S., and Gruebele, M. (2002). Absolute comparison of simulated and experimental protein-folding dynamics. Nature *420*, 102-106.

Stevens, F. J., and Argon, Y. (1999). Protein folding in the ER. Semin Cell Dev Biol *10*, 443-454.

Stone, E. M., Fingert, J. H., Alward, W. L., Nguyen, T. D., Polansky, J. R., Sunden, S. L., Nishimura, D., Clark, A. F., Nystuen, A., Nichols, B. E., *et al.* (1997). Identification of a gene that causes primary open angle glaucoma. Science *275*, 668-670.

Strnad, P., Zatloukal, K., Stumptner, C., Kulaksiz, H., and Denk, H. (2008). Mallory-Denk-bodies: lessons from keratin-containing hepatic inclusion bodies. Biochim Biophys Acta *1782*, 764-774.

Sun, T. X., Das, B. K., and Liang, J. J. (1997). Conformational and functional differences between recombinant human lens alphaA- and alphaB-crystallin. J Biol Chem *272*, 6220-6225.

Sun, T. X., and Liang, J. J. (1998). Intermolecular exchange and stabilization of recombinant human alphaA- and alphaB-crystallin. J Biol Chem *273*, 286-290.

Sun, Y., and MacRae, T. H. (2005). Small heat shock proteins: molecular structure and chaperone function. Cell Mol Life Sci *62*, 2460-2476.

Sung, C. H., Davenport, C. M., and Nathans, J. (1993). Rhodopsin mutations responsible for autosomal dominant retinitis pigmentosa. Clustering of functional classes along the polypeptide chain. J Biol Chem *268*, 26645-26649.

Tai, T. Y., Damani, M. R., Vo, R., Rayner, S. A., Glasgow, B. J., Hofbauer, J. D., Casey, R., and Aldave, A. J. (2009). Keratoconus associated with corneal stromal amyloid deposition containing TGFBIp. Cornea *28*, 589-593.

Takahashi, S., Sasaki, T., Manya, H., Chiba, Y., Yoshida, A., Mizuno, M., Ishida, H., Ito, F., Inazu, T., Kotani, N., *et al.* (2001). A new beta-1,2-N-acetylglucosaminyltransferase that may play a role in the biosynthesis of mammalian O-mannosyl glycans. Glycobiology *11*, 37-45.

Talla, V., Narayanan, C., Srinivasan, N., and Balasubramanian, D. (2006). Mutation causing self-aggregation in human gammaC-crystallin leading to congenital cataract. Invest Ophthalmol Vis Sci *47*, 5212-5217.

Tamarappoo, B. K., and Verkman, A. S. (1998). Defective aquaporin-2 trafficking in nephrogenic diabetes insipidus and correction by chemical chaperones. J Clin Invest *101*, 2257-2267.

Tatemichi, M., Nakano, T., Tanaka, K., Hayashi, T., Nawa, T., Miyamoto, T., Hiro, H., and Sugita, M. (2004). Possible association between heavy computer users and glaucomatous visual field abnormalities: a cross sectional study in Japanese workers. J Epidemiol Community Health *58*, 1021-1027.

Teter, S. A., Houry, W. A., Ang, D., Tradler, T., Rockabrand, D., Fischer, G., Blum, P., Georgopoulos, C., and Hartl, F. U. (1999). Polypeptide flux through bacterial Hsp70: DnaK cooperates with trigger factor in chaperoning nascent chains. Cell *97*, 755-765.

Thomas, P. J., Qu, B. H., and Pedersen, P. L. (1995). Defective protein folding as a basis of human disease. Trends Biochem Sci *20*, 456-459.

Tirasophon, W., Lee, K., Callaghan, B., Welihinda, A., and Kaufman, R. J. (2000). The endoribonuclease activity of mammalian IRE1 autoregulates its mRNA and is required for the unfolded protein response. Genes Dev *14*, 2725-2736.

Travers, K. J., Patil, C. K., Wodicka, L., Lockhart, D. J., Weissman, J. S., and Walter, P. (2000). Functional and genomic analyses reveal an essential coordination between the unfolded protein response and ER-associated degradation. Cell *101*, 249-258.

Trombetta ES, and Parodi AJ (2003). Quality control and protein folding in the secretory pathway. Annu Rev Cell Dev Biol *19*, 649-676.

Truscott, R. J. (2005). Age-related nuclear cataract-oxidation is the key. Exp Eye Res *80*, 709-725.

Tsai, B., Rodighiero, C., Lencer, W. I., and Rapoport, T. A. (2001). Protein disulfide isomerase acts as a redox-dependent chaperone to unfold cholera toxin. Cell *104*, 937-948.

Tveten, K., Holla, O. L., Ranheim, T., Berge, K. E., Leren, T. P., and Kulseth, M. A. (2007). 4-Phenylbutyrate restores the functionality of a misfolded mutant low-density lipoprotein receptor. Febs J *274*, 1881-1893.

Ueda, J., Wentz-Hunter, K., and Yue, B. Y. (2002). Distribution of myocilin and extracellular matrix components in the juxtacanalicular tissue of human eyes. Invest Ophthalmol Vis Sci *43*, 1068-1076.

Ueda, J., Wentz-Hunter, K. K., Cheng, E. L., Fukuchi, T., Abe, H., and Yue, B. Y. (2000). Ultrastructural localization of myocilin in human trabecular meshwork cells and tissues. J Histochem Cytochem *48*, 1321-1330.

Ueda, J., and Yue, B. Y. (2003). Distribution of myocilin and extracellular matrix components in the corneoscleral meshwork of human eyes. Invest Ophthalmol Vis Sci *44*, 4772-4779.

Ulloa-Aguirre, A., Janovick, J. A., Brothers, S. P., and Conn, P. M. (2004). Pharmacologic rescue of conformationally-defective proteins: implications for the treatment of human disease. Traffic *5*, 821-837.

Uttenweiler, A., and Mayer, A. (2008). Microautophagy in the yeast Saccharomyces cerevisiae. Methods Mol Biol *445*, 245-259.

Vanita, V., Singh, J. R., Hejtmancik, J. F., Nuernberg, P., Hennies, H. C., Singh, D., and Sperling, K. (2006). A novel fan-shaped cataract-microcornea syndrome caused by a mutation of CRYAA in an Indian family. Mol Vis *12*, 518-522.

Vollrath, D., and Liu, Y. (2006). Temperature sensitive secretion of mutant myocilins. Exp Eye Res *82*, 1030-1036.

Walter, P., and Johnson, A. E. (1994). Signal sequence recognition and protein targeting to the endoplasmic reticulum membrane. Annu Rev Cell Biol *10*, 87-119.

Wang, K., Cheng, C., Li, L., Liu, H., Huang, Q., Xia, C. H., Yao, K., Sun, P., Horwitz, J., and Gong, X. (2007). GammaD-crystallin associated protein aggregation and lens fiber cell denucleation. Invest Ophthalmol Vis Sci *48*, 3719-3728.

Wang, X., Garcia, C. M., Shui, Y. B., and Beebe, D. C. (2004). Expression and regulation of alpha-, beta-, and gamma-crystallins in mammalian lens epithelial cells. Invest Ophthalmol Vis Sci *45*, 3608-3619.

Webb, S. E., and Miller, A. L. (2003). Calcium signalling during embryonic development. Nat Rev Mol Cell Biol *4*, 539-551.

Wei, H., Kim, S. J., Zhang, Z., Tsai, P. C., Wisniewski, K. E., and Mukherjee, A. B. (2008). ER and oxidative stresses are common mediators of apoptosis in both neurodegenerative and non-neurodegenerative lysosomal storage disorders and are alleviated by chemical chaperones. Hum Mol Genet *17*, 469-477.

Weinreb, R. N., and Khaw, P. T. (2004). Primary open-angle glaucoma. Lancet *363*, 1711-1720.

Welburn, J. P., Tucker, J. A., Johnson, T., Lindert, L., Morgan, M., Willis, A., Noble, M. E., and Endicott, J. A. (2007). How tyrosine 15 phosphorylation inhibits the activity of cyclin-dependent kinase 2-cyclin A. J Biol Chem *282*, 3173-3181.

Welihinda, A. A., and Kaufman, R. J. (1996). The unfolded protein response pathway in Saccharomyces cerevisiae. Oligomerization and trans-phosphorylation of Ire1p (Ern1p) are required for kinase activation. J Biol Chem *271*, 18181-18187.

Werner, E. D., Brodsky, J. L., and McCracken, A. A. (1996). Proteasome-dependent endoplasmic reticulum-associated protein degradation: an unconventional route to a familiar fate. Proc Natl Acad Sci U S A *93*, 13797-13801.

Whiteman, P., Hutchinson, S., and Handford, P. A. (2006). Fibrillin-1 misfolding and disease. Antioxid Redox Signal *8*, 338-346.

Wickner, S., Maurizi, M. R., and Gottesman, S. (1999). Posttranslational quality control: folding, refolding, and degrading proteins. Science *286*, 1888-1893.

Wormald, M. R., and Dwek, R. A. (1999). Glycoproteins: glycan presentation and protein-fold stability. Structure *7*, R155-160.

Wright, J. M., Zeitlin, P. L., Cebotaru, L., Guggino, S. E., and Guggino, W. B. (2004). Gene expression profile analysis of 4-phenylbutyrate treatment of IB3-1 bronchial epithelial cell line demonstrates a major influence on heat-shock proteins. Physiol Genomics *16*, 204-211.

Xi, J. H., Bai, F., Gross, J., Townsend, R. R., Menko, A. S., and Andley, U. P. (2008). Mechanism of small heat shock protein function in vivo: a knock-in mouse model demonstrates that the R49C mutation in alpha A-crystallin enhances protein insolubility and cell death. J Biol Chem *283*, 5801-5814.

Yam, G. H., Bosshard, N., Zuber, C., Steinmann, B., and Roth, J. (2006). Pharmacological chaperone corrects lysosomal storage in Fabry disease caused by trafficking-incompetent variants. Am J Physiol Cell Physiol *290*, C1076-1082.

Yam, G. H., Gaplovska-Kysela, K., Zuber, C., and Roth, J. (2007a). Aggregated myocilin induces russell bodies and causes apoptosis: implications for the pathogenesis of myocilin-caused primary open-angle glaucoma. Am J Pathol *170*, 100-109.

Yam, G. H., Gaplovska-Kysela, K., Zuber, C., and Roth, J. (2007b). Sodium 4-phenylbutyrate acts as a chemical chaperone on misfolded myocilin to rescue cells from endoplasmic reticulum stress and apoptosis. Invest Ophthalmol Vis Sci *48*, 1683-1690.

Yam, G. H., Zuber, C., and Roth, J. (2005). A synthetic chaperone corrects the trafficking defect and disease phenotype in a protein misfolding disorder. Faseb J *19*, 12-18.

Yancey, P. H. (2005). Organic osmolytes as compatible, metabolic and counteracting cytoprotectants in high osmolarity and other stresses. J Exp Biol *208*, 2819-2830.

Yang, W. Y., and Gruebele, M. (2003). Folding at the speed limit. Nature *423*, 193-197.

Yang, Z., Huang, J., Geng, J., Nair, U., and Klionsky, D. J. (2006). Atg22 recycles amino acids to link the degradative and recycling functions of autophagy. Mol Biol Cell *17*, 5094-5104.

Ye, Y. (2005). The role of the ubiquitin-proteasome system in ER quality control. Essays Biochem *41*, 99-112.

Yoshida, H., Matsui, T., Yamamoto, A., Okada, T., and Mori, K. (2001). XBP1 mRNA is induced by ATF6 and spliced by IRE1 in response to ER stress to produce a highly active transcription factor. Cell *107*, 881-891.

Yoshida, T., Ohno-Matsui, K., Ichinose, S., Sato, T., Iwata, N., Saido, T. C., Hisatomi, T., Mochizuki, M., and Morita, I. (2005). The potential role of amyloid beta in the pathogenesis of age-related macular degeneration. J Clin Invest *115*, 2793-2800.

Zatloukal, K., Stumptner, C., Fuchsbichler, A., Fickert, P., Lackner, C., Trauner, M., and Denk, H. (2004). The keratin cytoskeleton in liver diseases. J Pathol *204*, 367-376.

Zeitlin PL (2000). Pharmacologic restoration of delta F508 CFTR-mediated chloride current. Kidney Int *57*, 832-837.

Zeng, L., Lu, M., Mori, K., Luo, S., Lee, A. S., Zhu, Y., and Shyy, J. Y. (2004). ATF6 modulates SREBP2-mediated lipogenesis. Embo J *23*, 950-958.

Zhang, H., Duncan, G., Wang, L., Liu, P., Cui, H., Reddan, J. R., Yang, B. F., and Wormstone, I. M. (2007a). Arsenic trioxide initiates ER stress responses, perturbs calcium signalling and promotes apoptosis in human lens epithelial cells. Exp Eye Res *85*, 825-835.

Zhang, L. Y., Yam, G. H., Fan, D. S., Tam, P. O., Lam, D. S., and Pang, C. P. (2007b). A novel deletion variant of gammaD-crystallin responsible for congenital nuclear cataract. Mol Vis *13*, 2096-2104.

Zhang, J., Yan, H., Harding, J. J., Liu, Z. X., Wang, X., and Ruan, Y. S. (2008). Identification of the primary targets of carbamylation in bovine lens proteins by mass spectrometry. Curr Eye Res *33*, 963-976.

Zhang, L. Y., Gong, B., Tong, J. P., Fan, D. S., Chiang, S. W., Lou, D., Lam, D. S., Yam, G. H., and Pang, C. P. (2009a). A novel gammaD-crystallin mutation causes mild changes in protein properties but leads to congenital coralliform cataract. Mol Vis *15*, 1521-1529.

Zhang, L. Y., Yam, G. H., Tam, P. O., Lai, R. Y., Lam, D. S., Pang, C. P., and Fan, D. S. (2009b). An alphaA-crystallin gene mutation, Arg12Cys, causing inherited cataract-microcornea exhibits an altered heat-shock response. Mol Vis *15*, 1127-1138.

Zhang, Y., Nijbroek, G., Sullivan, M. L., McCracken, A. A. (2001). Hsp70 molecular chaperone facilitates endoplasmic reticulum-associated protein degradation of cystic fibrosis transmembrane conductance regulator in yeast. Mol Biol Cell *12*, 1303-1314.

Zhou, Z., and Vollrath, D. (1999). A cellular assay distinguishes normal and mutant TIGR/myocilin protein. Hum Mol Genet *8*, 2221-2228.

Zhu, C., Johansen, F. E., and Prywes, R. (1997). Interaction of ATF6 and serum response factor. Mol Cell Biol *17*, 4957-4966.

Zietkiewicz, S., Lewandowska, A., Stocki, P., and Liberek, K. (2006). Hsp70 chaperone machine remodels protein aggregates at the initial step of Hsp70-Hsp100-dependent disaggregation. J Biol Chem *281*, 7022-7029.

Zolyomi, Z., Benson, M. D., Halasz, K., Uemichi, T., and Fekete, G. (1998). Transthyretin mutation (serine 84) associated with familial amyloid polyneuropathy in a Hungarian family. Amyloid *5*, 30-34.